Grafting of organic layers via bipolar electrochemistry

Chawanwit Kumsapaya

THÈSE EN COTUTELLE PRÉSENTÉE

POUR OBTENIR LE GRADE DE

DOCTEUR DE

L'UNIVERSITÉ DE BORDEAUX

ET DE l'UNIVERSITÉ DE KASETSART

ÉCOLE DOCTORALE SCIENCES CHIMIQUES

SPÉCIALITÉ : CHIMIE-PHYSIQUE

Par Chawanwit KUMSAPAYA

GREFFAGE DE COUCHES ORGANIQUES PAR ÉLECTROCHIMIE BIPOLAIRE

Sous la direction du Prof. Alexander KUHN
et du Prof. Jumras LIMTRAKUL

Soutenue le : 02.12.2014

Membres du jury :

M. BOPP, Philippe,	Professeur, Université de Bordeaux	Président
M. JONGSOMJIT, Bunjerd,	Associate Professor, Chulalongkorn University	Rapporteur
M. PROMARAK, Vinich	Associate Professor, Suranaree University of Technology	Rapporteur
M. PAVASANT, Prasert	Associate Professor, Chulalongkorn University	Examinateur
M. KUHN, Alexander,	Professeur, Institut Polytechnique de Bordeaux	Examinateur
M. LIMTRAKUL, Jumras,	Professor, Kasetsart University	Examinateur
M. ZIGAH, Dodzi,	Maître de Conférences, Université de Bordeaux	Membre invité
Mme. WARAKULWIT, Chompunuch,	Lecturer, Kasetsart University	Membre invité

Greffage de couches organiques par électrochimie bipolaire

Résumé :

Dans cette thèse, le concept d'électrochimie bipolaire qui permet de réaliser des réactions électrochimiques par l'application d'un champ électrique, sur un objet conducteur placé dans une solution électrolytique sans aucun contact avec les électrodes, a été utilisé pour générer des objets Janus possédant une partie organique et une partie inorganique. Comme preuve de principe, des billes de carbone vitreux de taille micrométrique ont été modifiées de manière asymétrique par électrochimie bipolaire en réduisant un sel d'aryl diazonium. La couche organique ainsi greffée a pu être observée après interaction avec des nanoparticules d'or, ou des molécules fluorescentes. Les résultats ont montré que la moitié de la surface des billes a pu être modifiée de manière sélective et avec une grande précision. En ajustant le temps et/ou le champ électrique utilisé pour la réduction du sel de diazonium, la surface greffée peut être modulée. Ce concept a été généralisé à l'échelle nanométrique sur des nanotubes de carbone alignés verticalement. Ces nanotubes de carbone ont été préparés par un dépôt chimique en phase gazeuse en utilisant un template d'oxyde d'aluminium poreux. L'électrogreffage bipolaire d'une couche organique uniquement sur une extrémité des nanotubes et uniquement sur la face interne de ces tubes, a été possible en conservant les nanotubes piégés dans le template d'oxyde d'aluminium. Cette technique ouvre donc la voie d'applications dans le domaine des piles à combustible, des bio-capteurs, et également pour la délivrance contrôlée de médicaments.

Mots clés : électrochimie bipolaire, particules Janus, électrogreffage, sels de diazonium, carbone, nanotubes de carbone, oxyde d'aluminium anodique

---

Grafting of Organic Layers via Bipolar Electrochemistry

Abstract :

In this thesis, the concept of bipolar electrochemistry, which allows carrying out electrochemical reactions on a free-standing conductive object in an electric field, was employed to generate Janus-type objects with a hybrid organic-inorganic composition. As a proof-of-concept micrometer-sized glassy carbon beads were modified asymmetrically via the bipolar electrochemical reduction of aryl diazonium salts. The grafted organic layers can be probed either with gold nanoparticles (AuNPs) or with fluorescent molecules. The results show that one-half sphere of the beads was modified selectively and with high precision. This concept was then generalized to vertically aligned carbon nonotubes (VACNTs). They were prepared via chemical vapor deposition using porous anodic aluminum oxide (AAO) as template. The bipolar electrografting of an organic layer onto the inner surface of the VACNTs was performed by using the tubes that were still embedded in the pores of the AAO membrane as the starting material. The grafted results can be visualized by coupling them with AuNPs. After the AAO removal, the results reveal a grafting of organic layers only at one end of the tubes along the inner wall. For both cases, fine tuning of the deposition time and/or the electric field used for the reduction of diazonium salts can control the geometric area of the grafting. This technique opens up applications of these objects in the fields of controlled drug delivery and storage.

Keywords : Bipolar Electrochemistry, Janus particles, Electrografting, Diazonium salts, Carbon, Carbon nanotubes, Anodic aluminum oxide

Unité de recherche

Chemistry Department and Center of Nanotechnology
Kasetsart University, 50 Ngamwongwan Road, Chatuchak, Bangkok, 10900 Thailand

Institut des Sciences Moléculaires (ISM) UMR 5255 CNRS Université de Bordeaux
351 cours de la libération 33405 Talence Cedex – France

ACKNOWLEDGEMENTS

Firstly, I would like to express my sincere gratitude to my supervisor in Thailand, Prof. Jumras Limtrakul for giving me the great opportunity to be a part of his group and contributing in several scientific projects. I am grateful for his patience, advice, knowledge, enthusiastic encouragement, and invaluable support throughout my Ph.D. study.

I am also deeply thankful to my co-supervisor, Prof. Alexander Kuhn, for all he has done for me, both academically and personally. I admire his positive attitude, insightful guidance, and vast majority of knowledge. He works hard, plays hard despite his busy schedule. I hope that one day I will be as smart as he is. In addition, I truly appreciate him and his wonderful family for the warm welcome. Their hospitality made my life in France a memorable experience.

I am forever grateful to my co-advisors, Assistant Prof. Dodzi Zigah, Dr. Chompunuch Warakulwit, Dr. Pipat Khongpracha, and Dr. Winyoo Sangthong. This thesis would not have been possible without their suggestion and support. I especially like to thank Assistant Prof. Dodzi for all the support, advice, discussion, and assistance, which kept my research and writing progress during these years. He taught me everything I need to know about electrochemistry in enthusiastic and patient way. I am also very grateful to Dr. Chompunuch, who introduced me to the challenge world of bipolar electrochemistry. She is the driving force behind this thesis. Her good spirit, intelligent idea, and stimulating discussion wholeheartedly inspired me beyond the scope of science.

It gives me great pleasure in acknowledge the constructive comments and suggestions of the members of my thesis committees, Prof. Philippe Anthony Bopp, Dr. Somkiat Nokbin, Assoc.Prof. Bunjerd Jongsomjit, Assoc.Prof. Vinich Promarak, and Assoc.Prof. Prasert Pavasant. Exclusively sincere thanks to Prof. Philippe who

gave me many helpful suggestions when I first got into Bordeaux. His kindness made me feel like he was family.

I would like to gratefully acknowledge the following organizations for their support: the Commission on Higher Education (CHE), Ministry of Education, under the program “Strategic Scholarships for Frontier Research Network for the Joint Ph.D. Program Thai Doctoral degree” and the “National Research University Project of Thailand (NRU)” and the “National Center of Excellence for Petroleum, Petrochemical and Advanced Materials (NCE-PPAM)”, the National Science and Technology Development Agency (NSTDA Chair Professor), the National Nanotechnology Center (NANOTEC Center of Excellence), and Kasetsart University Research and Development Institute (KURDI).

A Big thank to all the members of the groupe “Nanosystèmes Analytiques (NSysA)” of the “Institut des Sciences Moléculaires (ISM)”, Université de Bordeaux, France for their generous supports, particularly Janus people; Dr. Zahra Fattah, Dr. Nina Hüsken, Dr. Gabriel Loget, Dr. Jérome Roche, Dr. Michael Ongaro, and Marie-France Bakaï for the exciting work, the fruitful discussion, and the creative ideas we shared and inspired each other. My thanks also go to my wonderful friends from geek session, Dr. Chularat Wattanakit, Dr. Catherine Adam, Dr. Suresh Vajrala, Dr. Salem Ben-Amor, Dr. Lisa Peyrard, Dr. Léa Messager, Dr. María del Pozo, Dr. Emiline Girard, Dr. Laurent le Hanaff, Dr. Matthias Heim, Dr. Yémima Bon Saint Côme, Lorenzo Russo, Florent Pinaud, and Milica Sentic for the impressive discussions, the crazy experiences, and the kind helps. Deeply thanks to Aline Simon-Lalande for the family atmosphere she provided me. I would like to acknowledge all inputs and technical supports from Dr. Bertrand Goudeau, Patrick Garrigue, and Véronique Lapeyre.

I also indebted to all the laboratory for Computational and Applied Chemistry (LCAC), Kasetsart University, Thailand for their helps, supports and encouragement, especially Dr. Thana Maihom, Dr. Waraporn Jungtanasombat, Dr. Phongthep Prajongtat, Dr. Panvika Pannopard, Chaiyan Boonyuen, Sombat Ketrat, Oranit

Phuakkong, and Sudarat Yadnum. I do apologize that I cannot mention everyone. There are too many people involved in this process to list here. I thank you all.

Last but not least, I especially thank my parents, my sister, my best friends, particularly Ms. Krittaya Thipphayanon, and my beloved dog aka “Lapin” for their unconditional love and support 365 days a year. I would never make it this far without them.

Chawanwit Kumsapaya

December 2014

TABLE OF CONTENTS

Page

TABLE OF CONTENTS (Continued)

TABLE OF CONTENTS (Continued)

TABLE OF CONTENTS (Continued)

Page

LIST OF TABLES

LIST OF FIGURES

LIST OF FIGURES (Continued)

LIST OF FIGURES (Continued)

LIST OF FIGURES (Continued)

LIST OF FIGURES (Continued)

LIST OF FIGURES (Continued)

LIST OF FIGURES (Continued)

LIST OF FIGURES (Continued)

LIST OF FIGURES (Continued)

LIST OF FIGURES (Continued)

LIST OF FIGURES (Continued)

LIST OF FIGURES (Continued)

LIST OF FIGURES (Continued)

LIST OF ABBREVIATIONS

4-CP	=	4-carboxyphenyl
AAO	=	anodic aluminum oxide
AuNPs	=	gold nanoparticles
BPE	=	bipolar electrode
CABED	=	capillary assisted bipolar electrodeposition
CCVD	=	catalytic chemical vapor decomposition
CNTs	=	carbon nanotubes
CVD	=	chemical vapor decomposition
D	=	dimension
DI	=	deionized
DMF	=	*N,N*-dimethylformamide
DNA	=	deoxyribonucleic acid
EDC	=	1-ethyl-3-(3-dimethylaminopropyl) carbodiimide
EDX	=	energy dispersive X-ray
ESEM	=	environmental scanning electron microscopy
GO_x	=	glucose oxidase
HOPG	=	highly oriented pyrolytic graphite
HRP	=	horseradish peroxidase
IR	=	infrared spectroscopy
MWCNTs	=	multi-walled carbon nanotubes
NHE	=	normal hydrogen electrode
Ox	=	oxidized species
Red	=	reduced species
SEM	=	scanning electron microscopy
SHE	=	standard hydrogen electrode
SWCNTs	=	single-walled carbon nanotubes
TEM	=	transmission electron microscopy
TGA	=	thermogravimetric analysis
VACNTs	=	vertically aligned carbon nanotubes

LIST OF ABBREVIATIONS (Continued)

VACNT/AAO	=	VACNTs embedded in the AAO membrane
XPS	=	X-ray photoelectron spectroscopy
A	=	ampere
$A.cm^{-2}$	=	ampere per square centimeter
cm	=	centimeter
cm^{-1}	=	reciprocal wavelength
d	=	characteristic length or diameter
$E°$	=	standard potential
E_a	=	potential of the anode
E_c	=	potential of the cathode
E_{eq}	=	potential at equilibrium
E_{tot}	=	potential difference
eV	=	electron volt
g	=	gram
h	=	hour
kV	=	kilovolt
$kV.m^{-1}$	=	kilovolt per meter
L	=	distance between two feeder electrodes
M	=	molar
mA	=	milliampere
mg	=	milligram
min	=	minute
ml	=	milliliter
ml/min	=	milliliter per minute
mm	=	millimeter
mM	=	millimolar
mV	=	millivolt
mV/s	=	millivolt per second
MΩ.cm		mega-ohms centimeter

LIST OF ABBREVIATIONS (Continued)

n	=	number of electrons involved in an half-reaction
nm	=	nanometer
R	=	organic residue or substituted functional group
s	=	second
V	=	polarization potential at the substrate surface-solution interface
V	=	volt
$V.m^{-1}$	=	volt per meter
V_a	=	solution potential at anodic pole of BPE
V_c	=	solution potential at cathodic pole of BPE
V_{eq}	=	equilibrium potential
x	=	position along the BPE
X^-	=	inorganic or organic anion
x_0	=	position along the BPE where V is equal to V_{eq}
δ^-	=	cathodic pole of BPE
δ^+	=	anodic pole of BPE
ΔV	=	maximum polarization potential difference
ΔV_{min}	=	minimum potential value needed to drive the electrochemical reactions at BPE
Θ	=	angular position
µl	=	microliter
µm	=	micrometer
%w/v	=	weight-to-volume percent
(aq)	=	aqueous solution
(s)	=	solid
°C	=	degree of Celcius
°C/min	=	degree of Celcius per minute
$\mathcal{E}$	=	applied electric field

Chapter I: GENERAL INTRODUCTION

The present thesis is dealing with the controlled surface modification of carbon objects based on the concept of bipolar electrochemistry. Different approaches allowing the immobilization of ultrathin layers of organic molecules on the surface of isotropic or anisotropic particles will be explored with the final goal to obtain asymmetric Janus-type objects. In the following the most important ingredients for this work in terms of materials and mechanisms will be briefly described in order to set the fundamental scientific background for the understanding of the subsequent chapters.

1. Carbon materials

Carbonaceous materials have been widely used in various applications and technologies as they are present in different forms (ranging from powder to fibers) and allotropes (i.e. diamond, graphite, graphene, amorphous carbon, fullerenes, carbon nanotubes (CNTs), glassy carbon) and have a rich variety of dimensionality (ranging from 0D to 3D) and structural scale (ranging from micro- to nanoscale) as shown in Figure 1.

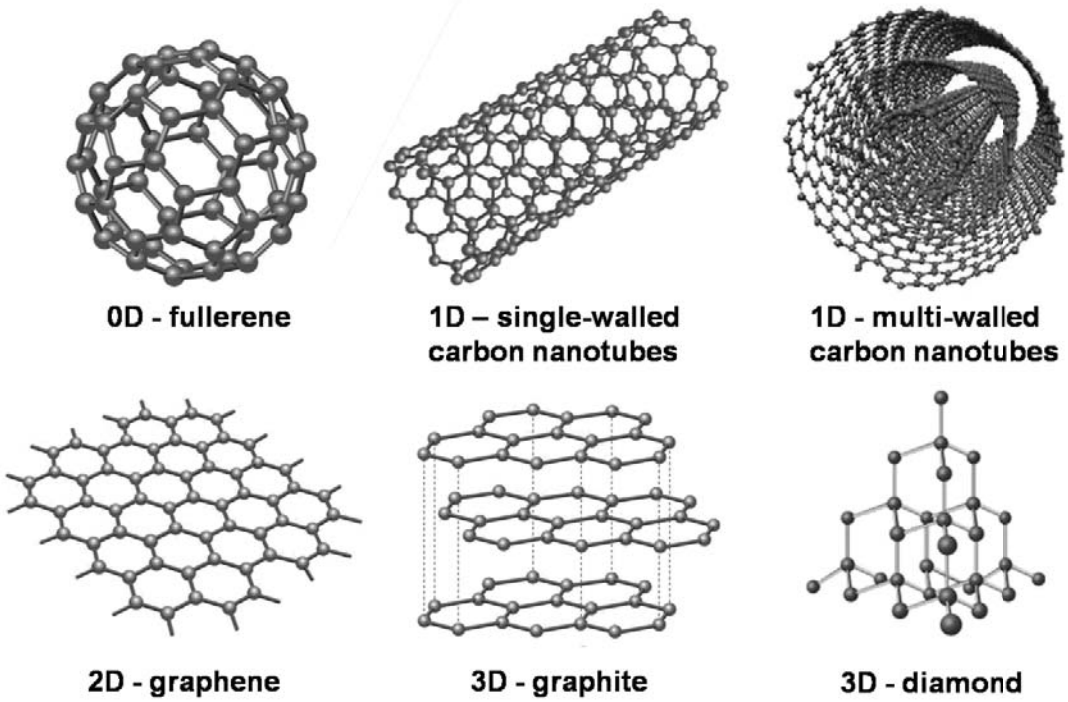

Figure 1 Six allotropes of carbon with all possible dimensionalities. The carbon forms structures of zero – dimension (0D) like fullerene, one – dimension (1D) as single- and multi-walled carbon nanotubes, two – dimensional (2D) graphene sheets, and, three – dimensional (3D) graphite and diamond.

The physical properties of carbon materials vary widely with their different forms even though all forms consist of pure carbon. For example, diamond is one of the hardest materials, it is colorless and transparent and has very low electrical conductivity (Collins, 1993) while graphite is very soft (can be used to write on paper), black, and it is a great electrical conductor (Deprez and McLachlan, 1988). Carbon materials with good electrical conductivity, chemical and mechanical stability, light-weight and a relatively low price (compared to noble metals) have been widely used for electrochemical applications. For example, glassy carbon has been traditionally used as an electrode material for electro-analytical applications (Van der Linden and Dieker, 1980). CNTs, graphene, activated carbon and porous carbon have been used as the electrode materials

for storage of electrochemical energy in batteries or supercapacitors (Chen and Dai, 2013; Frackowiak and Béguin, 2001). In addition, much attention has been paid to the use of graphene, CNTs and porous carbons as the supporting materials for electrocatalysts recently (Li *et al.*, 2012).

Glassy carbon is a non-graphitizing carbon. It has been fabricated since the early 1960s (Cowlard and Lewis, 1967; Lewis *et al.*, 1963; Ulrich *et al.*). Commonly, it is generated from polymeric precursors via heat treatment in the temperature range of 1000 - 3000 °C under an inert atmosphere. This treatment introduces its distinguishing properties including high mechanical strength, high thermal, oxidation (in the presence of water vapor, oxygen, or carbon dioxide) and chemical (especially for acids) resistance, as well as good electrical and thermal conductivity (Harris, 2004; Harris and Kawamura, 1976; Jenkins *et al.*, 1972). Due to these unique properties, glassy carbon has been used as material for high-temperature crucibles and electrodes. Glassy carbon has a highly disordered structure. Unlike graphite, which is an allotropic form of carbon possessing a structure with the sheets of the hexagonal (honeycomb) carbon lattices or graphene sheets, glassy carbon was proposed to have a fullerene-related microstructure in which the sp^2 hybridized carbon atoms arrange in planes with a hexagonal symmetry. The proposed structure consists of discrete fragments of the curved carbon planes. The five- and seven-membered rings are dispersed randomly throughout the networks of the six-membered rings and bend the hexagonal carbon planes (Harris, 2004).

CNTs have also attracted great attention from both experimental and theoretical points of view. This is because they possess a huge surface-to-volume ratio, remarkable thermal and mechanical properties, unique electrical and optical properties opening up various applications for coatings, composites, electronics, energy storage, catalysis, and biotechnology (De Volder *et al.*, 2013). CNTs were firstly observed in the carbon soot of graphite rods during an arc-discharge experiment in which carbon was evaporated at high temperatures via the arc discharge of high voltage under inert gas environment in 1991 by

Iijima (Iijima, 1991). Until recently, various methods have been utilized for the synthesis of CNTs. Among one of them, the catalytic chemical vapor deposition (CCVD) incorporating the catalyst-assisted thermal decomposition of carbon sources at high temperature (600 - 1200°C) (José-Yacamán *et al.*, 1993; Walker *et al.*, 1959) has the highest potential for large-scale production of CNTs because it is a simple, low-cost and easy to scale-up method (Endo *et al.*, 2006).

CNTs possess a cylindrical nanostructure. Their structure can be considered as the rolling rolled-up graphene sheets. Depending on the number of the rolled graphene sheet, CNTs can be categorized into two major types including single-walled carbon nanotubes (SWCNTs) and multi-walled carbon nanotubes (MWCNTs). CNTs have superior electrical properties as they are 1-D carbon structures with high aspect ratio (length-to-diameter ratio) in which electrons can move only forward or backward along the length of tubes and are not easy to scatter (Avouris *et al.*, 2003). In addition, their electronic properties can be varied depending on the morphology. For example, MWCNTs are metallic and can carry an electrical current of up to 10^9 A.cm^{-2} (Wei *et al.*, 2001) while SWCNTs may be metallic or semiconducting depending on the arrangement of the graphene lattice with respect to the tube axis or the chirality.

Nevertheless, due to the inert pristine surface leading the poor solubility of CNTs in most commonly-used solvents and the strong intertube forces keeping the tubes together in bundles, their manipulation is limited. As a result, their practical applications in many promising fields are hampered.

2. Surface functionalization

Surface functionalization offers the great advantage of producing soluble and easy-to-handle tubes. Furthermore, it is possible to introduce novel properties such as biocompatibility which allows using them as drug delivery agents in living systems in

drug therapy (Shim *et al.*, 2002; Wu *et al.*, 2008). Advanced modifications can not only improve the relevant properties of CNTs, but also can allow the fabrication of novel composites with desirable properties extending the application of CNTs. For example, functionalized CNTs can be used as catalyst support to enhance the catalytic activity for fuel cell (Guo and Li, 2005).

Chemical methods are typically used for the surface functionalization of CNTs. The chemical modification can be achieved via two approaches: covalent and non-covalent approaches. In the covalent approach, the functional groups are covalently attached to the tube sidewalls and/or the ends of the tubes. In the non-covalent approach, the functionalizations typically include wrapping by polymers (O'Connell *et al.*, 2001), encapsulation by surfactant molecules (Hu *et al.*, 2008) or π-stacking by conjugated macromolecules (Davis *et al.*, 2003). Comparing these approaches, the non-covalent functionalization can better maintain the original geometric structure and properties of CNTs including electronic properties due to little or no structural damage. However, it usually suffers from some disadvantages such as the requirement of specific complex, synthetic and/or expensive reagents. Although the covalent methods are more efficient for the tube functionalization providing a very stable derivatization compared to the non-covalent functionalization (Hoffman *et al.*, 1991; Wildgoose *et al.*, 2005), most of them require harsh reaction conditions such as using concentrated strong acids and thus significantly damage the tubes. Typically, CNTs are etched and shortened during the modification.

Electrochemically assisted covalent modification is an attractively alternative method for the modification of carbon materials. It is based on the electrogeneration of a highly reactive (radical) species near a carbon surface after a constant potential (potentiostatic) or a constant current (galvanostatic) is applied to the carbon electrode immersed in the solution that consists of a suitable reagent. Recently, two strategies involving the electrochemical reduction of aromatic diazonium salts (used in this thesis)

(Delamar *et al.*, 1992) and the oxidation of aromatic amines (Barbier *et al.*, 1990) have been reported in the literature. As an advantage over the common chemical functionalization, the electrochemically assisted modification does not require harsh chemical reagents, and thus, provides a modification without etching and shortening of carbon materials (Delamar *et al.*, 1992).

3. Aryl diazonium salts

Diazonium compounds or diazonium salts are organic compounds with a diazonium group (N_2^+). They have the general chemical formula R-N_2^+ X^- where R can be any organic residue such alkyl or aryl and X is an inorganic or organic anion. Diazonium salts with an aryl group, which is the functional group or the substituent derived from an aromatic ring, are important intermediates in organic synthesis, especially for the synthesis of azo dyes (Robert *et al.*, 2011; Zollinger, 2003). Typically, aryl diazonium salts are prepared in cold (0 ºC to 10 ºC) aqueous solution (Furniss *et al.*, 1989). They can generally react with various nucleophiles during the substitution reaction, producing the corresponding molecules with various functional groups including halogens, amino (-NH_2), hydroxyl (-OH), or cyano (-CN) groups (Allongue *et al.*, 1997). Diazonium compounds can also be coupling agents for linking polymers, biomacromolecules, and other species (e.g. metallic nanoparticles) to the surface of carbon materials (Mahouche-Chergui *et al.*, 2011).

The electrochemical reduction strategy using aryl diazonium salts was primarily developed by Jean Pinson and co-workers in 1992 (Delamar *et al.*, 1992). Soon after, it is further developed by a number of other groups (Allongue *et al.*, 1997; Delamar *et al.*, 1997; Kumsapaya *et al.*, 2013; Mahouche-Chergui *et al.*, 2011; Pinson and Podvorica, 2005; Radi *et al.*, 2008). The basic mechanism involved in the carbon modification via this strategy is shown schematically in Figure 2. The aryl radical is generated in the vicinity of the carbon surface by a one-electron electrochemical reduction of a diazonium

cation. Subsequently, the resulting radical species attach onto the carbon surface via a covalent bond (Andrieux and Pinson, 2003; Bahr *et al.*, 2001). The advantage of the use of aryl diazonium salts compared to other carbon surface modifiers lies in their ease of the preparation due to the rapid electrochemical reduction reaction and the resulting strong aryl-surface covalent bonding (Wildgoose *et al.*, 2005). In addition, as mentioned above, it provides a large choice of functional groups (Downard, 2000a). For these reasons, this strategy has been employed for a wide range of applications including sensing (Yang *et al.*, 2003), catalysis (Guo and Li, 2005), and materials science (Mahouche-Chergui *et al.*, 2011).

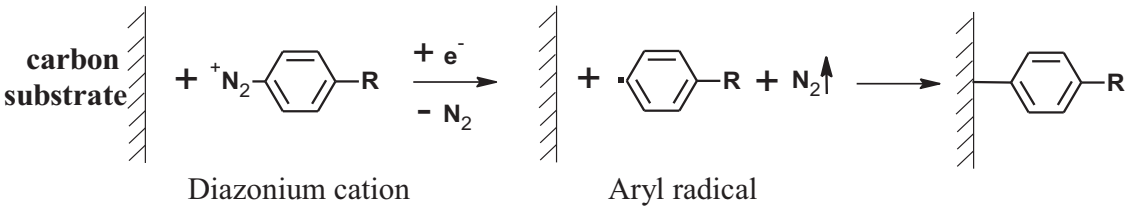

Figure 2 Schematic illustration of the basic mechanism involved in the carbon modification via the electrochemical reduction of aryl diazonium salts. R can be any organic residue such alkyl or aryl or substituted functional substituents such as halogens, amine or amino (-NH_2), hydroxyl (-OH), or cyano (-CN) groups.

In the beginning, the carbon modification via the electrochemical reduction of aryl diazonium salts was considered as a monolayer modification (Delamar *et al.*, 1992). However, multilayer films of organic compounds can be formed on the carbon substrate (Brooksby and Downard, 2005; Kariuki and McDermott, 1999; 2001; Marcoux *et al.*, 2004) due to the difficulty to precisely control the surface modification. The aryl multilayers are formed by the reaction of the electrochemically generated radicals with the aryl groups that are already bound to the carbon surface as illustrated in Figure 3.

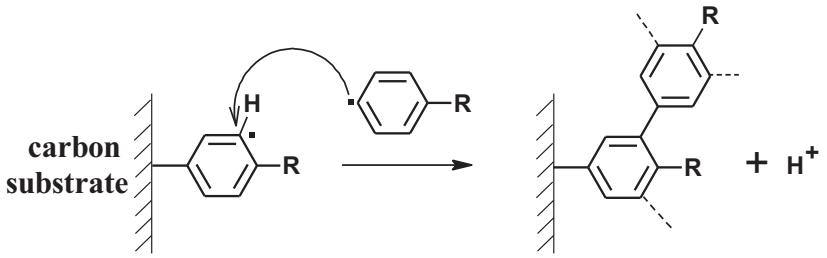

Figure 3 Schematic mechanism of multilayer formation during the modification on the carbon substrate via the electrochemical reduction of aryl diazonium salts. The dotted lines show the possible positions to form further bonds during the multilayer growth of phenyl units on the carbon substrate.

The magnitude of the applied potential is an essential parameter to control the film thickness (Brooksby and Downard, 2004; Downard, 2000b). The more the negative applied potential, the thicker the film (Downard, 2000b). Furthermore, the film thickness depends not only on the applied potential, but also on the type and the concentration of the diazonium salts, the employed substrate, and the duration of the electrochemical modification (Ceccato *et al.*, 2011). For example, Kariuki and co-workers (Kariuki and McDermott, 2001) demonstrated that multilayer films of diethylaniline were grown continuously over 30 min deposition time on the glassy carbon electrode with an average film thickness of 20 nm. Phenyl acetic acid and nitrophenyl films with a thickness of 15 – 25 nm can be produced by using this procedure. In fact, the thickness of a monolayer of phenyl and nitrophenyl groups are approximately 0.59 nm and 0.68 nm, respectively (Yang and McCreery, 1999). This indicates that multilayer aryl films with these functional groups are deposited on the glassy carbon electrodes by using the deposition times greater than 10 min for reducing the corresponding diazonium salts (Kariuki and McDermott, 2001). Allongue and co-workers demonstrated that 84% of the aryl radicals generated electrochemically (Figure 2) form bonds with a glassy carbon surface whereas only 56% form bonds with the basal planes of highly oriented pyrolytic graphite (HOPG) (the rest escapes into the solution) (Delamar *et al.*, 1997). Thus controllable modification

on carbon substrates via electrochemical reduction of aryl diazonium salts is still a challenge for developing further applications of CNTs.

Although the electrochemical reduction of diazonium salts has become very attractive for the derivatization of carbon surfaces, the main disadvantage of this approach is that the step for the salt synthesis (called as "diazotation", "diazoniation", or "diazotization") is required. The diazotization typically includes the treatment of aromatic amines such as aniline with nitrous acid, which is usually generated *in situ* from sodium nitrite ($NaNO_2$) and mineral acid (HX) such as HCl, as shown in Figure 4 (Allongue *et al.*, 1997; Furniss *et al.*, 1989; Yang *et al.*, 2003). As the products are rather unstable and tend to lose the N_2 molecule from their structure at temperatures above 5 °C in aqueous solutions (only diazonium compounds in the form of tetrafluoroborate salts can be kept almost indefinitely at room temperature) (Sagar, 1996), their isolation for further use is difficult. The stability of salts also depends on the acidity/basicity of medium. The salts are more stable in acidic medium (especially for a pH lower than 3) compared to neutral and alkaline media (Pazo-Llorente *et al.*, 2004).

In a simpler and efficient way, diazonium salts are generated in a medium via diazotization of aryl amines and are then immediately used in the further reaction without isolation from the medium. Because the results of the grafting obtained by either the isolated diazonium salts or the *in situ*-generated corresponding salts are comparable (Belanger and Pinson, 2011; Shul *et al.*, 2013), this *in situ* strategy has become very attractive for carbon modification. The modification of carbon surfaces based on aryl diazonium is usually achieved by the addition of either $NaNO_2$ in water or nitrosonium tetrafluoroborate ($NOBF_4$) in acetonitrile (Downard, 2000a; Pinson and Podvorica, 2005).

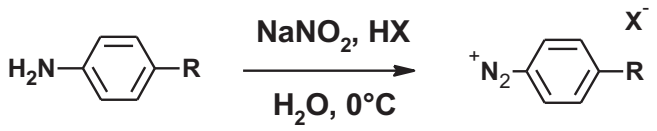

Aromatic amine Diazonium salt

Figure 4 Schematic illustration of the standard diazotization reaction. The diazonium salt is prepared from the reaction of aromatic amine and nitrous acid, which is generated *in situ* from sodium nitrite ($NaNO_2$) and mineral acid (HX).

Amine (-NH_2) and carboxylic acid (-COOH) functional groups are present in amino acids, which are the building blocks of proteins and of biologically important organic compounds. Amide functional groups (-CONH) are fundamental components of biological molecules. The amide coupling of carboxylic acids and amines is one of the most common methods employed to immobilize a protein or a peptide through a covalent bond onto the surface of supporting materials. Figure 5 is the schematic illustration of the strategy used to immobilize bio-molecules on the surface of materials. The amide bond is formed between the carboxylic acid group, which is introduced on the material surface via aryl diazonium chemistry, and the amine group of the bio-molecule. Therefore, amine and carboxylic acid groups are the key functional groups for the modification of carbon materials for exploring their potential in biological applications including bio-sensing (Yang *et al.*, 2003), bio-fuel cell (Pellissier *et al.*, 2008a), bio-electrocatalyst (Guo and Li, 2005) and drug delivery (Liu and Gooding, 2006; Liu *et al.*, 2007). Therefore we are going to use this versatile immobilization strategy also in the present thesis.

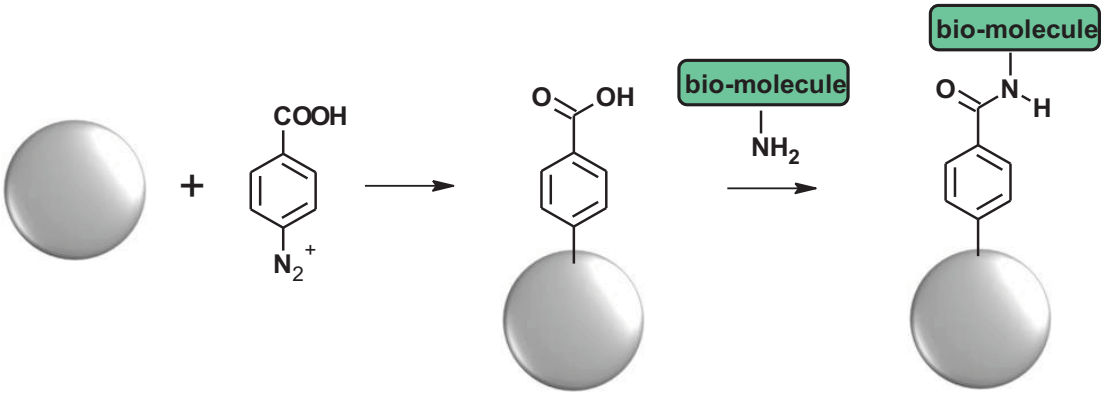

Figure 5 Schematic illustration showing a strategy to immobilize bio-molecules through the formation of an amide bond between the carboxylic acid functional group of the material surface modified by aryl diazonium and the amine functional group of the bio-molecule.

4. Janus particles

Asymmetry brings an additional degree of freedom when increasing the complexity of micro/nano-materials that is promising for advanced applications such as directed self-assembly, molecular electronics, sensing and catalysis (Fattah *et al.*, 2011; Himmelhaus and Takei, 2000; Loget and Kuhn, 2011a). Janus particles are asymmetrical functionalized particles with two different parts of surface compositions. The name of "Janus" is borrowed from the Roman god of beginnings and transitions whose two faces are looking into the opposite directions. Janus particles can have several geometric characteristics such as spheres (most commonly) (Nisisako *et al.*, 2006), cylinders (Loget *et al.*, 2011) and discs (Walther *et al.*, 2009). They can for example incorporate different chemical compositions (Paunov and Cayre, 2004), polarities (Cayre *et al.*, 2003a), and/or colors (Nisisako *et al.*, 2006) on their two parts upon design. Therefore Janus particles are very promising for diverse applications.

For example, the particles can be designed to have both hydrophilic and hydrophobic parts on their surface. These particles are called amphiphilic Janus particles. These particles behave like amphiphilic surfactants, which can stabilize water-in-oil or oil-in-water emulsions (Binks and Lumsdon, 2001). Amphiphilic Janus particles are sometimes used for the water-repellent textile applications. For this application, the hydrophilic side of the particles is bound to the surface of a textile such as polyethylene terephthalate fabric whereas their hydrophobic side is exposed to the environment providing water-repellent behaviors (Loget and Kuhn, 2010). Janus particles can be designed to have opposite charges on their both sides resulting in bipolar Janus particles (Cayre *et al.*, 2003b). They allow remote control of their position and orientation in an electric field (Cayre *et al.*, 2003a; b; Paunov and Cayre, 2004; Takei and Shimizu, 1997). If these particles are also bicolored by coating them with black color on one side and white color on the other side, they can be used for electronic ink applications in the electronic-paper display technology as shown in Figure 6 (Nisisako *et al.*, 2006).

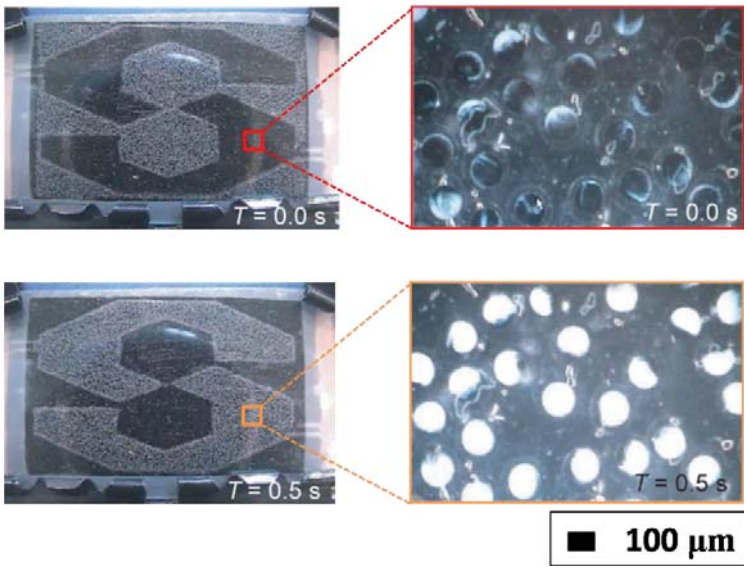

Figure 6 Top views and their magnified top views of color switching tests using bicolored Janus spheres with electrical and color anisotropies. Under an external electrical field within the display panel, these spheres turn to orient their black hemispheres (carbon black) to the negatively charged panel and their white hemispheres (titanium oxide) to the opposite panel. The particles flip after reversing the electric field gradient. Scale bar is 100 µm. Adapted from reference (Nisisako *et al.*, 2006).

Additionally, some Janus particles allow the evolution of gas from a catalytic reaction on one side of them due to their chemical composition. The gas evolution triggers propulsion of the particle. The particles then can act as jets or swimmers and be potentially applied as vehicles for drug delivery (Loget and Kuhn, 2010). Some types of Janus particles could be used as probes or sensors for some chemicals or bio-chemicals when modified with selective receptors or corresponding chemical active compounds. Apart from the applications mentioned above, some Janus particles can also be used as materials for targeting (Yang *et al.*, 2012) and as catalysts (Faria *et al.*, 2010; Fattah *et al.*, 2011; Mano and Heller, 2005).

Several techniques have been adopted to fabricate Janus particles. One of the simplest techniques is based on the use of surfaces to break the symmetry. For example, the particles are placed on a planar solid substrate, which functions as the protecting surface. Then the obtained surface is coated with a chemical substance or stamped with ink resulting in particles with two different faces (Casagrande *et al.*, 1989; Cayre *et al.*, 2003b). The uncoated side of the particles can also be further modified with different deposits leading to a higher control of the functionalities of the particles (Cayre *et al.*, 2003b). Nevertheless, the main disadvantage of this preparation technique is that a large scale production is limited. In order to obtain a relatively large quantity of Janus particles, the production in a liquid emulsion using interfaces to break the symmetry was employed. In this technique, the homogeneous particles are located at the interface of an emulsion of two immiscible phases. Then the particle surface is modified by the substances presented in one or both phases (Aveyard *et al.*, 2003; Hong *et al.*, 2006). Still, this technique does not allow an efficient and precise control of the modification (Nisisako *et al.*, 2006). Besides that, Janus particles can be also obtained by microfluidic techniques. This technique provides an outstanding control in the particle morphology (Nie *et al.*, 2006; Nisisako and Torii, 2007; Nisisako *et al.*, 2006). However, this technique requires sophisticated microfluidic devices. Additionally, the controlled nucleation and growth technique can be applied to produce Janus particles with different shapes e.g. dumbbells (Yu *et al.*, 2005), snowmen (Gu *et al.*, 2004) and acorns (Teranishi *et al.*, 2004). With this technique, a single particle of the second material is grown onto the surface of each original particle (Yu *et al.*, 2005). Nevertheless, the precise control of nucleation and growth of particles in that way is rather difficult.

Taking into account the above mentioned drawbacks it is still a very important challenge to develop scalable processes or bulk processes, yielding micro- and nanometer-sized objects in relatively large quantities, required for technological and commercial applications. Although a few methods providing bulk synthesis of Janus particles were reported, they still do not allow a fine-tuning of the particle characteristics.

Recently, a new approach based on bipolar electrochemistry has been suggested that satisfies such criteria.

5. Bipolar electrochemistry

5.1. Principle of bipolar electrochemistry

The concept of bipolar electrochemistry on microobjects was first described by Fleischmann and co-workers in 1986 (Fleischmann *et al.*, 1986). Under the influence of an external electric field, redox reactions, both oxidation (loss of electrons) and reduction (gain of electrons) reactions, can occur on a substrate placed between two feeder electrodes without any physical contact made between the conductive (or semi-conductive) substrate and the electrodes when the potential drop in the solution is high enough to drive the reactions (Loget and Kuhn, 2011b; Mavré *et al.*, 2010). For this reason, this approach allows a real bulk synthesis of Janus particles without any complexity related to the use of interfaces or surfaces to break the symmetry (Loget *et al.*, 2012).

Normally, the traditional electrochemical cell with a three-electrode setup consists of working, counter and reference electrodes. The potential of the working electrode is controlled relatively to the constant potential of the reference electrode by transferring electrons from or to the working electrode using a potentiostat, which means controlling the energy of electrons within the working electrode (Bard and Faulkner, 2001). Without the externally applied electric field, the solution potential is at a floating potential that relies on the composition of the solution (Mavré *et al.*, 2010). When the potential of the working electrode reaches a value more negative (the energy of electrons is raised) than that of an electroactive molecule in the solution, electrons may transfer from the electrode to the oxidize species in solution (reduction reactions) (Bard and Faulkner, 2001) (Figure

7). On the other hand, the oxidation reactions can occur when the electron transfer is in the opposite way as shown at left side in Figure 7.

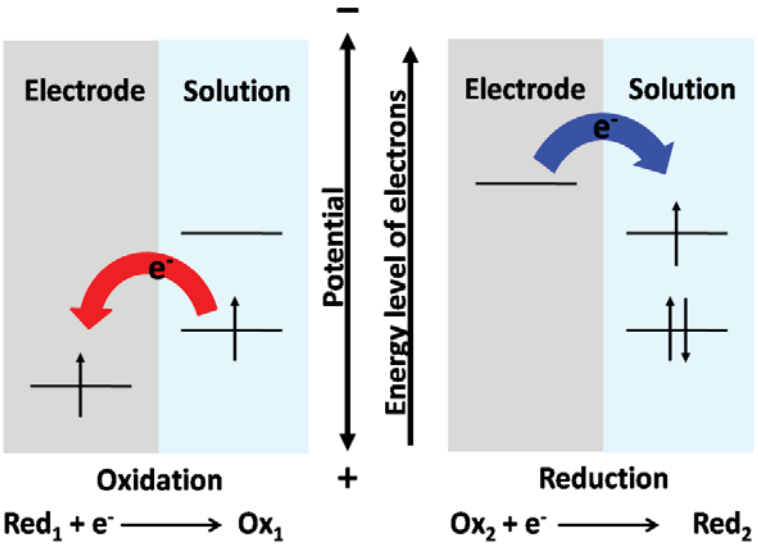

Figure 7 Schematic illustration of electron transfer across the electrode-solution interface for the oxidation (left) and the reduction (right) reactions involving two different redox couples in the solution, Ox_1/Red_1 and Ox_2/Red_2, respectively.

For bipolar electrochemistry, unlike the normal case of electrochemical reactions, the conducting substrate has no contact with the power supply, its potential thus cannot be controlled but it is the solution potential that is controlled by the power supply. Furthermore, in contrasts to common electrochemistry, the anodic process occurs at the negative side of the field set up in the solution while the cathodic reduction occurs at the positive one. This is a characteristic feature of bipolar electrode (BPE).

5.2. Open bipolar electrochemistry

Until recently, the strategies which have been used for bipolar experiments can be divided into two categories. In the first category that was used in this work, the redox reactions are taken place on a substrate, which is completely immersed in an electrolyte (Figure 8). This approach is called open bipolar electrochemistry.

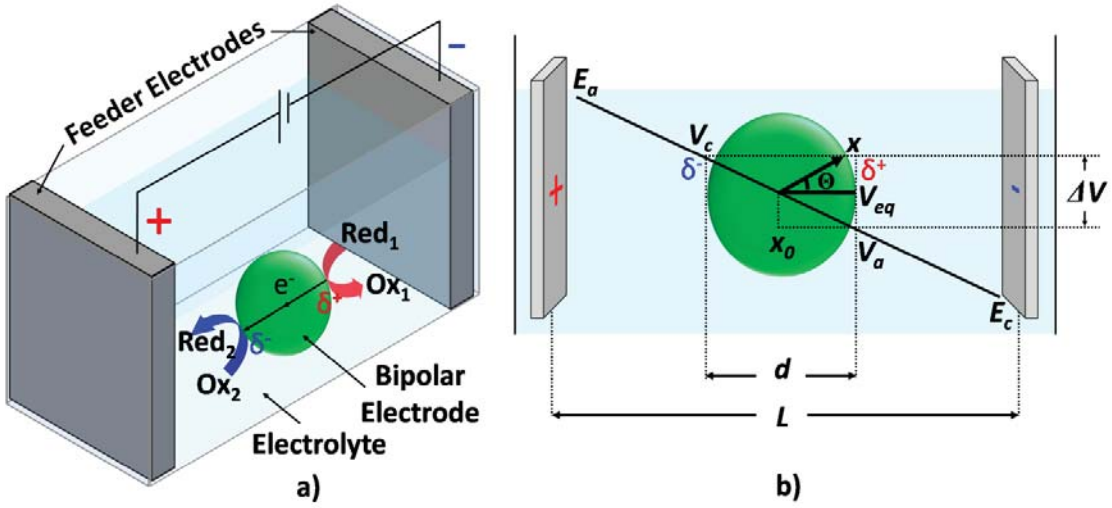

Figure 8 Scheme of (a) the open bipolar configuration. When a conductive (or semi-conductive) substrate is placed between two feeder electrodes in an electrolyte, and if the potential drop in the solution depicted in (b) is high enough, the redox reactions can occur at the bipolar electrode.

Figure 8a illustrates the experimental set-up corresponding to the open bipolar electrochemistry approach. The present set-up allows a direct observation of the individual redox reactions occurring at the ends of the conductive substrate in response to the applied field across the solution. A conductive (or semi-conductive) substrate is placed in an electrolyte in a reservoir. A potential difference, $E_{tot} = E_a - E_c$, where E_a and E_c represent the potential of anode and cathode, respectively is applied between two

feeder electrodes separated by a distance L. Due to the high resistance of the solution, the majority of E_{tot} drops linearly along the channel length (Mavré *et al.*, 2009) (Figure 8b). If we assume that the potential drop at the feeder electrode-solution interface is negligible, then E_{tot} drops linearly across the solution. The interfacial potential difference between the BPE and the solution becomes the driving force for the bipolar electrochemical reactions (Mavré *et al.*, 2010). Therefore, the resulting electric field ($\mathcal{E}$) in the solution is given by $\mathcal{E} = E_{tot}/L$.

When a BPE, either of spherical or tubular shape, is placed inside the electrolytic solution, a fraction of E_{tot}, denoted as ΔV, drops along its characteristic length (or diameter), d, following equation (1) (Duval *et al.*, 2001; Mavré *et al.*, 2010):

$$\Delta V = \frac{E_{tot}}{L} \times d = \mathcal{E} \times d \qquad \ldots(1)$$

The BPE potential floats (it is not controlled with respect to a reference value) at an equilibrium value (V_{eq}) situated between the solution potential at one end (V_c) and the other end (V_a) of the BPE (Mavré *et al.*, 2009). The value depends on the composition of the electrolyte solution and the object's position in the field.

The position x_0 in Figure 8b defines the position at which the solution potential is equal to V_{eq}, meaning that at that position no electrochemical reactions occur. This point separates the conductive substrate into two poles: the anodic pole (δ^+), where the solution potential is lower than V_{eq} and the cathodic pole (δ^-), where the solution potential is higher than V_{eq} at $x > x_0$ and $x < x_0$, respectively. Under the influence of the applied electric field, the potential difference at the substrate surface-solution interface induces a polarization potential (V), which may or may not be sufficient to drive an electrochemical reaction. If the electric field is considered to be constant, V varies linearly as a function of

the position x along the interface as calculated by equation (2) and equation (3) for a spherical and a tubular substrate, respectively:

$$V_{(x)} = \mathcal{E}(x - x_0) \cos \Theta \quad \ldots(2)$$

$$V_{(x)} = \mathcal{E}(x - x_0) \quad \ldots(3)$$

Accordingly, V increases when moving towards both ends of the substrate. The maximum polarization potential difference (ΔV) is present at the extremities of the substrate, according to the equation (1); $\Delta V = \mathcal{E} d$. The value of ΔV indicates the overall polarization between the ends of the substrate. This means that it controls directly the reactivity at the extremities of the polarized interface.

In general, two different redox couples, Ox_1/Red_1 and Ox_2/Red_2, are involved in the anodic and cathodic processes via two irreversible reactions (Figure 7):

$$Red_1 \text{ -----> } Ox_1 + n_1\, e^- \quad \ldots(4)$$

$$Ox_2 + n_2\, e^- \text{-----> } Red_2 \quad \ldots(5)$$

where, n_1 and n_2 represent the number of electrons involved in each half-reaction with the standard potentials of E_1° and E_2°, respectively.

In order to generate two redox reactions simultaneously, the minimum potential value (ΔV_{min}) needs to be at least equal to the difference between the standard potentials of the two redox couples (see equation (6)).

$$\Delta V_{min} = E_1^\circ - E_2^\circ \quad \ldots(6)$$

If the applied electric field induces a large enough polarization across the conductive substrate, that is $\Delta V > \Delta V_{min}$, then both electrochemical reactions in equation

(4) and (5) can occur at the opposite ends of the substrate. It is necessary that the oxidation reaction (equation (4)) occurs at the anodic pole (red arrow in Figure 8a) coupled electrically with the reduction reaction (equation (5)) at the cathodic pole (blue arrow in Figure 8a) to maintain the electroneutrality within the BPE (Mavré *et al.*, 2010).

Obviously, a BPE can be a material with any chemical composition and its structure can be of any dimension and scale, but its conductivity must be higher than that of the surrounding electrolyte. As this open bipolar electrochemistry approach can be generalized to various types of objects and can also be used to deposit various materials with different nature ranging from metals and semiconductors to polymers, this approach is therefore powerful and versatile opening up the way to a whole new family of complex objects with an increasingly sophisticated design, thus extending their potential applications (Loget and Kuhn, 2011b; Mavré *et al.*, 2010).

5.3. Closed bipolar electrochemistry

In the second category, the conducting substrate is placed as a barrier between two feeder electrodes. The electrolyte is therefore separated into two distinct parts: an anodic and a cathodic compartment as shown in Figure 9. As there is no direct contact and exchange of ions between these two compartments, the total amount of the current has to flow through the substrate as an electronic current. Therefore the relative conductivity of the substrate and the electrolyte is no longer playing an important role, in contrast to what has been explained for the open configuration. Generally this approach, also known as closed bipolar electrochemistry, needs lower field intensities to achieve a sufficient polarization of the substrate with respect to the solution phase. (Guerrette *et al.*, 2012). Thus experiments can be carried out under less drastic conditions and can lead to a very controllable functionalization of the substrate surface.

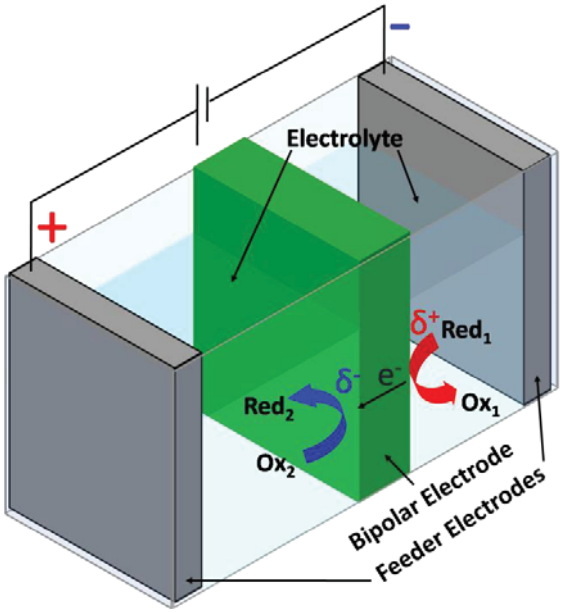

Figure 9 Scheme of a closed bipolar electrochemical cell showing the oxidation (red arrow) and reduction (blue arrow) reactions generated separately on the anodic and cathodic parts of the bipolar electrode under the influence of the global electric field.

5.4. Applications of bipolar electrochemistry

Bradley and Ma first used the bipolar electrochemical technique to modify microscale carbon particles (Bradley and Ma, 1999). Palladium (Pd) catalysts could be electrochemically deposited on various carbon materials including graphite (Figure 10), carbon nanofibers, carbon nanotubes, and carbon nanopipes (Bradley *et al.*, 2001; Bradley and Ma, 1999; Bradley *et al.*, 2005).

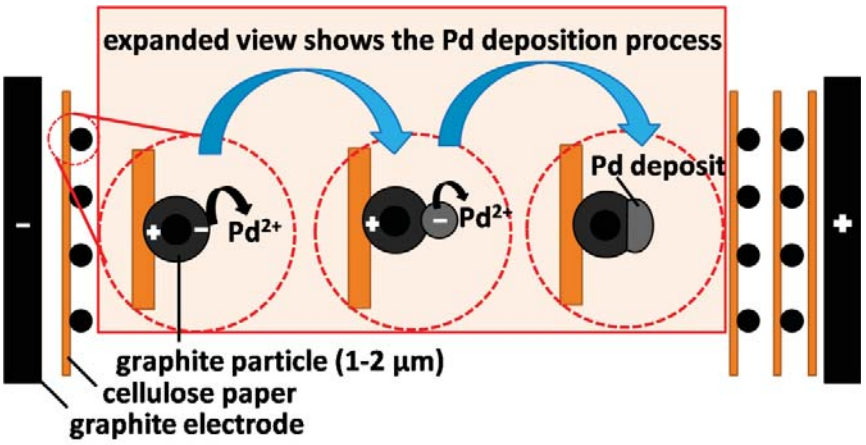

Figure 10 Scheme of the preparation of bipolar electrodeposited catalyst. The electric field is applied between two graphite electrodes to deposit asymmetrically Pd on graphite particles that are sandwiched between layers of cellulose paper in a solution of $PdCl_2$ in toluene/acetonitrile. Adapted from reference (Bradley and Ma, 1999).

This technique has also been used to deposit conducting polymer (Babu *et al.*, 2005). However, it was necessary to immobilize the substrates on the surface of a solid (Bradley and Ma, 1999). For this reason, the employed method is considered as a surface-confined method and not as a real bulk method. In addition, organic solvent was used to widen the potential window (Bradley and Ma, 1999) and to avoid problems related to side reactions such as water electrolysis, which generates macroscopic bubbles at both feeder electrodes and disturbs the orientation of the substrate in the electric field. Thus the employed technique is also not so attractive from an environmental point of view.

Later, the capillary assisted bipolar electrodeposition (CABED) was described and applied to the selectively asymmetric decoration of multi-walled carbon nanotubes (MWCNTs) at one end with gold nanoparticles (AuNPs). In the experiment, the gold deposition occurred via the reduction of gold salts at the cathodic pole of MWCNTs whereas the water oxidation occurred at the anodic pole (Warakulwit *et al.*, 2008). As

this procedure uses a real bulk-phase reaction in contrast to most of the literature methods based on interfaces to break the symmetry, this CABED process is very attractive for a mass production of asymmetric objects, especially nanoobjects.

Subsequently, nickel (Ni) (Loget *et al.*, 2010), platinum (Pt) (Fattah *et al.*, 2011), copper (Cu) (Fattah *et al.*, 2012) and silver (Ag) (Fattah *et al.*, 2013) were also electrodeposited asymmetrically on carbon tubes with a length at the microscale via the bipolar electrochemical technique. It has been shown that this technique can not only provide carbon microtubes with a metal decoration at one end, but that metal can also be deposited on both ends of the tubes via adjusting strength and time of the applied electric field. For this purpose, the metal decoration was carried out first on one side (cathodic or reduction side) of the tubes by applying an electric field pulse. After that the field was turned off. This allowed the tubes to re-orientate or relax in the capillary. During the second pulse, the deposition occurs at a position depending on the relaxation time (Loget *et al.*, 2011). The concept of bipolar electrochemical deposition has then be extended to the real bulk-phase reactions (Loget and Kuhn, 2011b). Janus objects with various types of substrates and deposits with diverse nature and shape have been successfully created (Fattah *et al.*, 2012; Loget *et al.*, 2010; Loget *et al.*, 2012; Loget *et al.*, 2013; Warakulwit *et al.*, 2008) as shown in Figure 11.

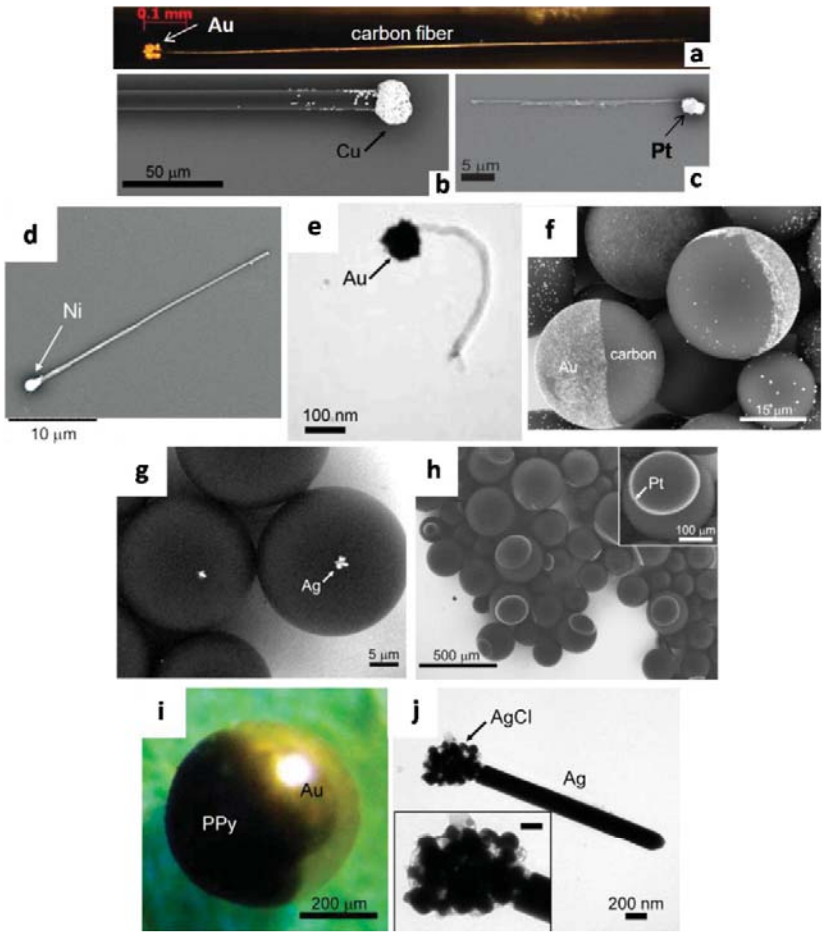

Figure 11 Janus objects with various types of substrates and deposits obtained by bipolar electrochemistry: (a) optical micrograph of a carbon fiber modified with gold. SEM micrographs of (b) a carbon microfiber modified with a copper deposit, a carbon tube (c) modified with platinum, and (d) modified with nickel. (e) TEM micrograph of MWCNT modified with gold. SEM micrographs of micrometric glassy carbon beads (f) modified with gold, and (g) modified with silver. (h) SEM micrograph of submillimetric glassy carbon beads modified with platinum rings. (i) Optical micrograph showing a gold bead modified with polypyrrole. (j) TEM micrograph of a silver nanowire modified with silver chloride. Adapted from references (Fattah *et al.*, 2012; Loget *et al.*, 2010; Loget *et al.*, 2012; Loget *et al.*, 2013; Warakulwit *et al.*, 2008).

The special features of the fabricated hybrid materials gives rise to many applications in various fields including electrochemical reactors and batteries (Loget, 2012), detection and separation (Mavré *et al.*, 2010; Sheridan *et al.*, 2011), microfluidic devices (Bouffier and Kuhn, 2013; Loget and Kuhn, 2010; 2011a; 2012), bipolar patterning (Inagi *et al.*, 2010; Ulrich *et al.*, 2008) and smart objects (Loget and Kuhn, 2011b; Loget *et al.*, 2011; Loget *et al.*, 2013; Warakulwit *et al.*, 2008).

In this work, we aim to fabricate for the first time Janus particles with an organic layer grafted selectively at one side. The organic layer is generated via a bipolar electrografting technique using aryl diazonium salts as reagents. In the first proof-of-principle experiments, micrometer-sized glassy carbon beads were used. Then the grafting technique has been generalized for another type of objects namely CNTs.

Chapter II: BIPOLAR ELECTROGRAFTING OF MOLECULAR LAYERS FOR JANUS-TYPE BEAD SYNTHESIS

Janus-type beads with hybrid organic-inorganic compositions, opening up biological applications, were fabricated via two different grafting strategies. These strategies lead to the grafting of different functional groups onto the carbon substrate, namely amino and carboxylic groups. The details are described in the following. In this part, the first proof-of-principle experiments were performed by using micrometer-sized glassy carbon beads as carbon substrate.

1. Modification of glassy carbon beads by bipolar electrochemical reduction of 4-nitrobenzenediazonium salt

First the bipolar electrochemical grafting of 4-nitrobenzene moieties onto the glassy carbon beads was carried out. The resulting immobilized 4-nitrobenzene moieties were used as the precursor of the amino-terminated aryl moieties. These amino groups are aimed for the further grafting of the carbon surface because they may be used as a very general platform for linking molecules or bio-molecules such as protein and DNA to the surface. This opens up the potential applications in fields of bio-sensing or biochemical micromotors (Mano and Heller, 2005).

The strategy proposed for asymmetrical grafting the carbon bead with the amino-terminated aryl groups is shown in Figure 12. In the first experimental step, asymmetric electrografting of 4-nitrobenzene moieties onto the bead is performed in an aqueous hydrochloric acid (HCl) solution. A 4-nitrobenzenediazonium tetrafluoroborate (BF_4^- $^+N_2$-C_6H_4-NO_2) salt is selected to be used as a reagent. This salt is one of the most common diazonium salts used for grafting nitro-phenyl groups to carbon based surfaces because it is commercially available, relatively stable (Sagar, 1996) and it has the nitro-phenyl group which allows to monitor electrochemically the surface coverage via its

electrochemical reduction to aminobenzene. By immersing the carbon bead in the electrolyte and applying an external electric field, the bead can act as BPE where the reduction of diazonium salts and the water oxidation can occur at the cathodic and the anodic poles, respectively, if the induced polarization potential (ΔV) (see equation (1) in Chapter 1) is high enough. In principle, ΔV has to be at least equal to the difference between the formal potentials of the two involved redox couples. For the electrochemical reduction of diazonium salts leading to the grafting of the nitrobenzene groups on to the bead surface, the reduction potential (E_1) equals to 0.15 V vs Ag/AgCl (Baranton and Bélanger, 2005). For the water oxidation reaction: $2H_2O \rightarrow O_2 + 4H^+ + 4e^-$, the oxidation potential (E_2) equals to 1.2 V vs Ag/AgCl. Then, a voltage of at least 1.05 V (calculated from the equation: $\Delta V_{min} = E_2 - E_1$) has to be presented across the bead in order to trigger these coupled redox reactions on the two sides of the bead. This means that for a glassy carbon bead with diameter of about 800 μm, an electric field of at least 1313 $V.m^{-1}$ (calculated from $E = \Delta V/d$ = 1.05 V/ 800 μm) is required for the bipolar experiments. If an electric field below this threshold value is applied, the electrochemical reduction of 4-nitrobenzenediazonium salts is impossible, and thus, no grafting can be obtained. This calculation demonstrates that the applied external voltage has to be at least 13.13*x V with a distance of x cm between the two feeder electrodes. Thus, if the distance between two feeder electrodes is ~10 cm, we need to apply a voltage of at least 131 V between the electrodes to obtain the organic layer grafted site-selectively onto the bead. Taking into account eventual reaction overpotentials and potential drops at the electrodes a voltage two times higher than the theoretical value is suggested for the experiments. For instance, for the set-up with a distance between two feeder electrodes of ~10 cm and a carbon bead with a diameter of ~800 μm, a voltage of more than 300 V is required.

The area on the bead that is modified by the organic layer is expected to be controllable by the variation of the applied voltage or electric field and the period of time that the voltage or the field is applied, namely the deposition time. The products containing the nitro-phenyl groups can be simply characterized by X-ray photoelectron

spectroscopy (XPS) and infrared spectroscopy (IR). The XPS presents a signal at ~406 eV corresponding to nitro group (Delamar *et al.*, 1997). Two strong IR bands corresponding to the antisymmetric and symmetric vibrations of the functional nitro groups are at ~1520 and 1340 cm^{-1} (Silverstein *et al.*, 1991).

In order to obtain amino groups attached onto the bead surface, the nitro groups of the grafted nitrobenzene moieties can be further electrochemically reduced to the amino groups. This reduction potential is -0.60 V vs Ag/AgCl (Brooksby and Downard, 2004). The obtained amino groups can then be further coupled with other functional groups such as carboxylic acid groups of molecules or bio-molecules such as proteins and DNA allowing their immobilization onto the carbon surface.

The functional amino groups presented on the beads can be protonated under acidic conditions leading to a positively charged surface due to the NH_3^+ groups. This allows an electrostatic attachment of the negatively charged species onto the bead surface. Electrostatic attachment of the negatively charged gold nanoparticles (AuNPs) onto the bead surface provides the labeling of the electrografted 4-aminobenzene layer (Bradley and Garcia-Risueño, 2011; Frens, 1973; Kimling *et al.*, 2006). The presence of AuNPs can be simply observed by scanning electron microscopy (SEM). The colloidal negatively charged AuNPs can be easily obtained, for example, by the chemical reduction of gold ions in an aqueous solution containing citrate species.

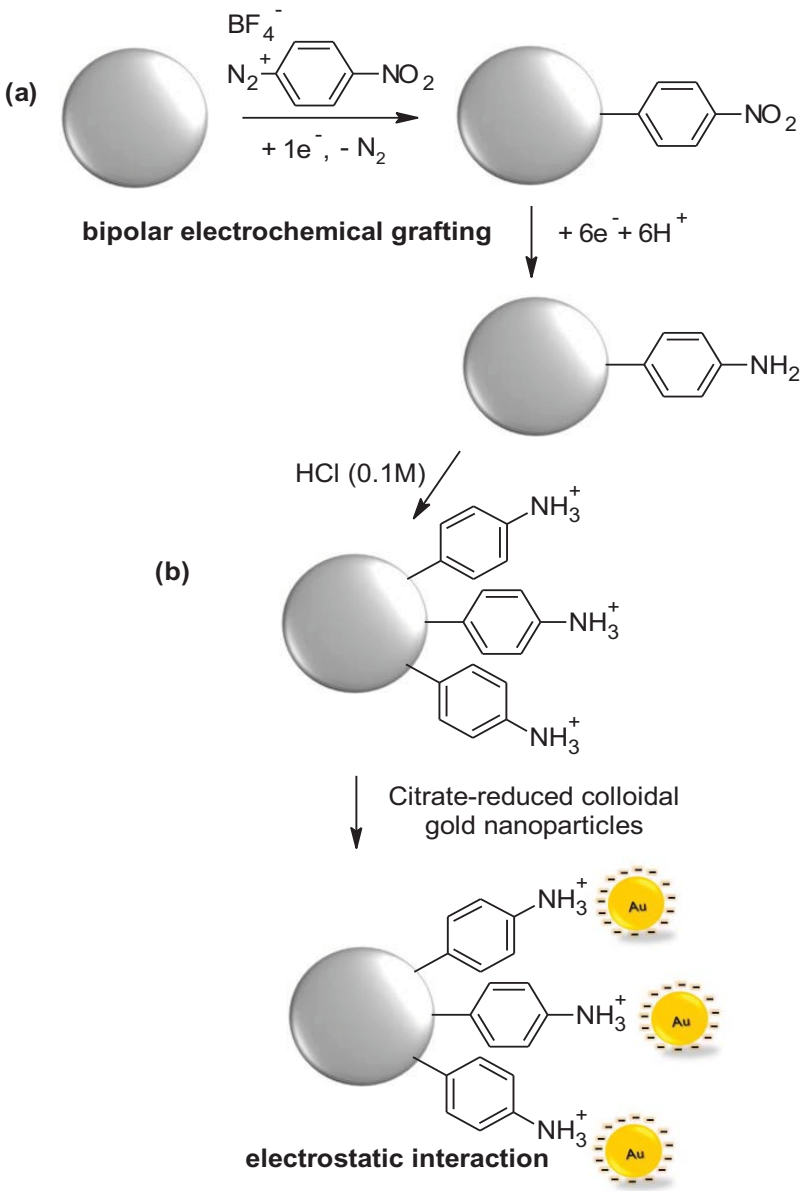

Figure 12 Schematic illustration showing the strategy employed for site-selective modification of a glassy carbon bead by the amino-terminated aryl groups. The experimental steps are (a) asymmetric electrografting of 4-aminobenzene moieties in an aqueous HCl solution and (b) electrostatic attachment of citrate-reduced colloidal gold nanoparticles to the grafted bead for visualization of the grafted molecules.

1.1. Materials and Methods

1.1.1. Materials

Major Chemicals

- Glassy carbon beads (spherical powder with diameter of 630-1000 μm, type 2, Alfa Aesar)
- Carbon rods (99.997%, diameter of 2 mm, Goodfellow Cambridge Limited)
- 4-Nitrobenzenediazonium tetrafluoroborate (97%, BF_4^- $^+N_2$-C_6H_4-NO_2, Sigma-Aldrich)
- Gold (III) chloride trihydrate (≥99.9%, $HAuCl_4 . 3H_2O$, Sigma-Aldrich)
- Citric acid-trisodium salt dihydrate (≥99%, $HOC(COONa)(CH_2COONa)_2 . 2H_2O$, Sigma-Aldrich)
- Hydrochloric acid (HCl, VWR International)
- Ethanol (96%, C_2H_5OH, VWR International)
- Deionized (DI) water (resistivity of 18 MΩ·cm, Milli-Q Integral 3, MILLIPORE)

Major Equipment

- High voltage power supply (6000V - 150 mA, CONSORT E862)
- Blowlamp (Soudogaz X 2000 PZ, CAMPINGAZ)
- Helping hand (tool) with adjustable arm ending in alligator clip
- Ultrasonic processor/bath
- Oven
- Combined hot-plate magnetic-stirrer device
- Glass Pasteur pipettes (with 0.53 mm wall thickness, 1.50 mm jet outer diameter, 230 mm long, VWR International)

- Scanning Electron Microscope (SEM) (performed with an accelerating voltage of 15 kV, TM-1000, Hitachi)
- Zetasizer (Nano-ZS90, Malvern) with disposable folded capillary cell

1.1.2. Methods

1.1.2.1. Purification of glassy carbon bead and carbon graphite

The commercial glassy carbon beads (diameter of ~800 μm) and carbon rods (diameter of 2 mm) were used as substrates and feeder electrodes, respectively. Both materials were cleaned by the sonication in absolute ethanol for half an hour. Then, they were allowed to dry at 100°C in an oven for 15 min before using them in the bipolar electrografting experiments.

1.1.2.2. Preparation of the negatively charged gold nanoparticles (AuNPs) via the citrate reduction method

In order to visualize the grafted 4-aminobenzene moieties on the bead surface that cannot be observed directly by eyes, the modified bead was exposed to the citrate-reduced AuNPs which have been prepared as follows (Kimling *et al.*, 2006) (Figure 13). Briefly, 1.7 mg of gold (III) chloride trihydrate was dissolved in 19 ml of DI water in an Erlenmeyer flask. The obtained solution was then boiled under magnetic stirring. Then, 1 ml of 0.5% w/v aqueous solution of trisodium citrate dihydrate was immediately added to the boiling solution. The color of the solution rapidly changed from pale yellow, colorless, dark purple to ruby red, respectively, within 15 s. After the ruby red color was obtained, the colloidal solution of AuNPs was removed from heat immediately. The solution was allowed to cool down to room temperature.

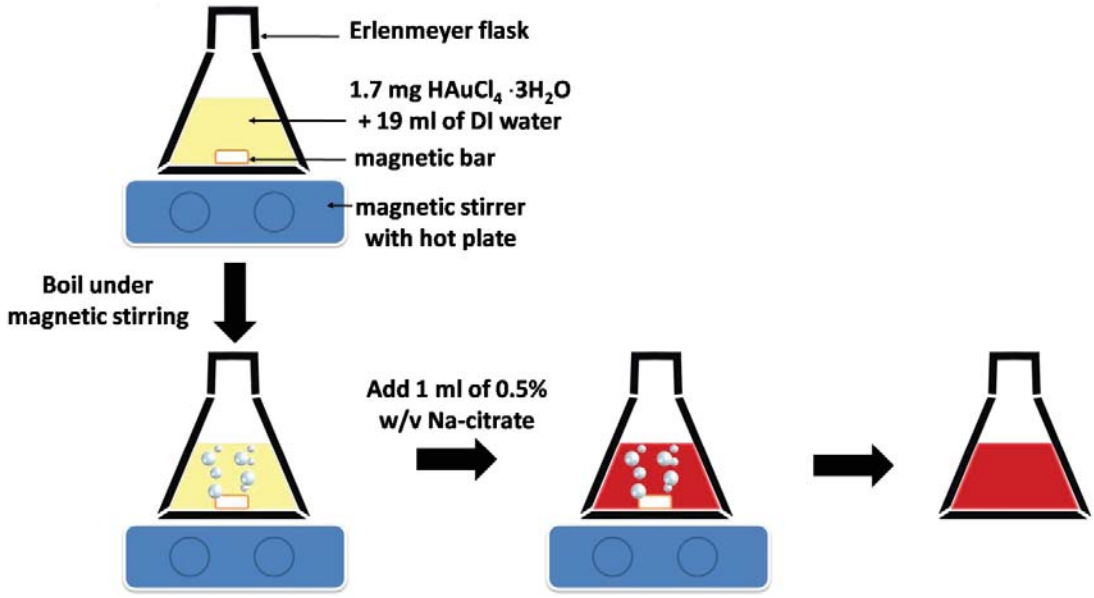

Figure 13 Schematic illustration showing the preparation of the negatively charged AuNPs via citrate reduction.

The prepared AuNPs were characterized by TEM. For this, a few drops of the colloidal solution were placed on the TEM grid (Formvar/carbon 200 mesh Cu grids, Agar Scientific). After that, a few drops of absolute ethanol were used for removing the residues from the citrate reduction (by soaking). The TEM characterization was performed using a FEI Technai 12 instrument equipped with an Orius SC1000 11MPx (GATAN) camera. The particle size and size distribution of these AuNPs were determined by using ImageJ, a Java-based image processing program developed by the National Institutes of Health (Collins, 2007).

Furthermore, the synthesized colloidal solution was characterized by zeta potential measurements (Figure 14) to measure the electrical charge of particles (Figure 14a). A disposable folded capillary cell with two gold electrodes (Figure 14b) was filled with the synthesized colloidal solution to apply an electric field. The zeta potential can be

obtained by characterizing the movement of the particles under the influence of the applied electric field.

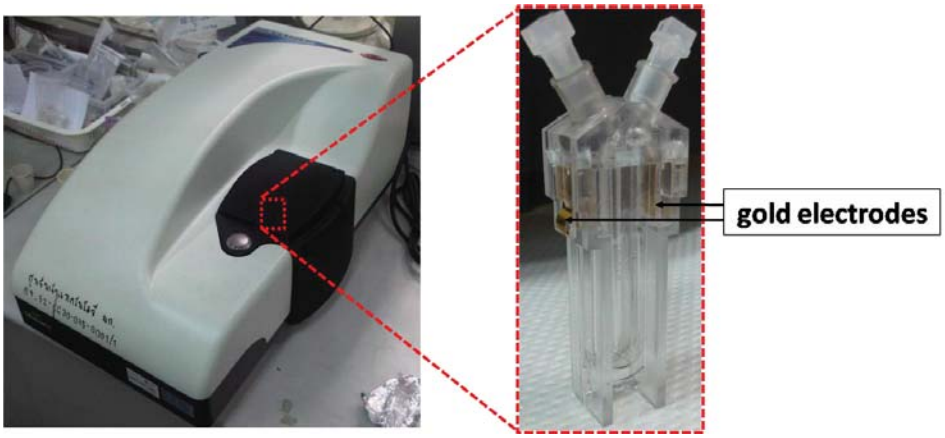

(a) (b)

Figure 14 Picture of (a) the zetaseizer and (b) the disposable folded capillary cell used for the zeta potential measurement of the synthesized colloidal solution of gold nanoparticles.

1.1.2.3. Control experiments

In order to confirm the grafting of the organic layer on the bead, five control experiments were performed prior to the bipolar experiments. Glassy carbon beads purified by the absolute ethanol under the sonication for half an hour and then dried in oven were used. The details of these experiments are shown in Table 1. These experiments were performed in order to examine 1) the raw glassy carbon beads, in order to exclude the possibility that the glassy carbon bead also interacts with the diazonium salt without applying an electric field to the system (Adenier *et al.*, 2006; Dyke and Tour, 2003) 2) beads with and 3) without the labeling by AuNPs, 4) the interaction between raw glassy carbon beads and the citrate-capped AuNPs and 5) the grafted organic layer on the bead by using the citrate-capped AuNPs.

Table 1 Details of control experiments performed in order to confirm the grafting of organic layer on the bead*

Details	1	2	3	4	5
Add 5 mM 4-nitrobenzenediazonium tetrafluoroborate /1 mM HCl	✗	✓	✓	✗	✓
Apply an electric field (4 kVm^{-1})	✗	✗	✗	✗	✓
Further interact with the citrate-capped AuNPs	✗	✗	✓	✓	✗

*The experiment was performed with (✓) and/or without (✗) the corresponding experimental step.

1.1.2.4. Fabrication of Janus-type carbon beads via bipolar electrochemical reduction of 4-nitrobenzene diazonium salt

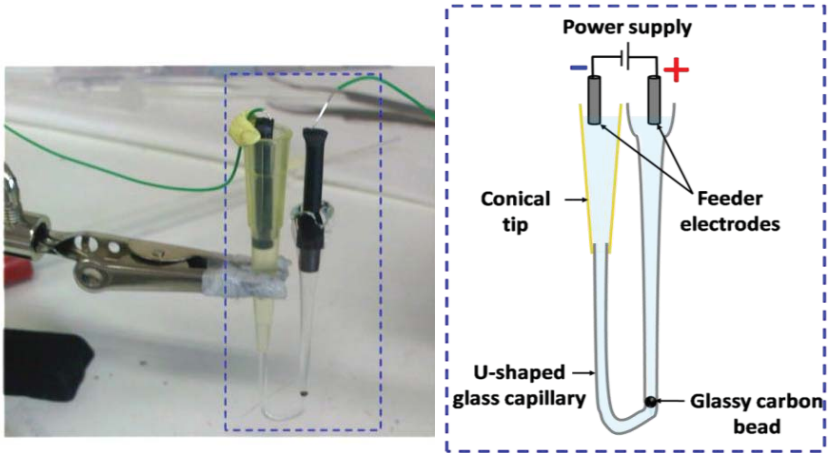

Figure 15 Schematic illustration showing the experimental set-up for the fabrication of Janus-type carbon beads with inorganic-organic composition via bipolar electrochemical reduction of 4-nitrobenzenediazonium salt. The bipolar cell was prepared from a U-shaped glass capillary connected with a conical tip. The distance between two feeder electrodes (carbon rods) was ~ 10 cm while the BPE (glassy carbon bead) was ~ 800 μm in diameter.

Figure 15 shows the experimental set-up for the fabrication of Janus-type carbon beads with inorganic-organic composition via bipolar electrochemical reduction of 4-nitrobenzene diazonium salt. Details of the experimental procedures are shown in Table 2.

Briefly, in order to modify a glassy carbon bead with 4-aminobenzene moieties, the bead (with an average diameter of ~800 μm) was placed between two carbon rod electrodes (acting as the feeder electrodes) in a bipolar cell. The cell was made from a U-shaped glass capillary. The capillary was then filled with 5 mM 4-nitrobenzenediazonium tetrafluoroborate in 1 mM glacial aqueous HCl solution. An electric field of desired amplitude was then generated by the high-voltage power supply and applied to the cell for a certain period of time. After the grafting process, the modified carbon bead was taken out from the cell and rinsed with 0.1 M HCl solution for several times in order to remove salt residues and to transform NH_2 into NH_3^+.

Table 2 Details of experimental procedures for the fabrication of Janus-type carbon beads with inorganic-organic composition via bipolar electrochemical reduction of 4-nitrobenzenediazonium salt

Procedure	Step	Details
Preparation of bipolar cell	1	Use blowlamps to manually shape the glass Pasteur pipette into a U-shaped glass capillary
	2	Lock the capillary in a vertical position with the helping hand
	3	Put one purified glassy carbon bead into one arm of the capillary until it is stopped by the surrounding capillary wall

Table 2 (Continued)

Procedure	Step	Details
Preparation of glacial 4-nitrobenzenediazonium salt solution	4	Dissolve 0.0122 g of 4-nitrobenzenediazonium tetrafluoroborate in 10 ml of 1 mM HCl cold solution prepared with DI water
	5	Keep the solution cold in an ice bath and keep it away from light.
Fabrication of Janus-type carbon beads with inorganic-organic compositions via bipolar electrochemical reduction of 4-nitrobenzenediazonium salt	6	Fill the capillary (obtained from the 3rd step) with 1 ml of 5 mM 4-nitrobenzenediazonium tetrafluoroborate/1 mM HCl (prepared from the 5th step)
	7	Insert the carbon rods (the feeder electrodes) on the top of each arm of the bipolar cell
	8	Connect the feeder electrodes to a high-voltage power supply without applying the electricity
	9	Apply the voltage of 400 V for 90 s
	10	Stop applying the voltage and transfer carefully the modified carbon bead into an Eppendorf cup.
	11	Rinse the modified bead gently with 0.1 M HCl

The bead with the grafted organic layer on the surface was further coupled with the citrate-reduced AuNPs by soaking it into the colloidal solution overnight. During this step, the mixture was kept away from light to avoid unwanted byproducts (Kimling *et al.*, 2006). Due to the electrostatic interaction between the negatively charged AuNPs that is

due to the citrate stabilizer and the positively charged bead surface originating from the protonated aryl amino groups that are site selectively grafted onto the surface, the AuNPs were attached to the surface of the carbon bead at the grafted fraction. The modified bead was carefully rinsed with 0.1 M HCl solution for several times before the SEM characterization in order to remove the non-specifically attached AuNPs from the bead surface. The bead was then allowed to dry in air. For the SEM characterization, the bead with the gold label was placed directly on a conductive double-sided sticky carbon tape. The SEM analysis was performed with an accelerating voltage of 15 kV.

To investigate the influences of the amplitude of the applied electric field and the deposition time on the grafting of the organic layer, experiments were performed with the same procedure but with various applied electric fields and deposition times.

1.2. Results and discussion

1.2.1. Preparation of citrate-capped AuNPs

The used sodium citrate plays a dual role as a reducing agent and a capping agent that stabilizes AuNPs. The solution of sodium citrate was added to the pale-yellow boiling $HAuCl_4$ solution, leading to an initial loss of color which indicates the complexation and the reduction of $AuCl_4^-$ ions to atomic Au. Within a few seconds, the solution became dark purple, witnessing the formation of metallic Au nuclei due to the collision of the Au atoms. The small crystalline structures will act as seeds for the growth of the final spherical particles presented in the ruby red solution (Frens, 1973). Figure 16 shows the synthesized citrate-capped AuNPs solution with the transparent color of red ruby. Its color reveals the formation of quite homogeneous spherical AuNPs having an average diameter of 10 – 20 nm as described by Turkevich (Turkevich *et al.*, 1951) and Frens (Frens, 1973). This was confirmed by Figure 17a, displaying the well-dispersed spherical AuNPs with an average particle size of 15.08±1.91 nm. A relatively narrow size

distribution of particles between 11 and 20 nm in diameter (Figure 17b) was obtained by analyzing with the ImageJ program.

Figure 16 Photograph showing the red ruby color of the colloidal solution containing the citrate-capped AuNPs.

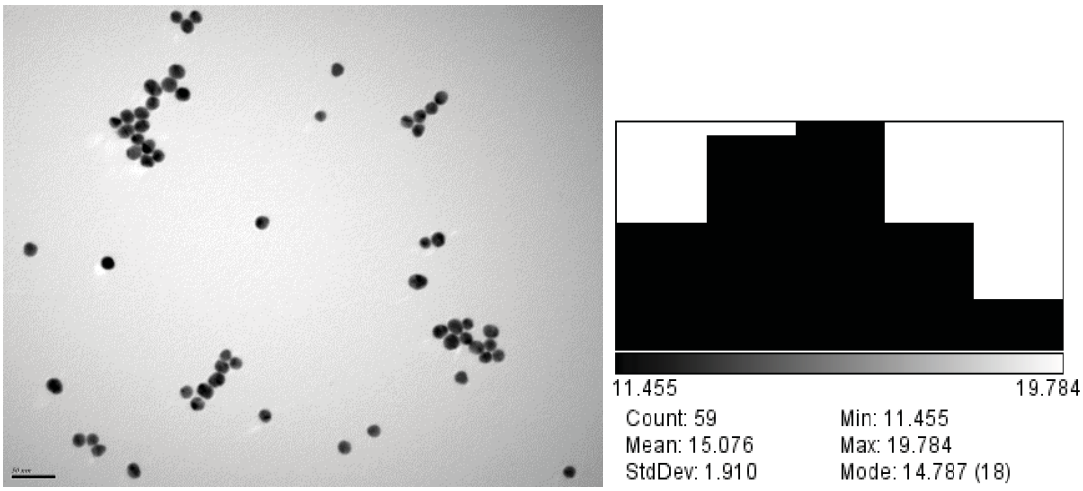

(a) (b)

Figure 17 (a) TEM micrograph and (b) the corresponding particle size distribution histogram obtained by the ImageJ processing program of the citrate-capped AuNPs in the colloidal solution showing a particle size of ~15.08±1.91 nm.

The zeta potential, indicating the particle charge (Hunter, 1981; 1993), was also measured. Briefly, the particles dispersed in a colloidal solution will carry a surface charge that attracts a thin layer of oppositely charged ions to the surface of the particle. While the particle moves through the solution by the applied electric field or the gravity, this electrical double layer moves together with it. The electric potential at the boundary of the double layer is defined as the zeta potential. It is a crucial tool for predicting the stability of the nanoparticles because if the particles have a large positive or negative zeta potential, they will have a strong enough repulsive force to repel each other and will maintain the particles dispersed. In other words, the greater the magnitude of zeta potential, the more stable the colloidal suspension will be.

In this study, the AuNPs have a large negative zeta potential (- 46.2 mV). This value resulted from the citrate ions adsorbing on the AuNPs surface, providing the AuNPs with overall negative charge.

1.2.2. Optimization of experimental conditions and control experiments

The external voltage applied in our bipolar experiment is one of the most important issues that should be considered first. The potential drop in the solution will generate variable overpotentials along the conductive object. We need to consider this point, particularly pH changes which might affect the required potential difference. In order to estimate the potential difference necessary to drive both redox reactions with sufficiently high kinetics, cyclic voltammetry has been used.

A normal electrochemical measurement was performed with a μAutolab type III potentiostat/galvanostat and controlled by GPES software with a three-electrode system. The three-electrode system comprised a carbon rod (graphite) as a counter electrode, a silver-silver chloride (Ag/AgCl) electrode as a reference electrode, and a glassy carbon electrode as a working electrode (Figure 18). This cyclic voltammetry was carried out in

5 mM 4-nitrobenzenediazonium tetrafluoroborate/1 mM HCl/0.1 M NaCl aqueous solution at a scan rate of 100 mV/s.

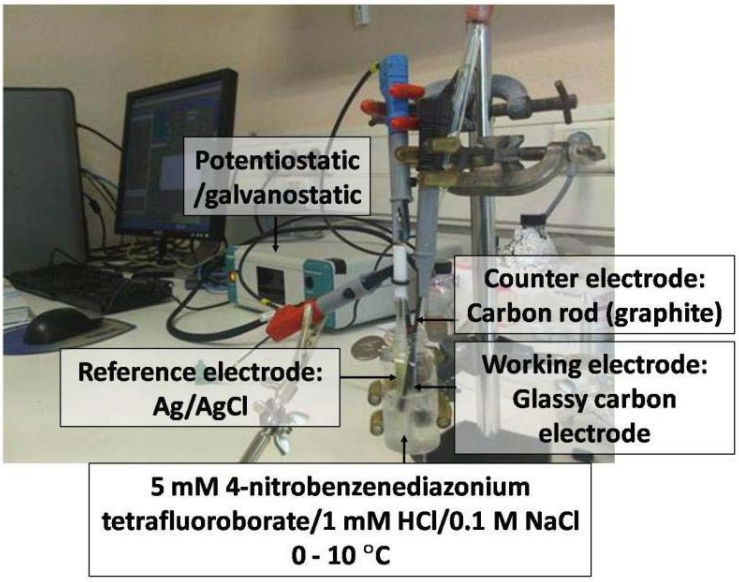

Figure 18 Photograph of the cyclic voltammetry set-up for determining the voltage to be applied to the bipolar cell for the bipolar electrografting of 4-aminobenzene onto carbon bead.

Figure 19 shows the first three cyclic voltammograms recorded during this experiment. The first scan (solid line) in a reductive direction shows a single, broad, reduction wave with a peak potential of approximately 0.23 V vs Ag/AgCl that corresponds to the reduction of aryl diazonium cations to radicals, which then react with and bind covalently to the glassy carbon surface (Andrieux and Pinson, 2003). This reduction wave disappeared during the following cycles, second (dashed line) and third (dotted line) scans, due to the blocking of the glassy carbon electrode by the organic layer generated on it. The modification of organic layers on the surface during the voltammogram recording results in a broadening of the wave.

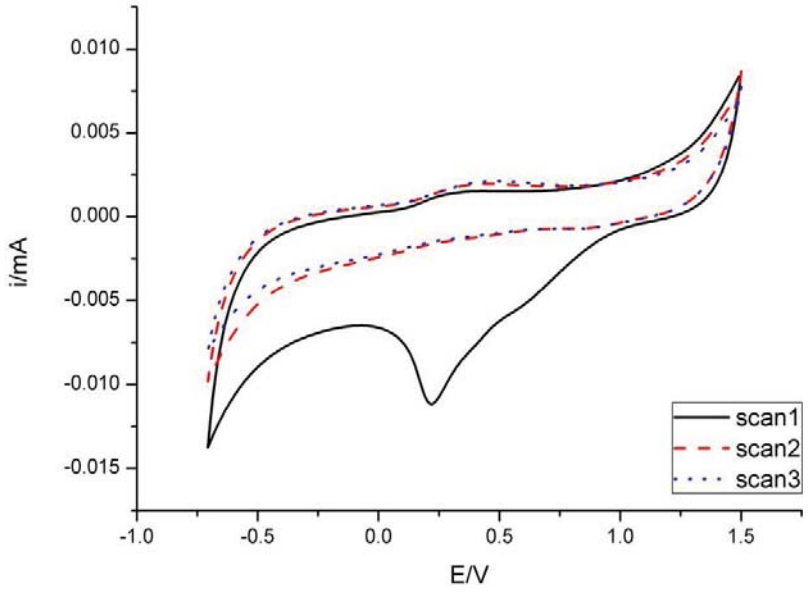

Figure 19 Cyclic voltammograms (solid line: first scan; dashed line: second scan; dot line: third scan) for 5 mM 4-nitrobenzenediazonium tetrafluoroborate/1 mM HCl in 0.1 M NaCl solution on a glassy carbon working electrode at a scan rate of 100 mV/s.

The potential used to drive the water oxidation reaction, $2H_2O \rightarrow O_2 + 4H^+ + 4e^-$; $E^\circ = 1.23$ V vs SHE, will also depend on the pH value of the solution. In this experiment, we used pH 3 obtained with a 1 mM HCl solution. From the relation between the potential at equilibrium (E_{eq}) and the pH value, E_{eq} (O_2/H_2O) = $E^\circ(O_2/H_2O)$ + $0.059\log[H^+]$, a potential of 1.05 V vs NHE (1.23 - (0.059)(3)) should be used for the water oxidation. However, due to the overpotential for water oxidation on a glassy carbon electrode, we observed in Figure 19 that a potential of 1.50 V is required to start this oxidation.

Therefore, in order to have a sufficient driving force for the two redox reactions, a polarization of the glassy carbon of at least 1.27 V (1.50 V - 0.23 V) is required. This

agrees with the potential calculated from the difference between the two standard reduction potentials (in the introduction part).

As mentioned before, in order to drive the desired redox reactions (the reduction of diazonium salt and the water oxidation) at two sides of a carbon bead with a diameter of ~800 μm placed between two feeder electrodes at a distance of ~10 cm, a voltage of more than 300 V is required in order to observe distinctly the grafted organic layer at one end of the bead. For this reason, we decided to apply a voltage of 400 V to the system in order to make sure to meet the reaction criteria.

In the beginning, two commercial gold coated slides (purchased from ACM) were used as the feeder electrodes. However, we found that these gold plates were not suitable to be used as feeder electrodes during the bipolar electrografting experiments. This is because the applied high potential induced a strong oxidation reaction that can destroy the deposited gold layer. The high potential of 400 V not only leads to the bipolar electrochemical reduction of diazonium salt at the carbon bead but also to many redox reactions at the feeder electrodes themselves, especially when the feeder electrodes are immersed in the same reservoir as the BPE. For example, the oxidation of the anchoring layer of the gold coated glass slides (chromium, Cr and Nickel, Ni), occurs at the anodic side of the feeder electrodes (Bard *et al.*, 1985).

$$Cr^{3+}\ (aq.) + 3\ e^- \text{ -----> } Cr\ (s),\ E^o = -\ 0.74.\ V/NHE$$
$$Ni^{2+}\ (aq.) + 2\ e^- \text{ -----> } Ni\ (s),\ E^o = -\ 0.25.\ V/NHE$$

, where E^o stands for the standard reduction potential. In addition, under very high electric field, it is possible to further trigger the oxidation of the gold layer itself (Bard *et al.*, 1985).

$$Au^{3+}\ (aq.) + 3\ e^- \text{ -----> } Au\ (s),\ E^o = 1.52\ V/NHE$$

$$Au^{+}\ (aq.) + e^{-} \text{ -----> } Au\ (s),\ E^{o} = 1.83\ V/NHE$$

These oxidation reactions result in the destruction of the electrode as shown in Figure 20. Simultaneously, the proton reduction occurs at the cathodic feeder electrode (Bard *et al.*, 1985), together with the reduction of the diazonium salt and of the gold ions dissolved from the anodic gold plate.

$$2\ H^{+}\ (aq.) + 2\ e^{-} \text{ -----> } H_2\ (g),\ E^{o} = 0.00\ V/\ SHE$$

Therefore metallic gold might also deposit on the bipolar electrode and it would be hard to distinguish this deposit from the citrate-capped AuNPs used for labeling the organic layer on the bead. As a consequence the gold plates are not suitable as feeder electrodes in this experimental set-up.

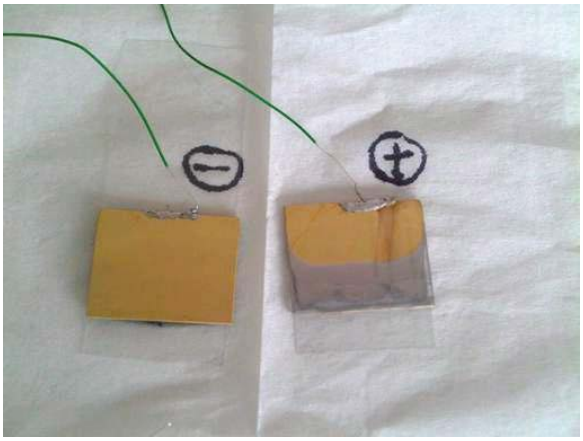

Figure 20 Photographs showing the corrosion of the gold plates used as feeder electrodes (left: (-) cathode, right: (+) anode).

For this reason, we used graphite rods as feeder electrodes. Next, we consider other redox reactions occurring in our system. Concerning water oxidation at the BPE, oxygen gas (O_2) is produced (coupled with the reduction of diazonium salt which can

generate N_2 gas). If this water oxidation occurs very slowly, O_2 can gradually dissolve in the solution. However, if the oxidation occurs rapidly, oxygen bubbles will be produced which might induce a rotation or a displacement of the bead thus disturbing the grafting process. Furthermore, in the extreme case when water oxidation occurs very rapidly, big bubbles can interrupt the current flow in the system and stop the electrochemical reactions in the cell.

In order to avoid or at least slow down the rotation or the movement of the bead , Loget and co-workers added gelling agents such as agarose into the solution of the reaction compartment to increase the viscosity of the medium (Loget *et al.*, 2012). Nevertheless, this strategy requires heating of the polymer in the solution (here containing also the diazonium salts). This thermal process can cause an undesired spontaneous reduction of diazonium salts and results in an unspecific grafting instead of the site-selective grafting. As a consequence, the citrate-capped AuNPs can couple with the carbon bead due to both spontaneous reduction and bipolar electrochemical reduction of diazonium salts as shown in Figure 21a. Even though there was no electric field applied to the system gold labeling was found on the carbon bead as shown in Figure 21b due to the grafted organic layer generated from the spontaneous reduction of diazonium salts.

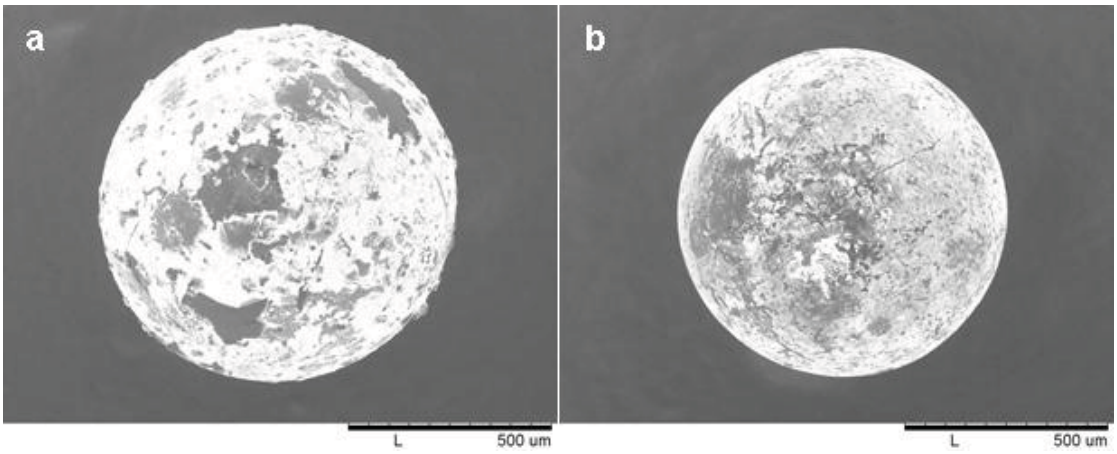

Figure 21 SEM images of the 4-aminobenzene-modified glassy carbon bead generated (a) by applying an electric field of 4 kVm^{-1} and (b) without applying an electric field in solidified agarose containing 5 mM 4-nitrobenzenediazonium tetrafluoroborate/1 mM HCl solution. To label the surface grafted organic molecules, the beads were immersed into a colloidal gold solution containing the citrate-capped AuNPs. Scale bar is 500 μm.

As a consequence, a closed bipolar electrochemical cell configuration was used in order to mechanically stabilize the position of the bead. The inner diameter of the capillary used in this study was adapted to fit the diameter of the carbon bead in order to avoid its rotation or movement during the grafting experiment. Before the grafting process, the bead was introduced into a capillary. Due to the approximately same diameter of the carbon bead and the capillary, the bead was physically blocked in the capillary. With this configuration, the reorientation and movement due to the macroscopic bubbles originating from the water oxidation at the BPE can be avoided.

In order to confirm the grafting of 4-aminobenzene moieties onto the bead via bipolar electrochemical reduction of 4-nitrobenzenediazonium salt, control experiments were performed prior to the bipolar experiments. A SEM image of raw glassy carbon

beads purified with ethanol is shown in Figure 22. The image shows that the surface of commercial glassy carbon beads is typically not smooth even if the beads are already purified.

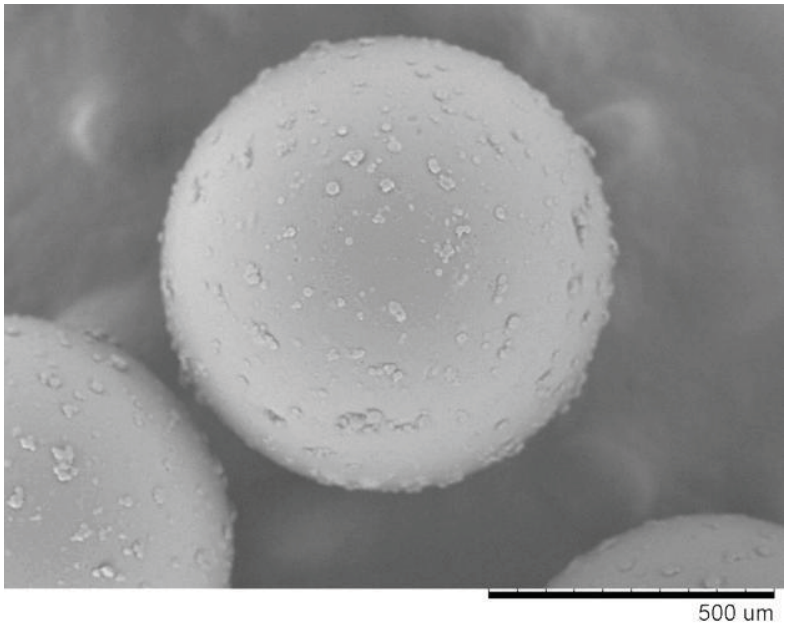

Figure 22 SEM image of raw carbon beads purified by ethanol. Scale bar is 500 μm.

In the second control experiment, a glassy carbon bead purified with ethanol was soaked in 5 mM 4-nitrobenzenediazonium tetrafluoroborate/1 mM HCl solution for 90 s. This period of time is similar to that used in the bipolar experiment. The resulting bead was then rinsed with 0.1 M HCl solution and further observed by SEM, not shown here because it is similar to that of the untreated one. This indicates that the treatment employed in this case did not lead to a grafting of the carbon surface by the organic layer.

Subsequently, another control experiment was performed by soaking a glassy carbon bead purified with ethanol into 5 mM 4-nitrobenzenediazonium tetrafluoroborate/1 mM HCl solution for 90 s. Then, the bead was isolated from the

solution and rinsed with 0.1 M HCl solution. Afterwards, it was immersed into the colloidal solution of AuNPs overnight. After this treatment it shows no gold labeling. The result confirms that when the electric field is not applied to the system, the grafting of the organic layer cannot occur spontaneously.

In order to validate the interaction between a raw glassy carbon bead and the citrate-capped AuNPs, a purified bead was soaked in the colloidal solution of the citrate-capped AuNPs overnight. After that, the bead was taken out from the solution and rinsed with 0.1 M HCl solution. The SEM results (not shown here) is similar to that of the previous control experiment, which shows no gold labeling on the carbon bead. The result indicates that the citrate-capped AuNPs can not directly attach to the raw bead surface.

The last control experiment was performed by using the same procedure as for the bipolar experiment but without exposing the modified bead to the citrate-capped AuNPs. The SEM observation (not shown here) reveals that without the citrate-capped AuNPs, the grafted area cannot be visualized. Thus, the step of the AuNP attachment is an important step for visualization of the grafted area by SEM.

1.2.3. Fabrication of Janus-type beads via bipolar electrochemical reduction of 4-nitrobenzenediazonium salt

The SEM image of a glassy carbon bead treated by applying an electric field of 400 V between the two feeder electrodes (with the distance of ~ 10 cm between them) for 90 s in 5 mM 4-nitrobenzenediazonium tetrafluoroborate/1 mM HCl after the purification by ethanol is shown in Figure 23. The bead was immersed in a colloidal AuNP solution overnight and then rinsed with 0.1 M HCl solution before the observation. The image indicates the presence of the gold label at one side of the modified glassy carbon bead.

The position of the gold labeling proves the successful bipolar electrochemical reduction of 4-nitrobenzenediazonium salts.

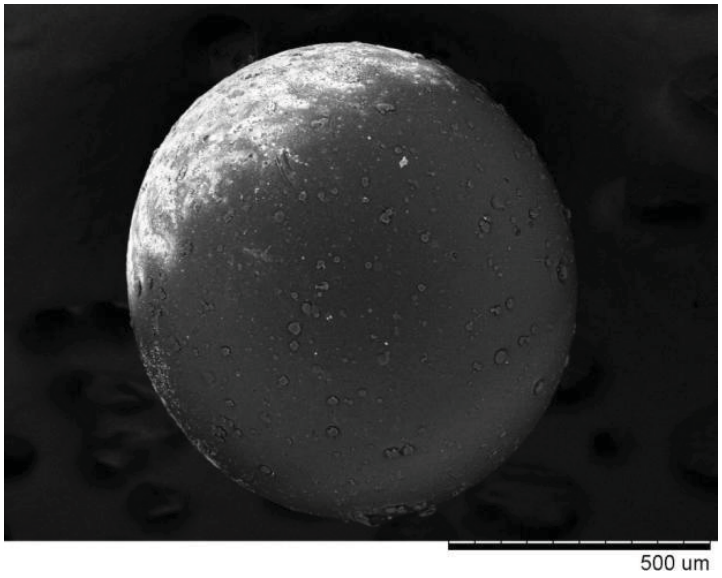

Figure 23 SEM image of a glassy carbon bead treated by applying a voltage of 400 V between two feeder electrodes for 90 s in 5 mM 4-nitrobenzenediazonium tetrafluoroborate/1 mM HCl after the purification by ethanol. The distance between the feeder electrodes was ~ 10 cm. The bead was immersed in a colloidal AuNP solution overnight and then rinsed with 0.1 M HCl solution before the observation. Scale bar is 500 μm.

Additional experiments were performed by applying various electric fields for various periods of time namely 1) an electric field of 4 kVm^{-1} for 66 s, 2) an electric field of 4.3 kVm^{-1} for 80 s and 3) an electric field of 6.7 kVm^{-1} for 40 s. The variability of the grafting obtained under these conditions and the previous conditions (an electric field of 4 kVm^{-1} for 90 s) are shown by the SEM images in Figure 24. The images indicate that the gold labeled area can be extended by increasing the deposition time and/or the

potential used for the reduction of the diazonium salts. Janus-type beads with hybrid organic–inorganic composition were obtained in all cases.

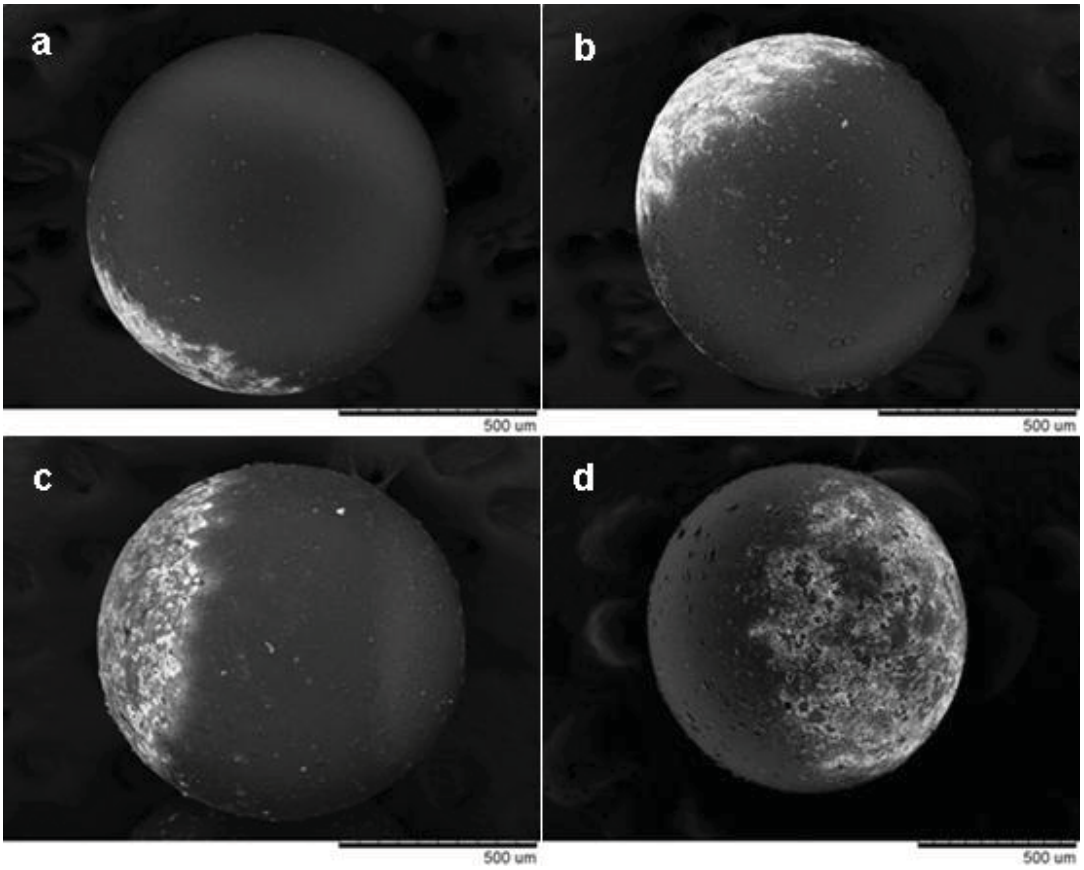

Figure 24 SEM images of glassy carbon beads treated by applying various electric fields for various periods of time namely (a) an electric field of 4 kVm^{-1} for 66 s, (b) an electric field of 4 kVm^{-1} for 90 s, (c) an electric field of 4.3 kVm^{-1} for 80 s, and (d) an electric field of 6.7 kVm^{-1} for 40 s in 5 mM 4-nitrobenzenediazonium tetrafluoroborate/1 mM HCl after the purification by ethanol. Before the observation, the beads were immersed in a colloidal AuNP solution overnight and then rinsed with 0.1 M HCl solution. Scale bar is 500 μm.

2. Modification of a glassy carbon bead by bipolar electrochemical reduction of *in situ* generated 4-carboxyphenyl diazonium salts

In order to demonstrate the general validity of this grafting concept, an asymmetrical grafting of an organic layer with different functional groups of carboxylic acid on the carbon surface was performed. The carboxylic acid groups are used for the grafting of carbon surfaces because they can be coupled with bio-molecules such as glucose oxidase (GO_x) (Bourdillon *et al.*, 1992; Pellissier *et al.*, 2008a; Pellissier *et al.*, 2008b) and horseradish peroxidase (HRP) (Radi *et al.*, 2008) via carbodiimide chemistry, opening up many applications in the fields of bio-sensing applications and enzymatic bio-fuel cells.

The strategy proposed for asymmetrical grafting the carbon bead with the carboxylic acid substituted aryl groups is shown in Figure 25. In the first step, 4-Carboxyphenyl (4-CP) diazonium salt ($^{+}N_2$-C_6H_4-COOH) is generated *in situ* by a standard diazotization reaction (Bourdillon *et al.*, 1992) using $NaNO_2$ and 4-aminobenzoic acid as reactants in a HCl solution (Baranton and Bélanger, 2005). The resulting molecule is immediately used for the asymmetric grafting of carboxylic acid substituted aryl groups on the surface of glassy carbon beads. The bipolar electrochemical grafting of 4-carboxy phenyl moieties occurred via one-electron reduction of 4-CP diazonium salts. This reaction results in the loss of a N_2 molecule and the covalent attachment of the 4-carboxy phenyl moieties to the cathodic side of the carbon bead.

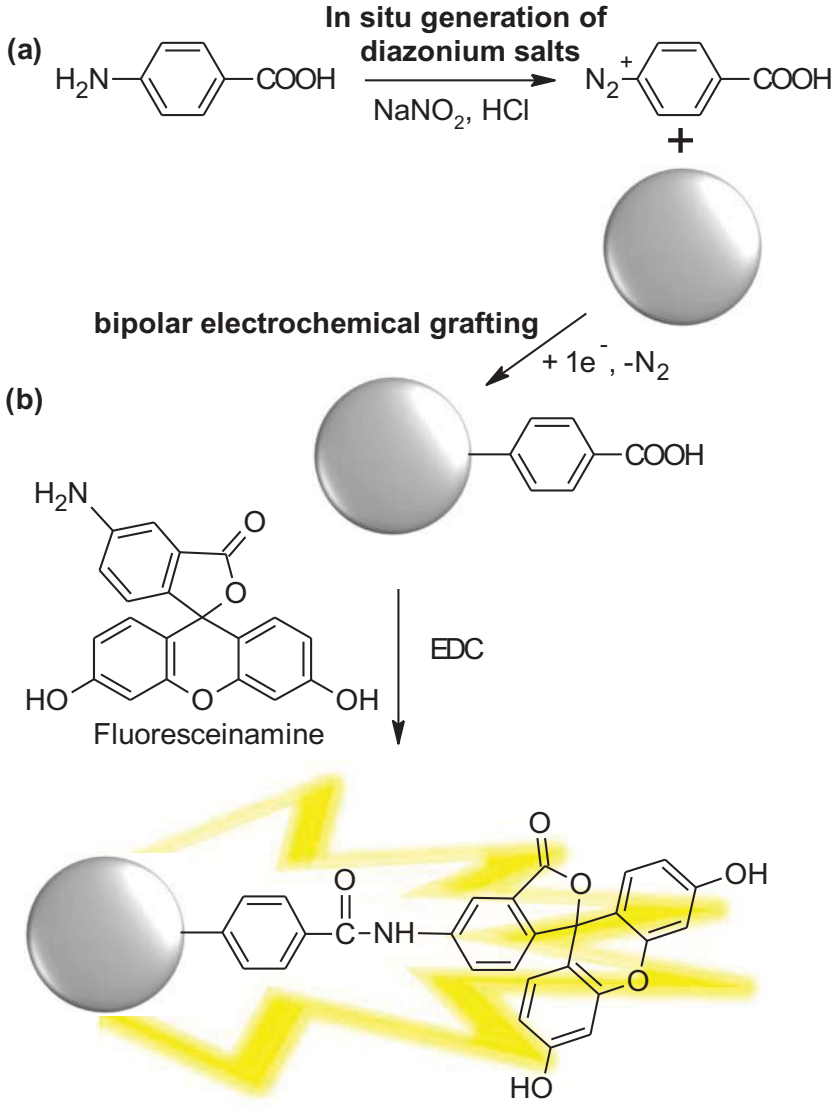

Figure 25 Scheme illustrating the strategy employed for site-selective modification of a glassy carbon bead by the carboxylic acid substituted aryl groups through (a) bipolar electrochemical reduction of *in situ* generated 4-carboxyphenyl (4-CP) diazonium in an aqueous $NaNO_2$/HCl solution and (b) followed by the coupling of the carboxylic acid groups of 4-CP presented on the bead surface to the functional amino groups of fluoresceinamine by using 1-ethyl-3-(3-dimethylaminopropyl) carbodiimide (EDC) as a coupling agent.

For the grafting of the carboxyphenyl groups on the bead surface, a voltage of at least 1.4 V (calculated from the equation: $\Delta V_{min} = E_2 - E_3$) has to be presented across the bead in order to trigger the coupled redox reactions (the electrochemical reduction of 4-CP with the reduction potential (E_3) of 0.2 V vs Ag/AgCl (Baranton and Bélanger, 2005) and the water oxidation with a formal potential (E_2) of 1.2 V vs Ag/AgCl). This means that for a glassy carbon bead with diameter of about 800 μm, an electric field of at least 1750 Vm^{-1} (calculated from $E = \Delta V/d$ = 1.4 V/ 800 μm) is required for the bipolar experiments. In order to be sure to observe site-selective grafting of the 4-carboxyphenyl moieties on the bead, an electric field of 4 kVm^{-1} was selected.

In order to observe the organic layer of 4-CP bound to the bead surface, a fluorescent labeling precursor allowing the observation by fluorescence microscopy, namely fluoresceinamine, is used. 1-Ethyl-3-(3-dimethylaminopropyl)carbodiimide (EDC), a water soluble carbodiimide, is used as a carboxyl activating agent for the coupling of the carboxylic acid groups of the 4-carboxy phenyl moieties presented on the bead surface to the primary amine groups of fluoresceinamine.

For the first step of the generation of 4-CP, the mechanism is according to the one reported in the literature (Clayden *et al.*, 2012). The proposed mechanism is shown as Figure 26. Nitrite ($NaNO_2$) reacts with acid producing a nitrosonium ion (Figure 26a). This nitrosonium ion then reacts with the amino group of 4-aminobenzoic acid producing the diazo group (Figure 26b).

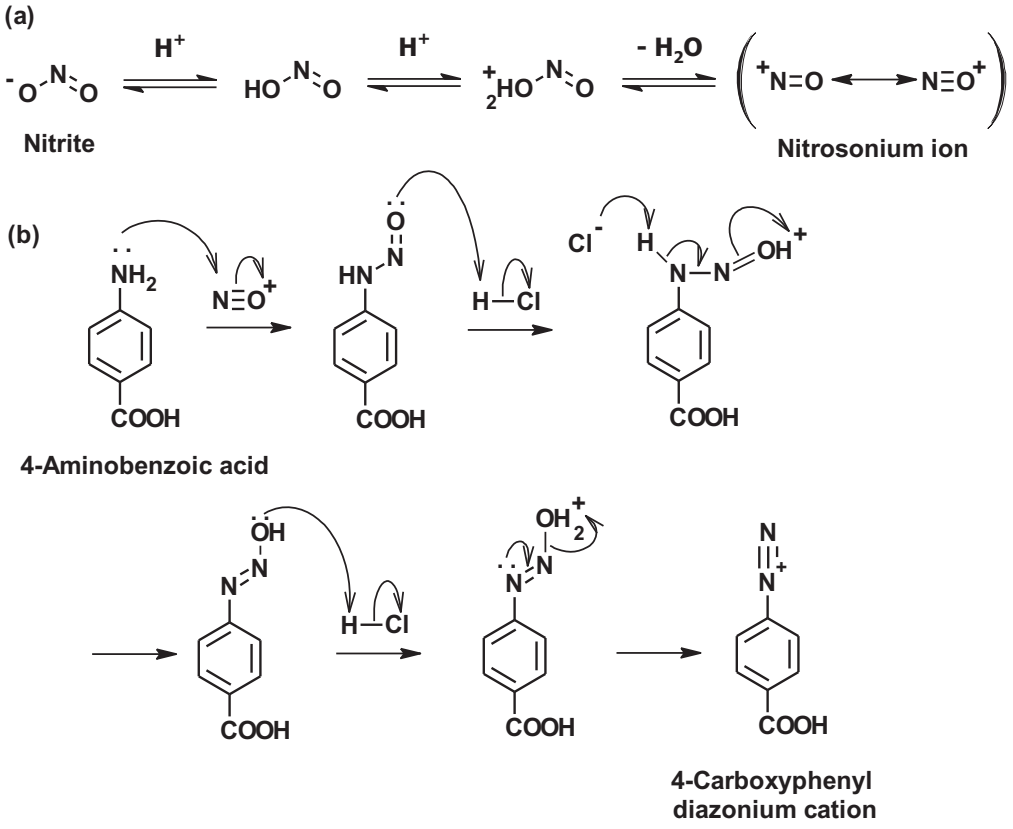

Figure 26 Reaction mechanism for the generation of 4-CP diazonium salt. (a) Generation of nitrosonium ion from the reaction between nitrite and acid. (b) Reaction of the nitrosonium ion and 4-aminobenzoic acid producing 4-CP.

2.1. Materials and Methods

2.1.1. Materials

Most of the ingredients and the equipments used in this section are similar to as described in the previous section (1.1.1. Materials). However, the preparation of diazonium salts and the visualization of modified organic layers are slightly adopt as follows:

Major Chemicals

- 4- Aminobenzoic acid (≥99%, $H_2NC_6H_4CO_2H$, Sigma-Aldrich)
- Sodium nitrite (≥97%, $NaNO_2$, ACROS ORGANICS)
- *N*-(3-dimethylaminopropyl)-*N′*-ethylcarbodiimide hydrochloride or 1-ethyl-3-(3-dimethylaminopropyl) carbodiimide (EDC) (≥98.0%, $C_8H_{17}N_3$.HCl, Sigma-Aldrich)
- Fluoresceinamine isomer I ($C_{20}H_{13}NO_5$, Sigma-Aldrich)
- *N,N*-Dimethylformamide or DMF (99.9%, $HCON(CH_3)_2$, Scharlau)

Major Equipment

- Epi-fluorescent microscope (DMI 6000B, Leica) equipped with a digital camera (DFC310 FX, Leica)

2.1.2. Methods

2.1.2.1. Purification of glassy carbon bead and carbon graphite

Similar to the previous bipolar experiments for grafting of the organic layer containing the functional amino groups, prior to the experiments, the commercial glassy carbon beads and carbon rods were purified with ethanol.

2.1.2.2. Synthesis of Janus-type beads by using bipolar electrografting of *in situ* generated 4-carboxyphenyl diazonium in an aqueous $NaNO_2$/HCl solution

Details of the experimental procedures used for the modification of glassy carbon beads with 4-CP are shown in Table 3. Briefly, a purified glassy carbon beads was introduced in a bipolar cell with the same set-up used for the previous section (see Figure

15) containing 4-CP diazonium salts in a glacial aqueous HCl solution. The feeder electrodes were connected to a high-voltage power supply. The electric field of 4 $kV.m^{-1}$ was applied to the cell for a certain period of time. After the grafting process, the modified carbon bead was taken out from the cell and rinsed by 0.1 M HCl solution for several times in order to remove salt residues.

Table 3 Details of experimental procedures for the fabrication of Janus-type carbon beads with inorganic-organic composition via bipolar electrochemical reduction of *in situ* generated 4-CP diazonium salt in an aqueous $NaNO_2$/HCl solution

Procedure	Step	Details
Preparation of glacial 5 mM 4-aminobenzoic acid/10 mM $NaNO_2$/ 10 mM HCl solution	1	Dissolve 0.69 g of $NaNO_2$ in 10 ml of cold DI water (solution A)
	2	Dissolve 0.007 g of 4-aminobenzoic acid in 10 ml of cold 10 mM aqueous HCl solution (solution B)
	3	Add 100 µl of solution A into the solution B
	4	Mix the mixture well
	5	Keep the mixture in a cold and dark place
Fabrication of Janus-type carbon beads with inorganic-organic compositions via bipolar electrochemical reduction of *in situ* generated 4-CP diazonium salt in an aqueous $NaNO_2$/HCl solution	6	Put a purified glassy carbon bead into one arm of the U-shaped glass capillary (see Figure 15)
	7	Fill the capillary with1 ml of glacial 5 mM 4-aminobenzoic acid/10 mM $NaNO_2$/ 10 mM HCl solution into the capillary (obtained from 5^{th} experimental step).
	8	Connect the feeder electrodes to a power supply

Table 3 (Continued)

Procedure	Step	Details
Fabrication of Janus-type carbon beads with inorganic-organic compositions via bipolar electrochemical reduction of *in situ* generated 4-CP diazonium salt in an aqueous $NaNO_2$/HCl solution	9	Apply an electric field of 4 $kV.m^{-1}$ for 120 s
	10	Stop applying the electric field and transfer the modified bead into an Eppendorf cup.
	11	Rinse that modified bead twice with DI water

2.1.2.3. Coupling the 4-carboxyphenyl (4-CP)-modified glassy carbon bead with a fluorescent labeling precursor

To observe the modification of the carbon bead by 4-CP, after rinsing the modified glassy carbon bead with DI water, the bead was immersed into 200 µl of 5 mM aqueous EDC solution for 10 min. Subsequently, 200 µL of 4 mM ethanolic fluoresceinamine solution was added to the system. The reaction was left under stirring at room temperature for 2 h. After 2 h, the solvent was removed. The resulting glassy carbon bead was then rinsed several times with DI water and DMF. Finally, the bead was allowed to dry in air at room temperature. The modification of the bead was then confirmed under a fluorescent microscope. For the observation, the bead was placed on a glass slide. One drop of oil (Leica, Immersion liquid, Type F) was thus added on the modified bead and left for 10 min. The characterization was then performed by an epi-fluorescent microscope with a mercury lamp as a light source. A filter cube I3, an excitation filter in the range of 450-490 nm, and an emission filter of 515 nm were used for the fluorescence mode. The microscope was equipped with a digital camera (Leica DFC310 FX) as shown in Figure 27.

Figure 27 Photograph of the epi-fluorescent microscope (DMI 6000B, Leica) equipped with a digital camera (DFC310 FX, Leica) used for the direct visualization of the grafted fluorescent molecule coupled with one side of the 4-CP-modified glassy carbon bead.

2.1.2.4. Control experiment

In order to confirm the grafting of the organic layer onto the bead, a control experiment was performed. The experiment was performed with the same procedure used for the bipolar experiments but without the bipolar cell and no electric field.

2.2. Results and discussion

In the same way as in the case of the bipolar electrografting of 4-aminobenzene, we first determined by the cyclic voltammetry the applied voltage needed to drive the involved redox reactions. We used the conditions and the experimental set-up (Figure 18) of the previous case but three electrodes were immersed in 0.1 M NaCl solution,

containing a 5 mM 4-aminobenzoic acid/10 mM $NaNO_2$/ 10 mM HCl solution instead of 5 mM 4-nitrobenzenediazonium tetrafluoroborate/1 mM HCl/0.1 M NaCl aqueous solution.

Figure 28 demonstrates three consecutive cyclic voltammograms from 0.5 to - 1.0 V vs Ag/AgCl for the 4-CP modification of the glassy carbon electrode in aqueous acidic medium containing *in situ* generated diazonium cations (5 mM 4-aminobenzoic acid/10 mM $NaNO_2$/ 10 mM HCl/0.1 M NaCl solution). In the reduction sweep, the first scan presents the reduction of the 4-aminobenzoic acid moiety, which starts at around 0.25 V and reaches a maximum at - 0.25 V. This irreversible reduction peak disappears during the following scans (dashed and dotted line) indicating the presence of a grafted organic layer. The process relates to the conversion of aryl amines to aryl diazonium salts by the treatment with HCl and nitrite. Then, the aryl group is attached covalently to the electrode surface by electrochemical reduction and N_2 is released.

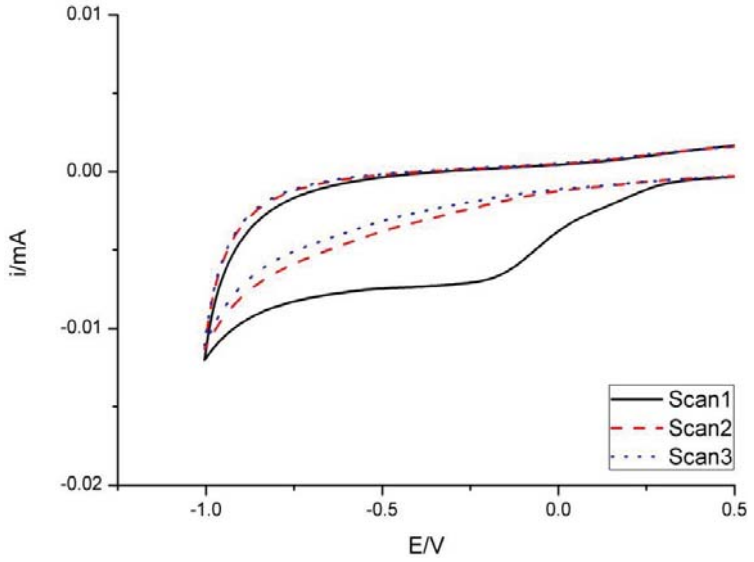

Figure 28 Cyclic voltammograms (solid line: first scan; dashed line: second scan; dot line: third scan) for a 5 mM 4-aminobenzoic acid/10 mM $NaNO_2$/ 10 mM HCl solution in 0.1 M NaCl solution on a glassy carbon working electrode at a scan rate of 100 mV/s.

As mentioned above, the potential required to drive the water oxidation reaction will depend on the pH value of the solution. For this experiment, pH 2.5 was measured for a 10 mM HCl solution. From the relation between the potential at equilibrium (E_{eq}) and the pH value, E_{eq} (O_2/H_2O) = E°(O_2/H_2O) + 0.059log[H^+], a potential of 1.08 V vs NHE, or 0.87 V vs Ag/AgCl should be used for the water oxidation. But as indicated by Figure 19 the overpotential for the water oxidation on a glassy carbon electrode allows the reaction to occur only around 1.50 V. In order to have a sufficient driving force for two redox reactions, a polarization of the glassy carbon of at least 1.75 V (1.50 V - (-0.25 V)) should be applied. This corresponds to the potential calculated from the difference between the two standard reduction potentials (1.4 V, in the introduction part). To drive the desired redox reactions (the reduction of diazonium salt and the water oxidation) over a carbon bead with diameter of ~800 μm placed between two feeder electrodes at a distance between each other of ~10 cm, a voltage of at least 219 V is

needed to be applied to the system. However, in order to make sure to observe the grafted organic layer at one end of the bead, we decided to apply 400V (4 kVm^{-1}).

Figure 29 shows the fluorescent micrograph of the carbon bead obtained from the control experiment where the experiment was performed with the same procedure used for the bipolar experiments but without the use of the bipolar cell and the application of any electric field to the system. The image indicates that no fluorescence can be observed. The result indicates that without the electrochemical reduction of 4-CP diazonium salts the 4-carboxy phenyl moieties cannot attach to the surface of the carbon bead. Therefore, the coupling with the fluorescent labeling precursor providing the observation by fluorescent microscopy cannot occur.

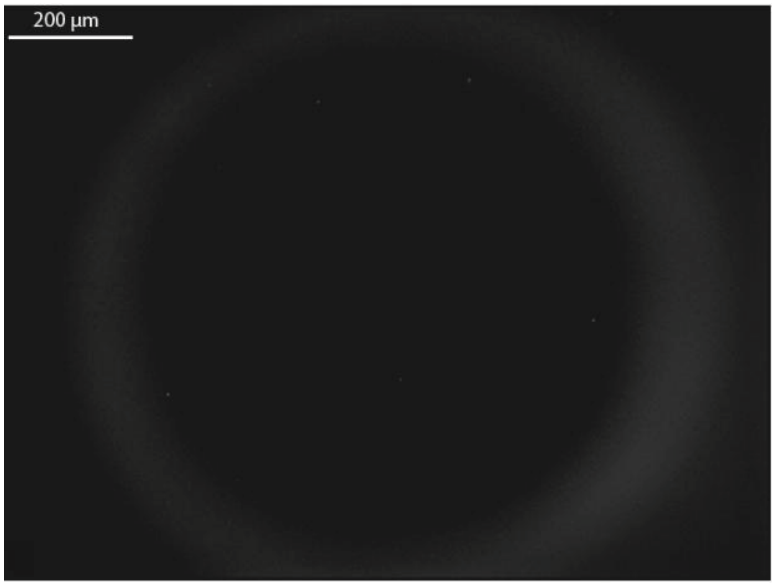

Figure 29 Fluorescent micrograph of a carbon bead obtained from the control experiment where the experiment was performed with the same procedure used for the bipolar experiments but without the use of the bipolar cell and the application of any electric fields to the system. Scale bar is 200 µm.

Figure 30 shows the fluorescent micrograph of a carbon bead obtained from the bipolar experiment. The fluorescence was selectively observed at one side of the glassy carbon bead confirming the formation of an amide bond between amine and carboxylic acid functional groups of the fluoresceinamine and the 4-carboxypheynyl moieties, respectively. Some spots appear darker and others brighter. We suggest that this is because the commercial glassy carbon beads have a rough surface, and the organic layer cannot be uniformly deposited because of this roughness.

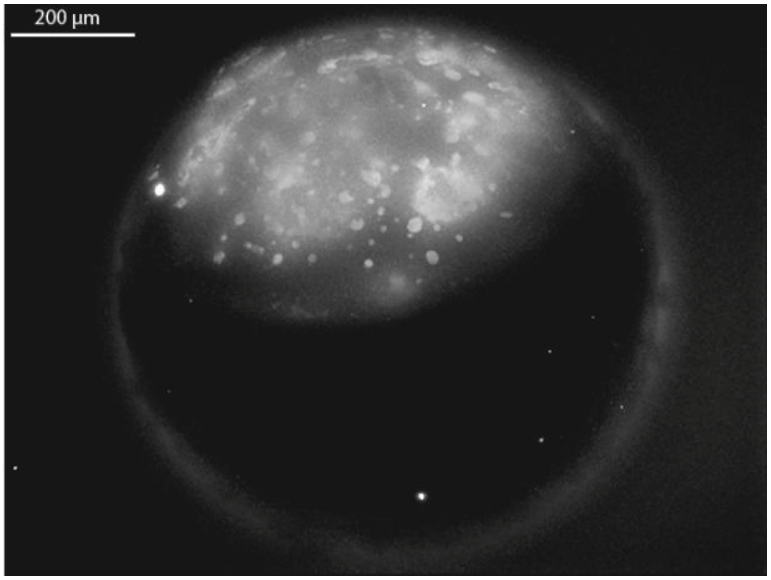

Figure 30 Fluorescent micrograph of a glassy carbon bead obtained from a bipolar experiment with the application of a 4 kVm^{-1} electric field for 120 s to an aqueous solution of 5 mM 4-aminobenzoic acid/10 mM $NaNO_2$/10 mM HCl. Before the observation, the bead was subsequently reacted with EDC and fluoresceinamine. Scale bar is 200 µm.

Figure 31 shows the fluorescent micrographs of the carbon beads obtained from additional bipolar experiments. The images reveal Janus-type beads with fluorescence on

one-half side in every experiment. This indicates that the results of the bipolar experiments can be obtained in a reproducible way.

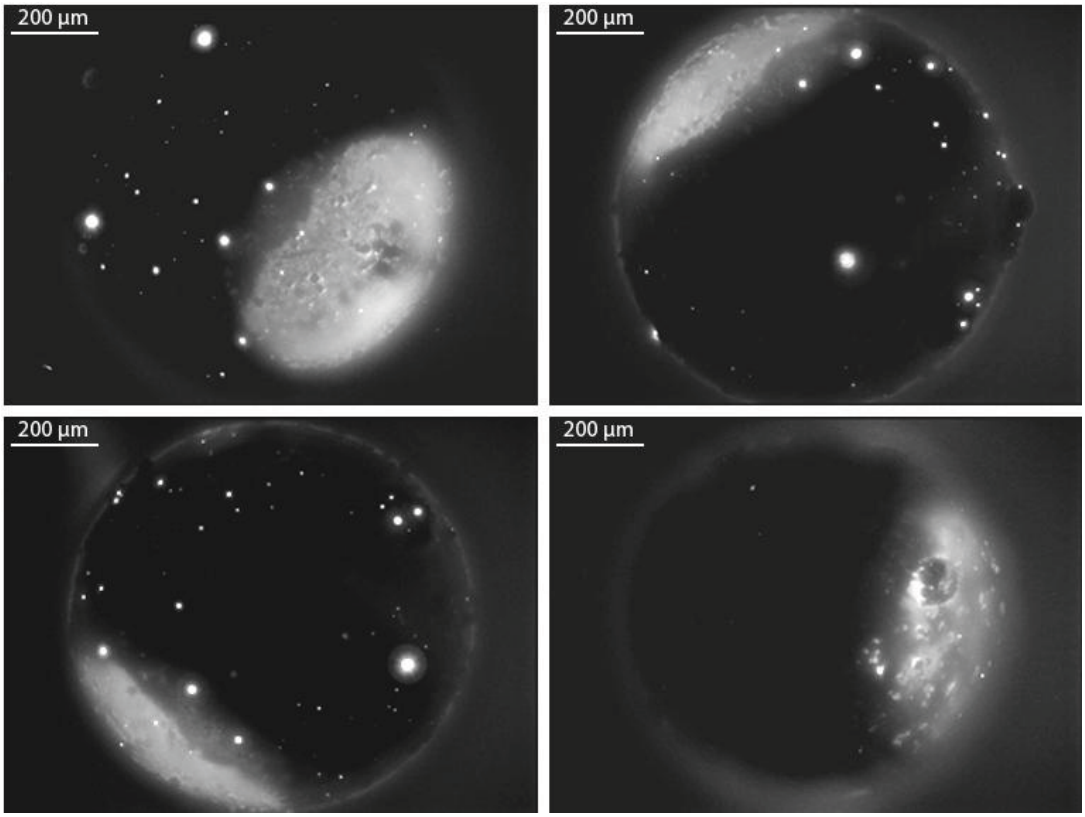

Figure 31 Fluorescent micrographs showing the possibility to obtain Janus-type beads in every experiment when modifying the glassy carbon bead by the application of a 4 kVm^{-1} electric field for 120 s to an aqueous solution of 5 mM 4-aminobenzoic acid/10 mM $NaNO_2$/10 mM HCl and subsequent interaction with EDC and fluoresceinamine. Scale bar is 200 µm.

3. Conclusions

In summary, the micrometer-sized glassy carbon beads (~630-1000 μm in diameter) were used as carbon substrates in the first proof-of-principle bipolar experiments for producing Janus-type objects with hybrid organic-inorganic composition. The bipolar electrochemical asymmetric covalent grafting of amino-terminated and carboxylic acid substituted aryl moieties was performed via the reduction of diazonium salt precursors coupled with the water oxidation. The one-electron reduction of the diazonium salt occurred in the vicinity of the surface of the carbon bead and leads to the loss of dinitrogen from the precursor molecules. As a result, the aryl radical species with functional groups form a covalent bond at the cathodic side of the glassy carbon. Depending on the redox couples, an electric field was applied to the home-built bipolar cell containing the substrate or bipolar electrode, the precursors, and electrolyte solution for a certain time period. The bead was confined in the capillary in order to limit its motion during the experiment. This configuration allows that almost all the current goes directly through the bead without any physical contact to feeder electrodes. In the first case, a diazonium salt, namely 4-nitrobenzenediazonium tetrafluoroborate, was used as a reagent. The bipolar electrografting of 4-aminobenzene moieties on glassy carbon bead was obtained. The amino groups functionalized on the bead surface were then positively charged under acidic conditions. Then, they can be coupled with negatively-charged gold nanoparticles produced by a simple reduction of gold ions in the presence of citrate stabilizer. This leads to an indirect visualization of the organic layer presented on the bead surface. In the latter case, 4-carboxyphenyl diazonium salt was generated *in situ* via the diazotization reaction between 4-aminobenzoic acid and sodium nitrite under acidic conditions. Consequently, this salt was immediately used for the bipolar electrografting of 4-carboxyphenyl moieties on the bead. The subsequent coupling between the carboxylic acid groups and the functional amino groups of fluoresceinamine by using 1-ethyl-3-(3-dimethylaminopropyl) carbodiimide (EDC) as a coupling agent allows the visualization of the grafted layer under a fluorescent microscope. The results show that

both types of organic layers can be successfully grafted on one half of the bead selectively and the modified area can be simply tuned by varying the applied electric field and/or the deposition time. The finding demonstrates that bipolar electrochemistry is a very attractive method for the production of such asymmetric objects bearing organic functionalities. The asymmetric grafting of aryl diazonium compounds with various substituents can be easily imagined, thus allowing the generation of platforms for the linking of other molecules. These open promising possibilities for using Janus-type beads with hybrid organic-inorganic composition as model objects in the field of biochemical sensing devices or micromotors. As the approach allows by definition objects to be electromodified without physical contact to electrodes, it constitutes an important enrichment of the chemical methods used in micro and nanoscience.

Chapter III: ASYMMETRICALLY ELECTROCHEMICAL MODIFICATION OF VERTICALLY ALIGNED CARBON NANOTUBES BY ORGANIC LAYERS VIA A BIPOLAR ELECTROCHEMICAL APPROACH

1. Introduction

In the previous chapter, we highlighted the fact that the bipolar electrochemical technique is well adapted for the production of microscale Janus-type objects with hybrid organic-inorganic composition. This technique is also very attractive for the production of nanoscale Janus-type objects. For this reason, in this chapter we studied the possibility to use this technique for nanoscale objects. Multi-walled carbon nanotubes (MWCNTs) were selected as the nanoscale objects studied here due to their excellent and unique properties offering numerous breakthrough applications. The electrochemical modification of MWCNTs was performed in order to create selectively an area with organic functionalities on the tubes.

Relating to the principle of bipolar electrochemical modification, under an electric field, the maximum potential drop will be along the part of the object that is parallel to the field. This means that if the object can be aligned with the electric field or be arranged in a straight line parallel to the field direction, the maximum potential difference will be between both ends of the object. As a result, the electrochemical modification will take place selectively at both extremities of the object (Warakulwit, 2007). In contrast, for objects which cannot be aligned with the field, the modification will not selectively occur at both extremities. Taking the advantage that CNTs will be automatically aligned with the electric field, they were used here in order to promote their selective modification.

Until recently, CNTs have been prepared by several techniques. Arc discharge is the first technique used for synthesis of CNTs. In 1991, Ijima discovered MWCNTs with

4-30 nm in diameter, grown at the cathode (negative side) of high-purity graphite electrodes during direct current (dc) arc-discharge evaporation of carbon under an inert gas atmosphere (100 Torr) (Iijima, 1991). With this technique, SWCNTs can be generated in the presence of transition metal catalysts (Iijima and Ichihashi, 1993). For example, SWCNTs with diameters ranging from 0.75 to 1.37 nm were successfully prepared between Fe-graphite electrodes in a methane-argon atmosphere during the dc current discharge at 200 A and 20 V. In general, the production costs of CNTs via this technique are rather high because inert gas such as helium (He) or argon (Ar) with high-purity and sacrificial graphite electrodes are required, limiting the production at large or industrial scale.

Later, laser-ablation (vaporization) was used to produce CNTs. With this technique, MWCNTs can be produced by high-power laser vaporization of a pure graphite target in a chamber at a relatively high temperature of about 1200 °C under an inert atmosphere (Guo *et al.*, 1995). This method can also generate SWCNTs by adding a metal catalyst such as cobalt (Co) or nickel (Ni) to the graphite target (Thess *et al.*, 1996). The growth mechanism of the tubes produced via this technique is quite similar to that produced via the arc discharge technique. This technique can provide SWCNTs with a yield of more than 70% (Thess *et al.*, 1996) . However, due to the requirements of high laser power sources and high-purity graphite targets this technique is also not economically advantageous for large scale production.

Apart from the above mentioned methods, CNTs can also be produced via chemical vapor decomposition (CVD). With this technique, hydrocarbon molecules are decomposed into carbon atoms, and are precipitated as CNTs over a supporting material. The metal catalyst is usually involved in the process in order to lower the reaction temperature. This technique is called catalytic CVD (CCVD) technique. Until recently, many kinds of catalysts and supporting materials have been used for the CNT production via the CCVD technique. These include Fe particles (José-Yacamán *et al.*, 1993), Fe or

Co on glass (SiO_2) (Fonseca *et al.*, 1996; Li *et al.*, 1996), Fe or Co on zeolite support (Fonseca *et al.*, 1996; Hernadi *et al.*, 1996), and Fe on alumina (Al_2O_3) substrate (Ohno *et al.*, 2008; Qin *et al.*, 1998). Various hydrocarbons can be used as carbon sources. These include methane (Kong *et al.*, 1998; Qin *et al.*, 1998), ethylene (Fan *et al.*, 1999), acetylene (José-Yacamán *et al.*, 1993; Li *et al.*, 1996), carbon monoxide (CO) (Nikolaev *et al.*, 1999), and ethanol (Ohno *et al.*, 2008). In the process, N_2 or Ar is typically used as carrier gas. In order to prevent the catalyst deactivation, H_2 or NH_3 may be used as reducing gas. The reaction temperature for this technique can be varied in the range of 650-900 °C (Fonseca *et al.*, 1996; José-Yacamán *et al.*, 1993).

With the CCVD technique, both SWCNTs and MWCNTs can be produced. For the production of SWCNTs, the metal catalyst is typically formed through the thermal decomposition of organometallic compounds such as iron pentacarbonyl ($Fe(CO)_5$) and ferrocene ($Fe(C_5H_5)_2$). For example, Thess and co-workers (Thess *et al.*, 1996) produced SWCNTs by using CO and $Fe(CO)_5$ as the carbon source and catalyst, respectively. Apart from main metal catalysts used for the CNT production (Fe, Co and Ni), molybdenum exhibits also potential for the production of SWCNTs using CO as the carbon source (Dai *et al.*, 1996).

Compared to the arc-discharge and the laser-ablation techniques, the CVD technique is more versatile and better adapted for a large scale production of CNTs. This is because it can be operated at a relatively low temperature. In addition, it provides CNTs with a relatively high yield and controllable characteristics. Based on the simple set-up of the equipment required for this technique (such as temperature-programmable reactor and gas system), this technique is easy to scale up, leading to the possibility of a large scale production of CNTs (Iijima and Ichihashi, 1993; Kong *et al.*, 1998; Qin *et al.*, 1998). Although, the CVD technique, especially the catalytic one that operates at relatively low temperature, is used for the industrial scale production with acceptable production cost, the commercially produced CNTs are typically spaghetti-like (non-

oriented or disordered) in terms of morphology and contain a lot of structural defects, such as tube twisting and bending. In addition, they are bound into intractably entangled macroscopic aggregates (Wong *et al.*, 2004). For this reason, they cannot be well aligned with the electric field, and thus, they are not suitable for the bipolar electrochemical deposition, which is studied in this work. Consequently, for a well-defined selective grafting of the organic layer on the tube surface, obtaining arrays of aligned CNTs is crucial.

Vertically aligned carbon nanotubes (VACNTs) with the array aligned perpendicular to the substrate surface exhibit many attractive characteristics and properties that are interesting for electronic and functional devices such as scanning probes and field emitters and for interface and composite materials (Dai, 2006; Harris, 1999). In order to obtain VACNTs in a large quantity, several CVD techniques have been adopted (Gong *et al.*, 2008; Hata *et al.*, 2004; Meyyappan *et al.*, 2003; Singh *et al.*, 2003; Xu *et al.*, 2006; Zhong *et al.*, 2009). These techniques include the use of template materials such as mesoporous silica (Che *et al.*, 1998a; Li *et al.*, 1996), zeolites (Zhao *et al.*, 2012), alumina (Suh and Lee, 1999)and patterned catalysts.

Due to the relatively low amount of mesopores (diameter < 2-50 nm) and macropores (diameter > 50 nm), which are suitable for the growth of CNTs in mesoporous silica and zeolite materials, the use of patterned catalysts is more attractive in the context of high-yield production. Unfortunately, the VACNTs obtained via this technique are contaminated with catalyst particles, and thus, require purification steps after the synthesis and are therefore impractical. In addition, the growth process often involves a tip growth mechanism, which leads to the fact that the obtained VACNTs are capped or closed with catalyst particles (Andrews *et al.*, 1999; Fan *et al.*, 1999; Li *et al.*, 1996; Ren *et al.*, 1998; Terrones *et al.*, 1997; Zhang *et al.*, 2002). This results in the difficulties for filling other particles or materials into the tubes, and thus, limits the applications in the fields of storage and delivery. Although, post-treatment techniques

have been reported for opening the closed tips such as the oxidation by acid solution (Hiura *et al.*, 1995; Tsang *et al.*, 1994), these treatments usually destroy the tube structure. Consequently, the use of alumina template that can be produced commercially with a simple and scalable technique such as an electrochemical technique and with high pore densities has attracted a great interest for the production of VACNTs. This technique not only yields tube arrays with uniform orientation but also with high purity and identical tube length and diameter.

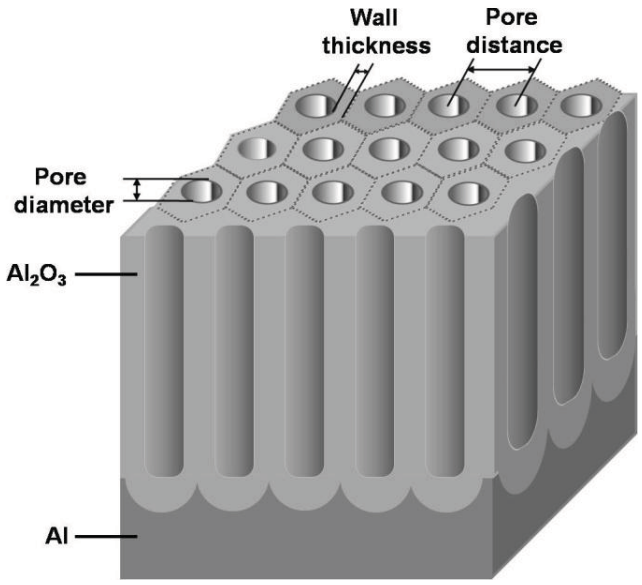

Figure 32 Schematic illustration of the AAO chemical composition and structure in which a porous anodic Al_2O_3 layer with well ordered hexagonal pore structure, narrow pore size distribution and uniform interpore spacing is situated on an Al substrate.

Anodic aluminum oxide (AAO) membranes are alumina (Al_2O_3) membranes with well-ordered pore structure, narrow pore size distribution and uniform interpore spacing. These membranes are commonly obtained from the anodic oxidation of aluminum (Al) metal (located at the anodic side of the circuit), in a strongly acid electrolyte, to

aluminum oxide (Keller *et al.*, 1953; Masuda and Fukuda, 1995; Sulka and Parkoła, 2007). These membranes are commercially available. Their structure can be considered as hexagonally close-packed arrays of parallel cylindrical pores with a high aspect ratio or length to diameter ratio (see Figure 32).

Apart from the mentioned advantageous characteristics and properties, AAO membranes have good thermal, mechanical and chemical stabilities. Their stabilities facilitate their use as template for the preparation of CNTs, which is typically performed at an elevated high temperature. In addition, their textural properties are tunable leading to a diversity in the CNT characteristics when they are used as template. The AAO membranes do not exhibit the potential only for the preparation of VACNTs but also for the numerous applications such as molecular separation (Jirage *et al.*, 1997), sensors (Heilmann *et al.*, 2003) and drug delivery (Losic and Simovic, 2009). Furthermore, they can be utilized as a template in the preparation of other materials ranging from polymers to metals (Martin, 1994; Masuda and Fukuda, 1995).

For the preparation of VACNTs, Kyotani and co-workers firstly used AAO films as template for the tube synthesis in 1995. The CVD process was performed without adding any additional catalyst (Kyotani *et al.*, 1995; 1996). In this process, an elevated high temperature within a hot-wall tubular reactor, in which the AAO template is located, promotes the decomposition of the gaseous carbon source. This results in the coating of a uniform carbon layer on the inner wall of the AAO nanochannels. After the template removal by immersing in hydrofluoric (HF) acid solution, CNTs are obtained as residue (Kyotani *et al.*, 1995; 1996) (see Figure 33)

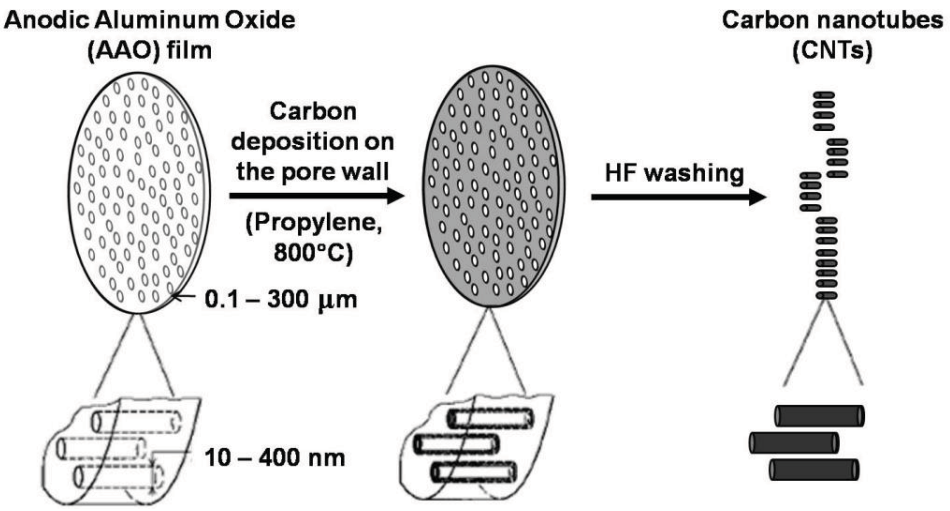

Figure 33 Schematic illustration of the process used for the VACNT production by using an AAO template. The illustration is adapted from that presented in the literature (Kyotani *et al.*, 1996).

It has been reported that this synthesis technique provides the parallel and straight arrays of CNTs with uniform and controllable characteristics (length and diameter) that reflect the characteristics of the AAO channels. The length of the whole tubes is derived from the thickness of the parent AAO template while the outer diameter of the tubes directly relates to the pore diameter of AAO (Che *et al.*, 1998b; Kyotani *et al.*, 1995). AAO is easily removable from the synthesized carbon by a simple chemical treatment using an acidic or alkaline solution (HF or sodium hydroxide (NaOH)) without affecting the structure of the CNT product confined inside its pores. In addition, it can yield MWCNTs without using any metal catalysts (Altalhi *et al.*, 2010). This is because AAO can itself play a catalytic role in the decomposition of the gaseous carbon source (Sui *et al.*, 2001). By considering that purification steps are not required in the process, this synthesis technique is practical for the production of VACNTs (Altalhi *et al.*, 2010). In addition to the advantage of the well-defined structure and alignment of the tubes, the use of AAO templates also yields tubes with open-ends. Thus, it is possible to fill foreign materials inside the hollow channel of the tubes.

In order to extend the applications of CNT in the fields of bio-fuel cell, bio-electrocatalyst and bio-sensing (Guo and Li, 2005; Wang and Lin, 2008), both non-covalent (Barone and Strano, 2006; Das and Das, 2009; Nativ-Roth *et al.*, 2007; Yan *et al.*, 2008) and covalent (Datsyuk *et al.*, 2008; Nayak *et al.*, 2007; Philip *et al.*, 2005; Rahimi-Razin *et al.*, 2012) approaches have been employed to create surface functional groups on the tube surface. The introduction of the key biocompatible functional groups including amine and carboxylic acid groups to the surface of the tubes is the fundamental process. Although both covalent and non-covalent functionalization can be employed for immobilizing bio-molecules including proteins, enzymes and DNA, the covalent functionalization offer a better mechanical, thermal and chemical stability than the non-covalent one. Nevertheless, as a main disadvantage, it usually damages the tube structure during the modification (Mittal, 2011).

In 2001, Bahr and co-workers reported for the first time an alternative and efficient way to modify the tubes without leading to structural damage of the tubes. The electrochemical grafting on CNTs via diazonium chemistry was employed (Bahr *et al.*, 2001). CNTs were modified with various degrees of aryl groups by an electrochemical reduction technique using a metal catalyst. It was found that via this technique the aryl groups are widely dispersed onto the tube surface. As the substituent of the aryl group of the diazonium molecules allows the coupling with other molecules such as polymers and other materials such as nanoparticles, the surface properties of the modified tubes can be tuned. Accordingly, the modification technique of CNTs using diazonium has attracted great interest.

The mechanism of the attachment of the molecules to the CNT surface using diazonium has been explored. Steven and co-workers suggested that via the electrochemical modification the covalent bonds are established between the carbon atom of substituted aryl groups (derived the diazonium molecules) and the lattice of CNTs (Kooi *et al.*, 2002). It was found that a highly reactive radical generated by the

electrochemical reduction of diazonium can not only interact and attach to the ends of CNTs but also to the sidewall of the tubes. This leads to a high degree of functionalization of the tubes (~5% of carbon atoms bear the functional groups) (Kooi *et al.*, 2002). Until recently, the selective modification of CNTs via the bipolar electrochemical reduction of diazonium that can increase the complexity of CNTs and make them promising for some specific applications such as storage and drug delivery, has not been reported.

In this section, we studied the selective modification of CNTs by an organic layer of 4-aminobenzene via the bipolar electrochemical approach. VACNTs were firstly prepared via the CVD technique by using AAO as the template. Then, the bipolar electrografting was performed without the removal of AAO from the carbon product. The main ideas for using the as-prepared VACNT/AAO product without removing of AAO are i) to simplify the setup because no membranes are needed ii) prevent the reaction on the outer surface of the tube walls. Keeping the tubes in the bundle form allows fixing the tubes between the two feeder electrodes, and as a consequence the tubes cannot get in contact with the feeder electrodes during the bipolar experiment and the reactions occur on the tube via bipolar electrochemistry. The template block protects the outer surface of the tubes from the covalent attachment of 4-aminobenzene, and thus, leads to the selective modification with the organic layer on the inner surface of the tubes and at one side of the tubes. Similar to the previous section, citrate-capped gold nanoparticles (AuNPs) were used for labeling the area that is modified by the organic layer in order to verify the asymmetric modification. In the last step, the AAO template was removed leading to the desired material.

2. Methods

The experimental steps for the selective modification of CNTs with the organic layer of 4-aminobenzene via the bipolar electrochemical approach are depicted in Figure 34. In the first step, VACNTs were prepared via the CVD technique by using AAO as the template. In this step, the additional metal catalyst was not used. Thus, the step for the metal catalyst removal is not required. After that the bipolar electrografting of 4-aminobenzene moieties onto the inner surface of the tubes was performed. Then in order to create the positive charges on the surface area that is modified by 4-aminobenzene moieties allowing the verification of the modification, the protonation of the amine groups of 4-aminobenzene moieties was performed by soaking the product in an acid solution. Then the material was coupled with the negatively charged AuNPs and analyzed. In the final step, the AAO template was removed. The asymmetrically modified tubes were then isolated, washed and dried. The details for each experimental step are as follows.

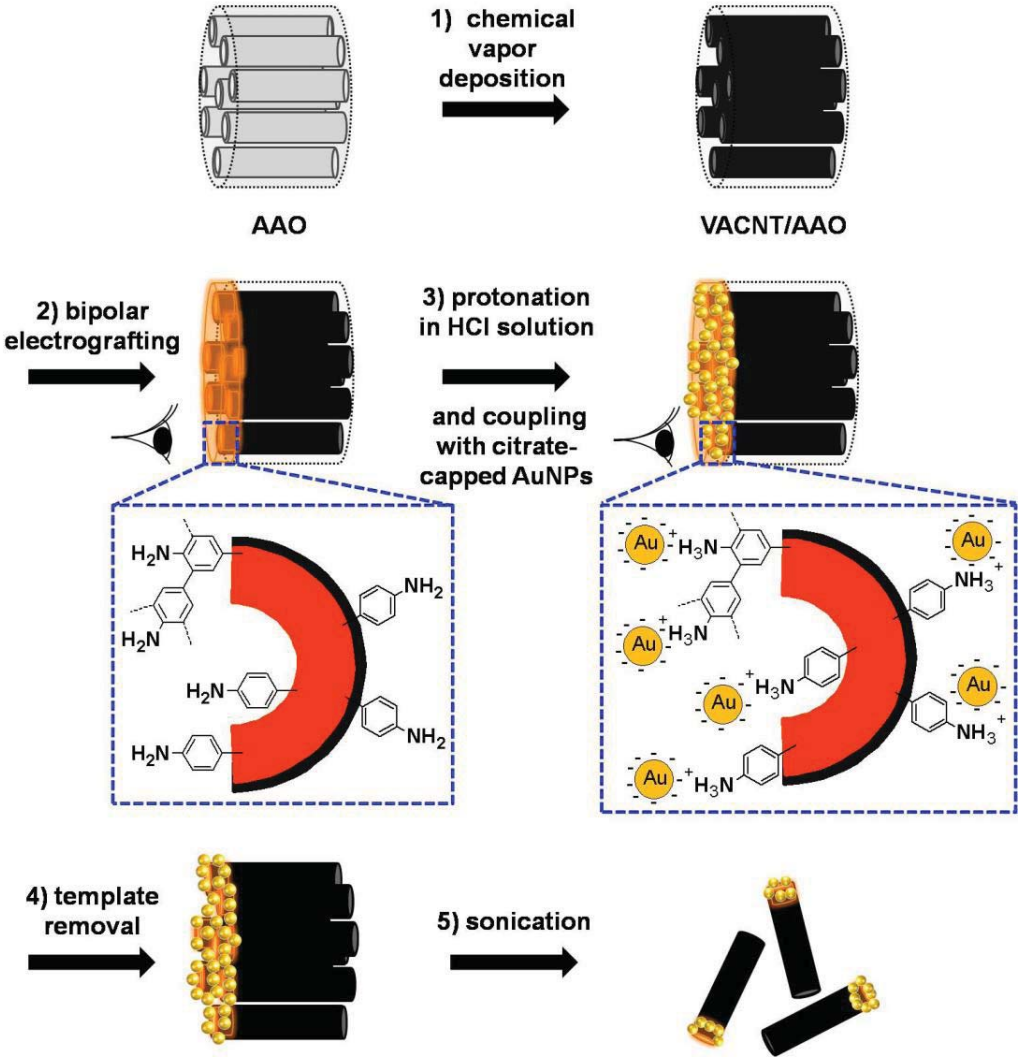

Figure 34 Schematic illustration of the experimental steps for the selective modification of CNTs with an organic layer of 4-aminobenzene via the bipolar electrochemical approach.

2.1. Preparation of VACNT/AAO

2.1.1. Pretreatment of AAO membrane

Commercial AAO membrane filters (Anodisc 47, WHATMAN) with a membrane diameter of 47 mm, average pore diameter of < 200 nm and thickness of 60 μm (without the polymer support) were used as templates for the synthesis of VACNTs. In order to avoid the wrapping of the membrane at an elevated temperature (at the reaction temperature for the tube synthesis) that originates from the transition of alumina, the membranes were annealed at the highest temperature used for the tube synthesis (the discussion about the optimized experimental conditions for the synthesis of VACNTs is included in the next section). During this annealing step, each AAO membrane was placed between crucibles with their bottoms facing the membrane and annealed in a muffle furnace (LV3/11/B180, NABERTHERM) at 1000 °C for 1 h with a heating rate of 3 °C/min. The annealed membranes were then used for the synthesis of CNTs.

2.1.2. Synthesis of VACNT/AAO

The experimental set-up used for the synthesis of VACNT/AAO in this work is quite similar to that used in the literature (Warakulwit, 2007). A few pieces of the annealed AAO membrane were placed on quartz wool (ALTECH) within a vertical aluminum porcelain work tube at the middle position as a fixed bed as shown in Figure 35. The work tube was then introduced in a vertical wire-wound tube furnace (LENTON LTF 12/38/250) equipped with a temperature controller. The mass flow controllers (AALBORG) were used to control the flow rate of acetylene (C_2H_2) and nitrogen (N_2) gases. A liquid trap was included in the system to condense the hydrocarbon residue gas to liquid.

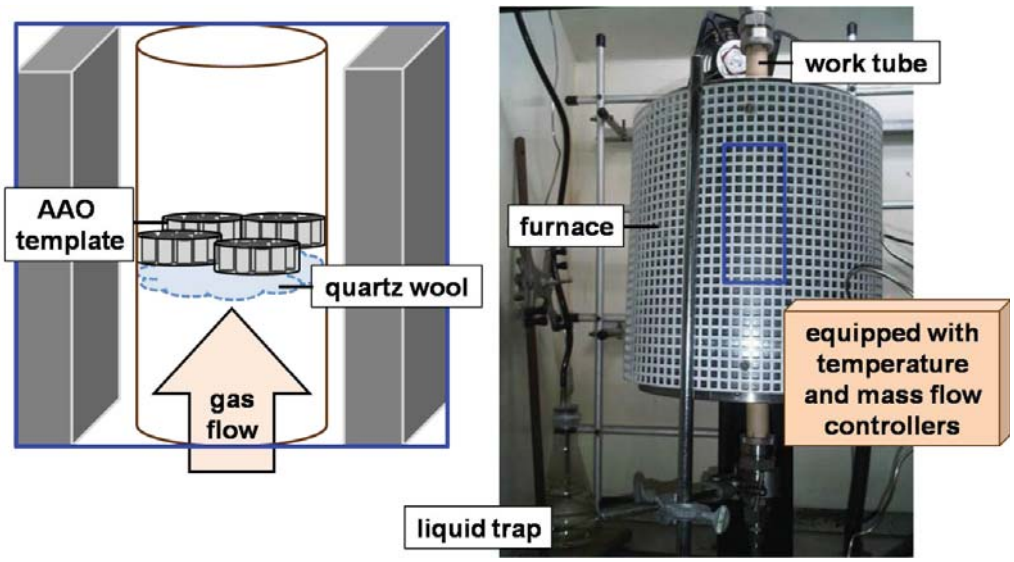

Figure 35 Schematic illustration and photo showing the setup of the equipment used for the synthesis of VACNT/AAO in this study.

Under a N_2 atmosphere (flow rate of N_2 was fixed at 90 ml/min), the temperature of the reactor was increased gradually from room temperature to 750 °C with a heating rate of 10 °C/min. The reactor was left under this condition for 5 min in order to ensure a steady temperature of the reactor before starting the reaction. Next, C_2H_2 gas (99.9% purity) was passed through the work tube by using N_2 as the carrier gas. The flow of N_2 and C_2H_2 was 90 and 10 ml/min, respectively. After 1 h (the reaction time), the C_2H_2 flow was stopped. The reactor was left to cool down to room temperature under the N_2 flow (90 ml/min). This process usually takes about 2 h. After each synthesis, the work tube was cleaned via an air oxidation at 1000 °C for 6 h in the horizontal furnace (LTF 12/50/610, LENTON).

2.1.3. Post-treatment of the VACNT/AAO product

Because no additional metal catalyst is used in this work in order to avoid the catalyst removal step, vertically aligned MWCNTs with low graphiticity (the proportion

of crystallinity and amorphousness) were obtained together with amorphous carbon (see later in the Results and Discussion section). Due to a relatively low electrical conductivity of the tubes which can lower the efficiency of the bipolar electrochemical grafting, a post-treatment of the tubes was performed. For this purpose, we firstly attempted to use manual polishing (by using a sand paper, DCC#2000, TOA, Thailand) to remove amorphous carbon from the top surface of the tube array and later employed a thermal annealing of the polished sample at 1000 °C under inert N_2 atmosphere . Unfortunately, we found that via this procedure, the structure of CNTs was severely damaged (see details in the Results and Discussion section). Therefore we avoided the manual polishing in order to preserve the tube structure. The steps of the thermal annealing of tubes and the air oxidation (of amorphous carbon from the carbon product) were employed instead in order to obtain VACNTs with high purity, improved graphiticity and preserved tube structure.

The treated VACNT/AAO material can be obtained by using a procedure similar to the one described above, but with some modifications. Afterwards the VACNT/AAO material was prepared via the decomposition of C_2H_2 at 750 °C for 1 h. The thermal annealing of the as-prepared VACNT/AAO material was immediately performed by continuously ramping up the temperature of the reactor to 1000 °C with a heating rate of 10 °C/min. The work tube was kept at this temperature for 4 h. Then, the reactor was left to cool down to room temperature (about 2 h) under the N_2 flow. After each synthesis, the work tube was cleaned via an air oxidation at 1000 °C for 6 h. After that the air oxidation of amorphous carbon from the carbon product was performed. The obtained sample was further transferred from the reactor into a crucible. The crucible was then placed in a muffle furnace (LV3/11/B180, NABERTHERM) and heated at 500 °C for 1 h with a heating rate of 3 °C/min.

2.1.4. Opening of both ends of the VACNT bundle

In order to enhance the efficiency of the bipolar electrografting, we attempted to liberate the ends of the VACNT bundle embedded in the AAO membrane by partly removing of the AAO top surface. For this purpose, hydrofluoric acid solutions with different concentrations were used to remove partly alumina from the top surface at both ends of the prepared VACNT/AAO membrane. A suction filter system was used in order to offer a short contact time between the membrane surface and the HF solution. This is because only a small area of the alumina on the top surface at both ends of the membrane is expected to be removed as shown in Figure 36.

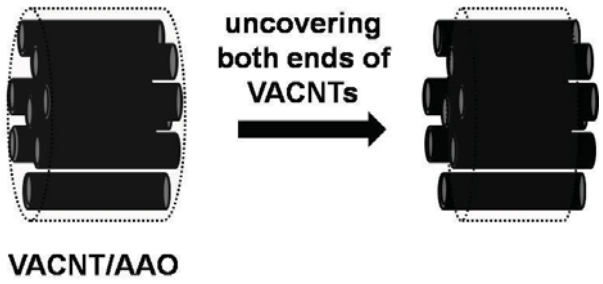

Figure 36 Schematic illustration showing the process to remove alumina from the top surface in part at both ends of the prepared VACNT/AAO membrane in order to facilitate the polarization of the tubes in the electric field, and thus, promoting the bipolar electrografting by the organic layer.

HF solutions with various concentrations were prepared from a concentrated solution of HF (50%, CARLO ERBA). A few droplets of the HF solution were carefully dropped on the top surface of the prepared VACNT/AAO membrane, which was placed on a polytetrafluoroethylene (Teflon) membrane filter (MILLIPORE) equipped with a suction filter system to remove the solution quickly from the membrane by using a water-jet vacuum pump (WJ-20, SIBATA) connected to the suction flask (see Figure 37). Then

ultrapure water was used to rinse the membrane. This procedure was repeated for the other side of the membrane surface.

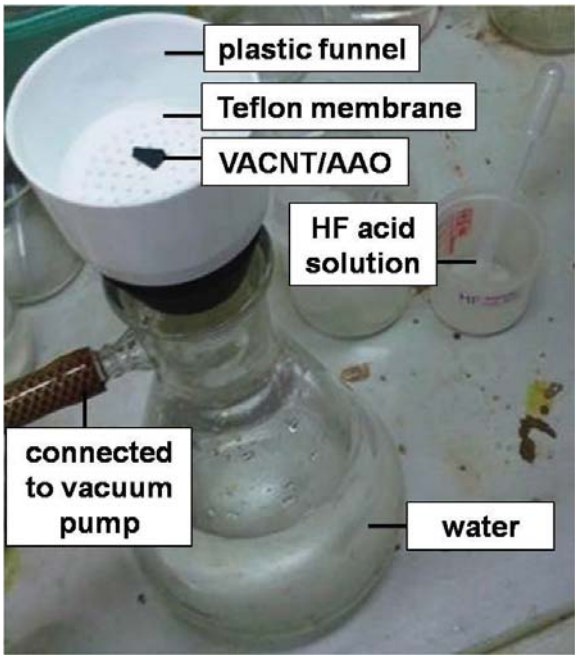

Figure 37 Photo showing the equipment used for the removal of alumina from the top surface in part at both ends of the prepared VACNT/AAO membrane.

2.2. Asymmetric electrografting of 4-aminobenzene on VACNTs via bipolar electrochemical reduction of 4-nitrobenzenediazonium salts

For an asymmetric electrografting of 4-aminobenzene on VACNTs via bipolar electrochemical reduction of 4-nitrobenzenediazonium salts, the obtained membrane was positioned in an electrochemical cell filled with a cold solution of 4-nitrobenzenediazonium salts (5 mM), which is prepared by dissolving 0.0122 g of 4-nitrobenzenediazonium tetrafluoroborate in 10 ml of cold 1 mM HCl solution (see Figure 38). A plastic container was used as the solution reservoir. The water cooling system consisted of ice, water, and salt was added into the container around the reaction

compartment. The resin was used to protect the flow of outer solution into the reaction compartment and vice versa. About 1 ml of glacial nitrobenzenediazonium tetrafluoroborate/1 mM HCl solution was filled into the reaction compartment. Two carbon rods were cleaned by sonicating in absolute ethanol, dried and used as the feeder electrodes. The feeder electrodes arranged horizontally were connected to a high-voltage power supply with steel crocodile clips. It should be noted that only the membrane and two feeder electrodes were suspended in the solution.

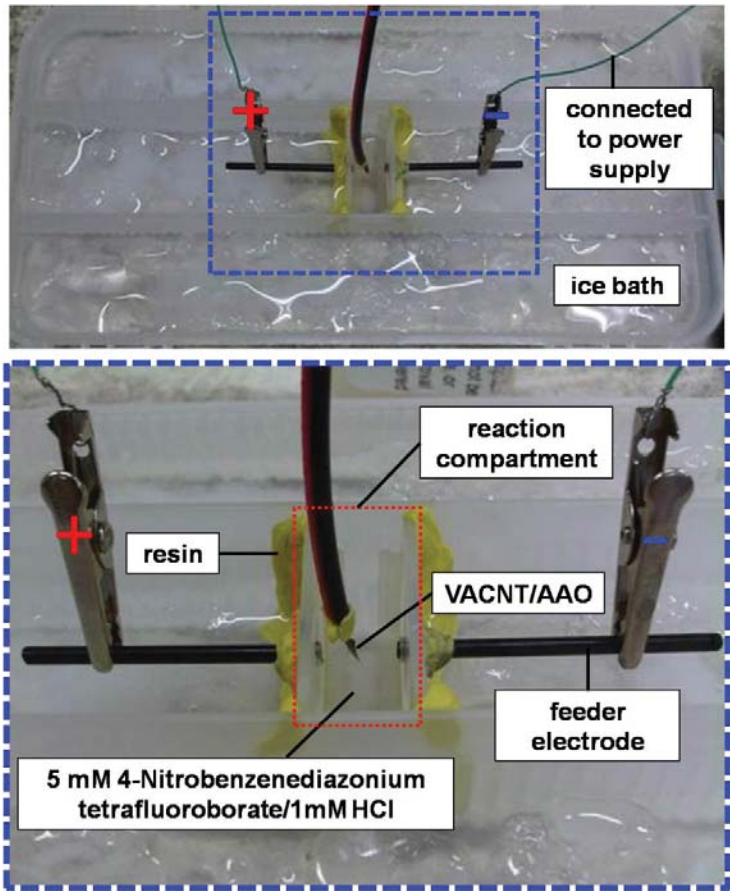

Figure 38 Schematic illustration and photo showing the experimental set-up of the equipments used for asymmetric electrografting of 4-aminobenzene on VACNTs by using bipolar electrochemical reduction of 4-nitrobenzenediazonium salts.

In order to drive the redox reactions leading to the bipolar electrografting of 4-aminobenzene moieties onto the tube inner surface (the average length of the tubes or the membrane thickness was < 60 μm) in the electric field (*E*) generated between the feeder electrodes with the distance between the electrodes of 1 cm (see equation (1)), a voltage of 400 V was applied for 30 s to the system. After that, the sample was carefully transferred into an Eppendorf cup and rinsed with 0.1 M HCl to protonate the amine groups of the 4-aminobenzene moieties grafted onto the inner surface of the tubes. Then, the obtained material was isolated from the acid solution and immersed overnight in the colloidal Au-citrate solution prepared according to the procedure described in the last chapter. The product was characterized by field-emission scanning electron microscopy (FE-SEM, S-4700, HITACHI with an accelerating voltage of 5 – 10 kV) and environmental scanning electron microscopy (ESEM, Quanta 450, FEI with an accelerating voltage of 30 kV). The chemical composition of the product was investigated by energy dispersive X-ray (EDX) analysis.

For the transmission electron microscopy (TEM) characterization, the alumina matrix was completely removed from the resulting material by immersing the membrane in an excess amount of 50% HF solution overnight. The precipitate was collected by the centrifugation. Consequently, the HF solution was removed from the precipitate. The precipitate was washed with ultrapure water several times until the pH of the supernatant was < 7. Then, the precipitate was dried in an oven at < 100 °C. A part of the precipitate was re-dispersed in absolute ethanol by using an ultrasonic bath (RK106, BANDELINE, LECTRONIC). A few drops of this suspension were put on a copper grid for the TEM characterization (HT-7700, HITACHI and JEM-2100, JEOL with an accelerating voltage of 120 kV).

3. Results and discussion

3.1. Preparation of VACNT/AAO

Figure 39 shows the photo and the SEM images of the as-obtained commercial AAO membrane. The top-view SEM image shows that the membrane is composed of the highly ordered structure of a hexagonal array of pores (see Figure 39b). By observing the two extremities of the membrane, the pores were found to be open at both ends. However, there is a slightly difference in the feature of the pore opening on both sides. The pores with an average diameter of about 200 nm can clearly be observed from the back side of the membrane (see Figure 39b). While at the opposite side, we found that the pores have a smaller diameter, about 165 nm in average (obtained by analyzing by ImageJ program). This feature is typically found for the commercially available Whatman® Anopore (Anodisc) membrane. Nevertheless, at the main entrances (the black pores beneath the openings at the top), we can observe also pores with an average diameter of about 200 nm (see Figure 39c) similar to that observed at the other side of the top-view surface. Then the difference in the feature of the pore openings at both extremities is expected to not have any influence on the main characteristics of the prepared CNTs, and thus, can be neglected. On the SEM image of the membrane cross-section (figure 39d) we observed the uniform length (~ 60 μm) of the pores. The high magnification image (Figure 39e) of this cross-section image shows pores with a straight, parallel and cylindrical structure and the openings of the pores. This finding corresponds well to that reported in the literature (Masuda and Fukuda, 1995; Poinern *et al.*, 2013). It should be noted that, from the cross-section SEM image, the sample does not look so clean and contains small pieces of the membrane fracture due to the cracking of membrane (by hands) in the preparation step of the sample for the SEM side-view observation.

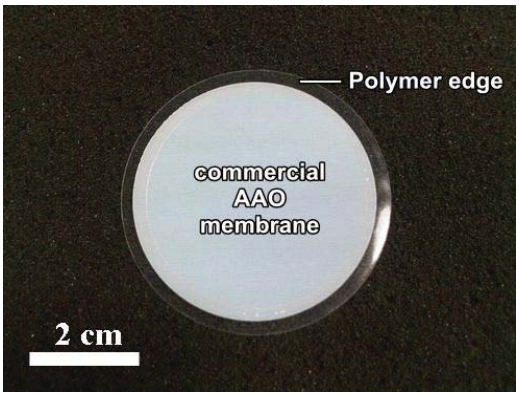

(a)

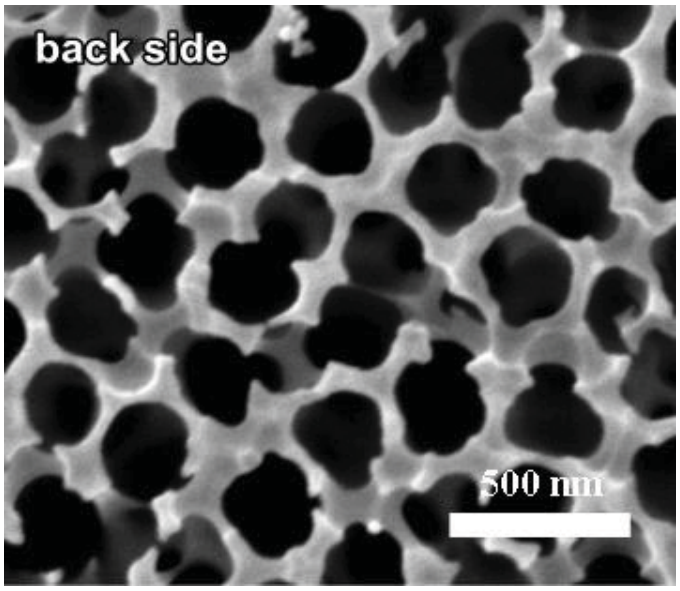

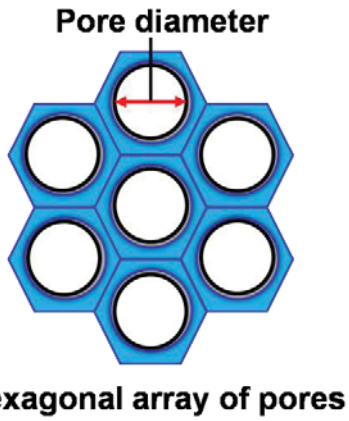

(b)

Figure 39 (a) Photograph and (b-e) SEM micrographs of a commercial AAO membrane filter with average pore diameter of about 200 nm. (b-c) The images show the top-view surfaces of the membrane: (b) back side and (c) front side. (d) The images with the cross-section view and (e) high magnification.

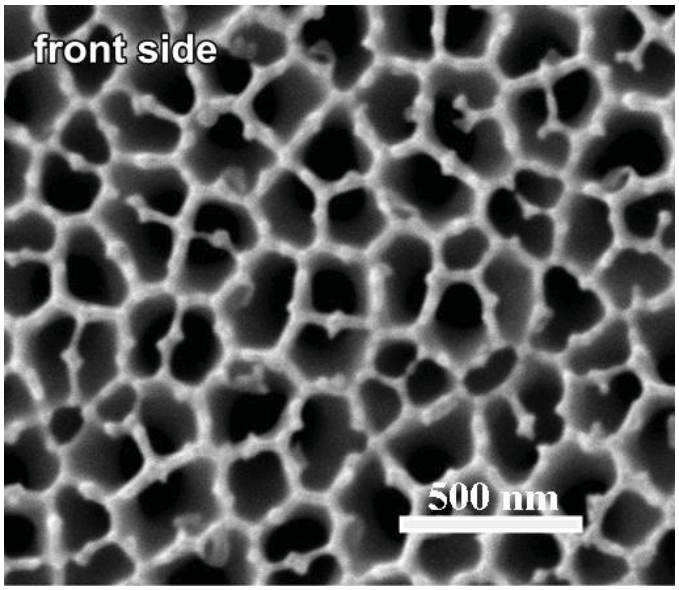

(c)

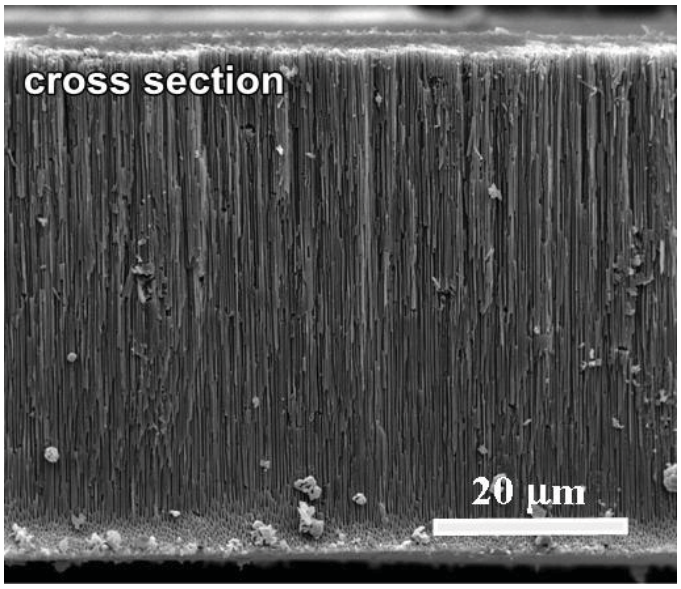

(d)

Figure 39 (continued)

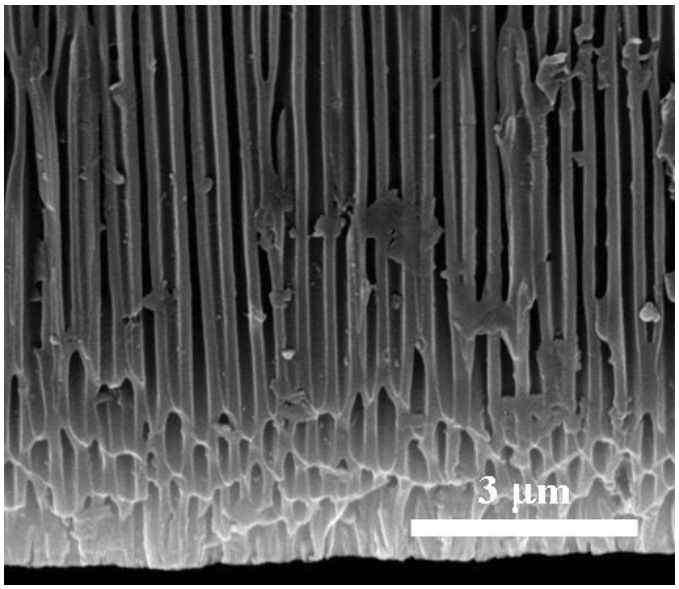

(e)

Figure 39 (continued)

Figure 40a shows the photo of the AAO membrane after the removal of the polymer support at the edge of the membrane (the transparent part in Figure 39a) by using a scissor and after a thermal treatment at 1000 °C for 1 h in air. It can be seen that the membrane splits in several pieces, rolled up almost into a semicircle. The SEM images of this membrane (see Figure 40b-c) do not show any modification in the pore characteristics. They are still highly ordered with a hexagonal arrangement. The average pore diameter, the straight, parallel and cylindrical structure was not changed during the treatment. It can be seen from the cross-section SEM image (Figure 40d) that there is a distortion of the surface plane of the membrane. The reason for the membrane to roll up and have a distorted surface plane is that there is a phase transformation of the alumina from amorphous to polycrystalline. This transformation is suggested to occur at a temperature of around 830 – 840 °C (Mardilovich *et al.*, 1995). Because of this wrapping feature, the membrane is not suitable anymore to be used for the bipolar experiment. In order to avoid the membrane wrapping at the temperature where the CNTs are prepared,

the membrane was placed between two crucibles that face their bottoms to the membrane and heat treated at 1000 °C as a pre-treatment.

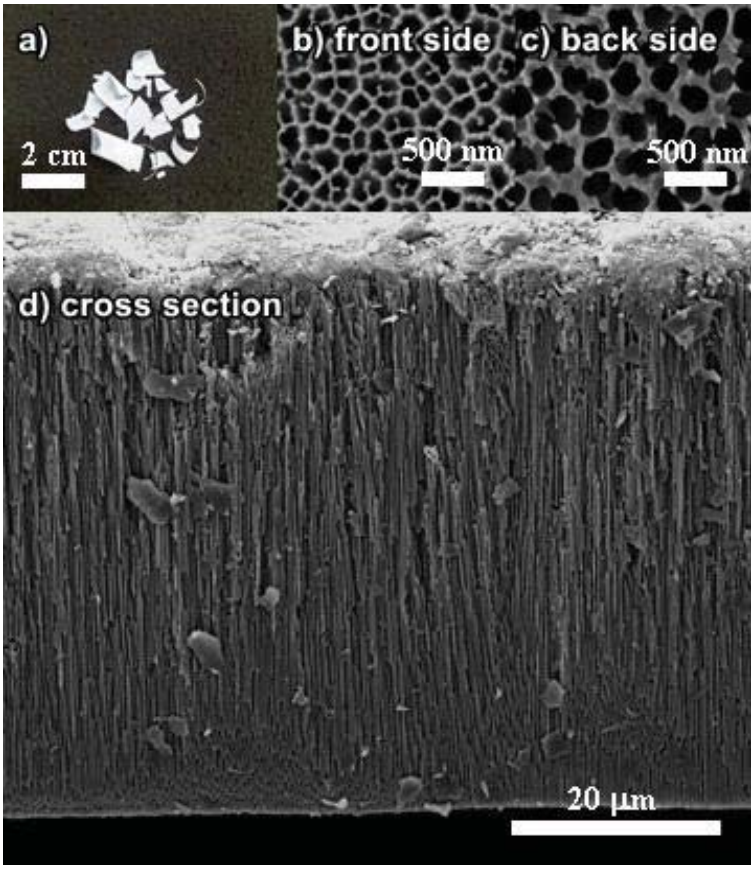

Figure 40 (a) Photograph of an AAO membrane obtained after the heat treatment at 1000 °C for 1 h in air and its SEM images taken from the top of (b) the front side and (c) the back side. (d) Its cross-section SEM image.

3.1.1. Pretreatment of AAO membrane

Figure 41a shows a photo of the membrane pretreated by placing between the crucibles that face their bottoms to the membrane during the heating at 1000 °C for 1 h in air. It was found that the wrapping of the membrane due to the transformation of the

alumina phase can be reduced (see Figure 41a). The SEM images (see Figure 41b-d) of the membrane show that the distortion of its surface plane is diminished and the pore characteristics including the highly ordered structure of hexagonal arrangement, the average pore diameter, and the straight, parallel and cylindrical structure are preserved. This pretreatment technique is thus used for the membrane prior to the synthesis of VACNTs.

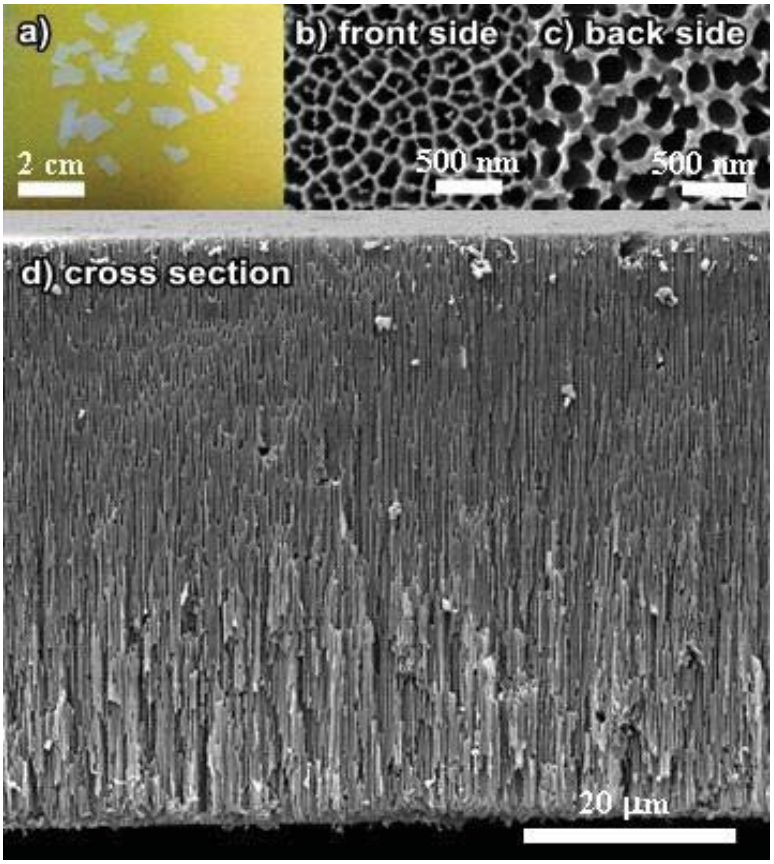

Figure 41 (a) Photograph of an AAO membrane pretreated by placing between crucibles that face their bottoms to the membrane during the heating at 1000 °C for 1 h in air and its SEM images taken from the top of (b) the front side and (c) the back side. (d) Its cross-section SEM image.

3.1.2. Synthesis of VACNT/AAO

Figure 42a shows a photo of the VACNT/AAO sample prepared at 750 °C. The membrane is now black because of the formation of carbon materials. Figure 42b shows the cross-section SEM image of the sample confirming a successful synthesis of VACNTs. The characteristics of the tubes including the straight, parallel and cylindrical structure, and the average diameter of ~ 200 nm are reflected from the pore characteristics of the AAO membrane (see inset of Figure 42b). The top-view image (Figure 42c) shows the average tube length of < 60 μm that is related to the membrane thickness. Nevertheless, it can be seen also from the image that, via the pyrolysis of acetylene under the current experimental conditions, apart from VACNTs, amorphous carbon is also formed at the surface of VACNT/AAO as a thin layer (indicated by the white arrows in Figure 42c). Because the tubes are formed without the catalyst in AAO template, playing the role of a catalyst, via the pyrolysis of the hydrocarbon precursor (acetylene), it is possible that amorphous carbon is generated over the top surface of the AAO (Schneider *et al.*, 2008). Due to the presence of the amorphous carbon, we expect that the prepared tubes are not completely open at the end. As the modification of the inner surface of the tubes is the objective of the bipolar experiments we did not use the as-prepared tubes (with the amorphous carbon) because i) the amorphous carbon layer can prevent the penetration of the organic precursors into the tubes ii) the bipolar modification will not occur at the end of the tubes but will occur at the amorphous layer leading to undesirable results and iii) the presence of the carbon coverage can prevent the removal of AAO by using HF. For all these reasons, a post-treatment is required in order to obtain the VACNT/AAO sample without the amorphous carbon that is not suitable for the bipolar experiments. We firstly attempted to remove the amorphous carbon by a simple manual polishing. The obtained results are described in the next part.

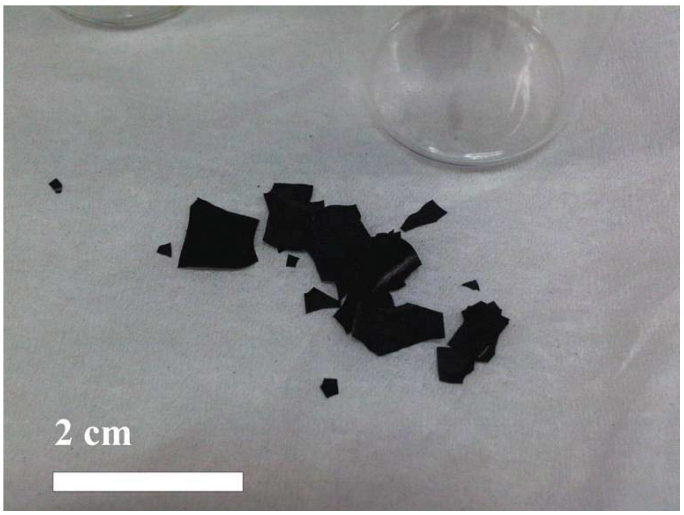

(a)

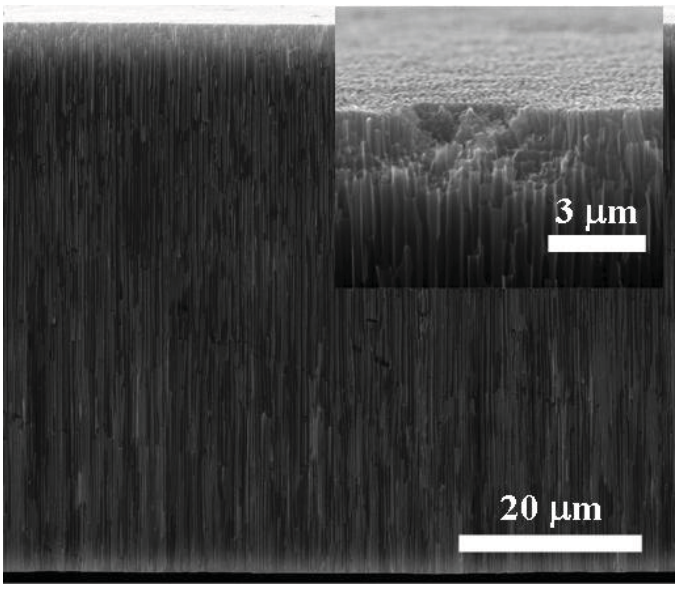

(b)

Figure 42 (a) Photograph and (b-c) SEM images of the VACNT/AAO sample prepared via the decomposition of acetylene at 750 °C for 1 h. (b) SEM image taken from the cross-section view (inset: the image with high magnification). (d) SEM image taken from the top-view.

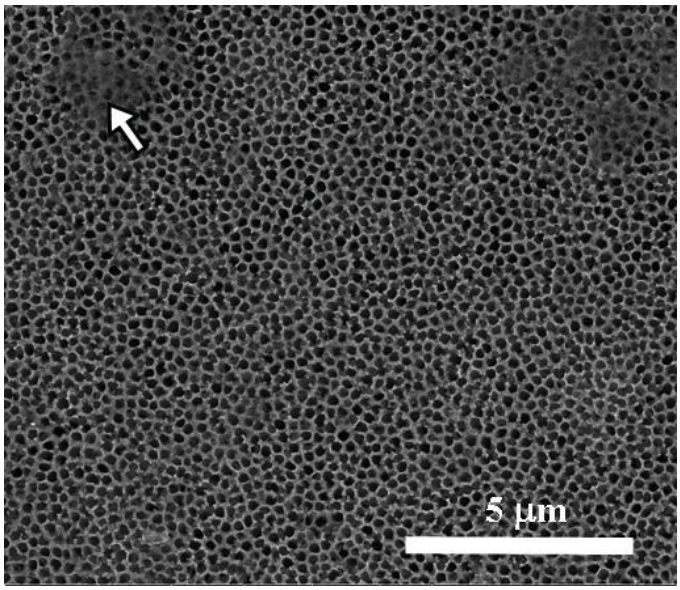

(c)

Figure 42 (continued)

3.1.3. Post-treatment of the VACNT/AAO product

The manual polishing was performed by using waterproof abrasive sandpaper (DCC#2000, TOA, Thailand). The membrane was mildly polished by hands at both front and back sides. We found that it is easy to get rid of the tiny black powder from the membrane without any severe breakages of the membrane (Figure 43a). After that, the polished membrane was thermally treated at 1000 °C and kept constant at this temperature for 1 h under the inert atmosphere of N_2 as an annealing step (heat treatment that alters the physical and sometimes chemical properties of a material to improve its workability) to improve the graphiticity (carbon crystallinity i.e. the presence of sp^2 hybridized or graphitic configuration) of the tubes, and thus, their mechanical strength. The SEM images of the obtained membrane are shown in Figure 43b-d. It can be seen from the images that the characteristics of the synthesized tubes are mainly preserved, however, the tubes were decomposed into tiny pieces at the ends and these pieces are

expected to block the entrance of the tubes. For this reason, we decided that the employed technique is not suitable for the post-treatment of the VACNT/AAO product.

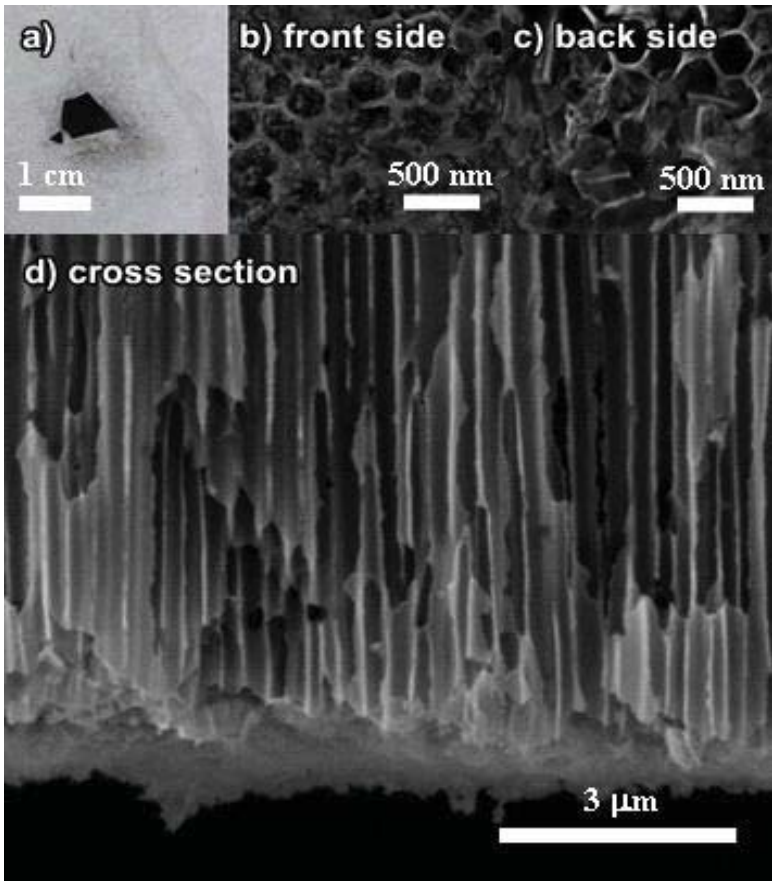

Figure 43 (a) Photograph of the VACNT/AAO sample prepared at 750 °C via the decomposition of C_2H_2 and post-treated by manual polishing using sand paper and (b-c) SEM images of the VACNT/AAO sample prepared at 750 °C via the decomposition of C_2H_2 and post-treated by manual polishing using sand paper and thermal annealing at 1000 °C. (d) SEM image taken from the cross-section view.

Next, we attempted to use a different technique to remove amorphous carbon from the product instead of the manual polishing. Typical purification techniques that

have been used to remove amorphous carbon from CNTs after the synthesis are wet-chemical treatments that use acids and bases as the oxidants for amorphous carbon (Colomer *et al.*, 2000; Li *et al.*, 2003). These treatments, however, extensively damage the tube sidewall and cause many defects on the tube sidewall (Hou *et al.*, 2008). In addition, the procedures, like filtering and drying, performed after the chemical etching also typically lower the yield of the tubes considerably. Then, an alternative purification approach, namely air oxidation, was used in this work. This technique is based on the gas-phase thermal oxidation by using air as the gaseous oxidant (Haddon *et al.*, 2004). Typically, via air oxidation, the carbon materials are oxidized at a temperature in the range of 200-500 °C depending on the type of the materials (Dementev *et al.*, 2009). The amorphous carbon is typically oxidized in air in the temperature range of 200-300 °C, whereas CNTs are thermally stable up to 400-650 °C (Lehman *et al.*, 2011; Osswald *et al.*, 2005). As reported in the literature the graphiticity or cystallinity of CNTs prepared via the CVD method without the use of metal catalysts is generally not high (Jeong *et al.*, 2004), thus we expected that the air oxidation might damage easily the sidewalls of the tubes obtained from our CVD synthesis, and thus decreasing the electrical conductivity of the tubes (leading to the inefficient bipolar experiments). For this reason, after the step of the tube synthesis at 750 °C, we employed thermal annealing by increasing the temperature of the work tube to 1000 °C and keeping it constant for 4 h (under the inert atmosphere of N_2) as the thermal annealing step should increase the graphiticity of the tubes in order to strengthen the tubes (Huang *et al.*, 2003; Kowalska *et al.*, 2006; Lin *et al.*, 2010) and preserve the tubes from the severe structural damage during the air oxidation step. Then, we performed the air oxidation at 500 °C for 1 h in air. The decomposition of VACNTs can be avoided at this temperature (see details in Appendix A).

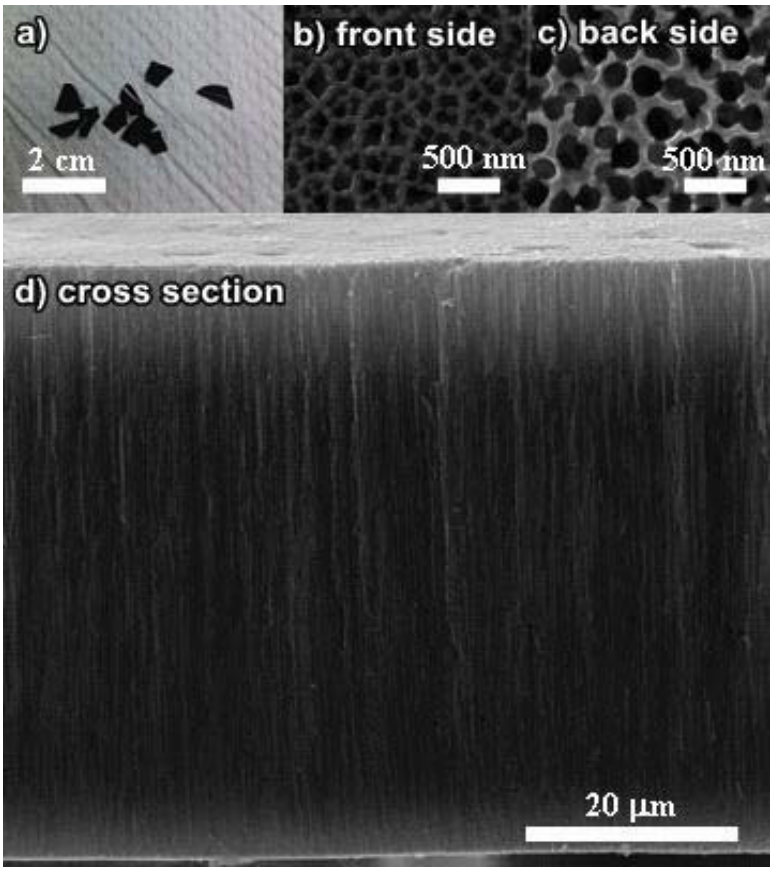

Figure 44 (a) Photograph and (b-c) SEM images of the VACNT/AAO sample prepared at 750 °C via the decomposition of C_2H_2, post-treated with the thermal annealing at 1000 °C for 4 h (under N_2 atmosphere) and the air oxidation at 500 °C for 1 h. (d) SEM image taken from the cross-section.

Figure 44a shows a photo of the VACNT/AAO sample prepared at 750 °C via the decomposition of C_2H_2 and post-treated by thermal annealing at 1000 °C for 4 h (under N_2 atmosphere) and air oxidation at 500 °C for 1 h. The black color of the sample indicates the existence of carbon materials. Figure 44b-d shows the SEM images of the sample confirming a successful removal of amorphous carbon from the VACNT/AAO product.

Figure 45a shows a photo of VACNTs prepared at 750 °C via the decomposition of C_2H_2 and post-treated by the thermal annealing at 1000 °C for 4 h (under N_2 atmosphere) and air oxidation at 500 °C for 1 h after the removal of the AAO template. It was found that although the AAO template was removed (by using HF), the tubes still stay together as bundles. It is due to the van der Waals interactions between them (Hertel *et al.*, 1998; Ruoff *et al.*, 1993). Additionally, the characteristics of the tubes including the straight, parallel and cylindrical structure, the average diameter of ~200 nm and the tube length of 60 μm were found to be preserved after the removal of the template (see Figure 45b-c).

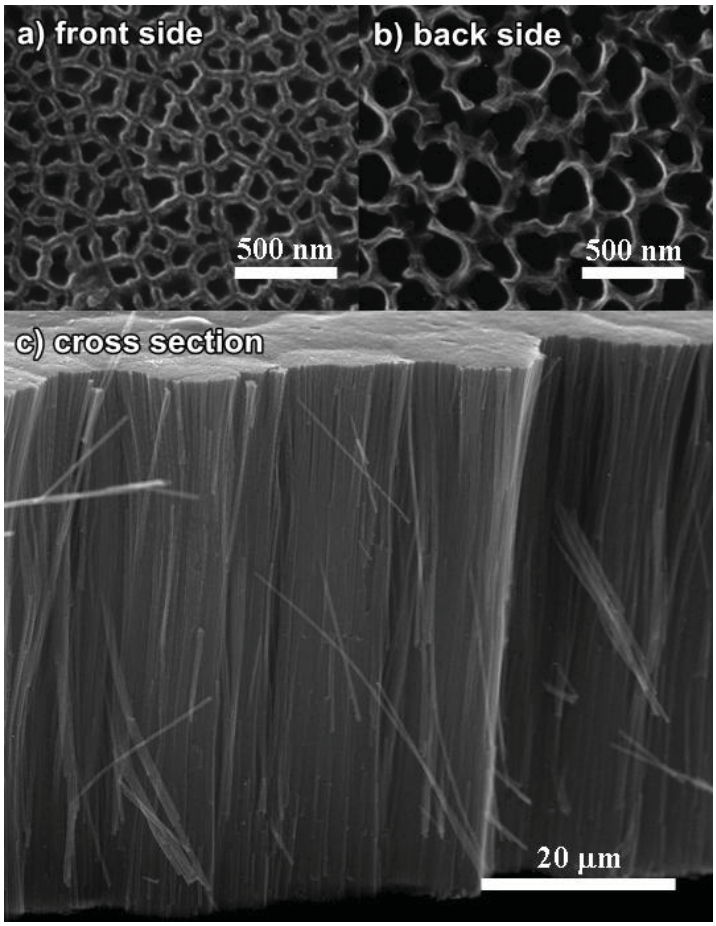

Figure 45 SEM images of the VACNT sample prepared at 750 °C via the decomposition of C_2H_2 through AAO template, post-treated with the thermal annealing at 1000 °C for 4 h (under N_2 atmosphere) and air oxidation at 500 °C for 1 h after the removal of the AAO template by using HF taken from the (a-b) top-view (from both sides) and (c) cross-section view.

The high-magnification cross-section SEM images focusing at both ends of the tubes (see Figure 46a-b) demonstrate that the tubes are open at both ends. As mentioned, this opening feature serves for the filling of the tubes with foreign molecules, ions or nanomaterials, and thus, opens up many related applications. It can also be observed from

the images that some tubes are branched in nature. This is due to the branched channels of the commercial AAO template.

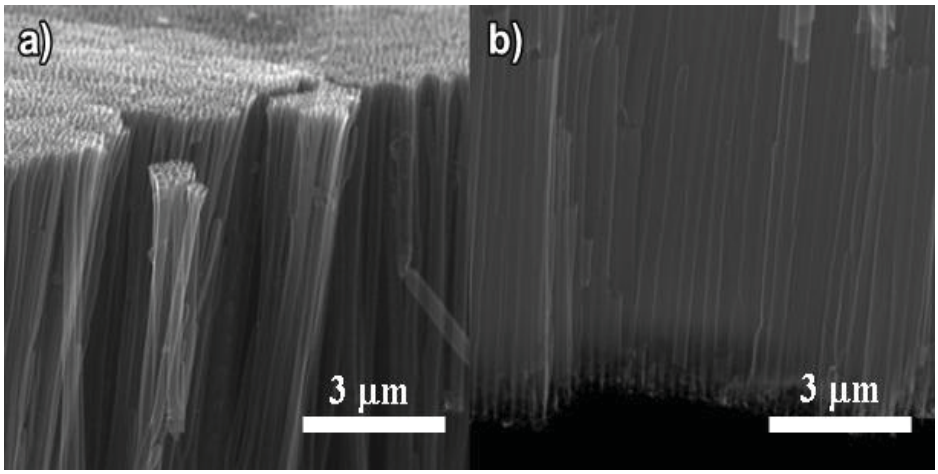

Figure 46 High magnification SEM images of the VACNT sample prepared at 750 °C via the decomposition of C_2H_2 through AAO template, post-treated by thermal annealing at 1000 °C for 4 h (under N_2 atmosphere) and air oxidation at 500 °C for 1 h after the removal of the AAO template by using HF taken from the cross-section view (from both sides) (a-b).

Raman spectroscopy , a non-destructive characterization technique that is widely employed for the characterization of CNTs, was used to provide information about the structural changes occurring during the treatments (Colomer *et al.*, 2000; Geng *et al.*, 2002; Lee *et al.*, 1999; Wepasnick *et al.*, 2010). Two main features in the Raman spectra of MWCNTs include D-band, the band at ~1350 cm^{-1}, which is associated with the disordered carbon defects of MWCNTs, and G-band, the band in the range of 1500-1600 cm^{-1}, which is attributed to the tangential vibrations of the graphitic carbon atoms (the fundamental Raman modes of crystalline graphite) (Eklund *et al.*, 1995; Geng *et al.*, 2002; Tuinstra and Koenig, 1970). The ratio between the D-band and the G-band (I_D/I_G) was used to evaluate of the degree of disorder of the tubes (Geng *et al.*, 2002; Tan *et al.*,

1997). A small I_D/I_G ratio suggests CNTs with the few defects and less amorphous carbon.

Raman spectra and the I_D/I_G ratios of the tubes prepared at 750 °C via the decomposition of C_2H_2 ("*as-synthesized VACNTs*"), the tubes prepared at 750 °C via the decomposition of C_2H_2 and post-treated with the thermal annealing at 1000 °C ("*as-annealed VACNTs"*) and the tubes prepared at 750 °C via the decomposition of C_2H_2, post-treated with the thermal annealing at 1000 °C for 4 h (under N_2 atmosphere) and air oxidation at 500 °C for 1 h (*"as-purified VACNTs"*) are shown in Figure 47. The D-band and G-band, which are the characteristics of MWCNTs, were found for all samples confirming the formation of the tubes via the synthesis and the preservation of the tubes during the treatment. The I_D/I_G ratio of the *as-annealed VACNTs* (1.04) is slightly lower than that of the *as-synthesized VACNTs* (1.07) indicating a slight improvement of the graphiticity of the tubes via the annealing process (at 1000 °C). The I_D/I_G ratio of the *as-purified VACNTs* (1.06) is slightly higher than that of the *as-annealed VACNTs* (1.04) indicating a lowering of the graphiticity of the tubes due to the air oxidation (at 500 °C). Nevertheless, the I_D/I_G ratio of the *as-purified VACNTs* (1.06) is almost comparable to that of the *as-annealed VACNTs* (1.04) indicating that, via the post-treatment, the graphiticity of the tubes was mainly preserved. Then the post-treatment performed in this study is considered to be a suitable process for the removal of amorphous carbon from the tube product.

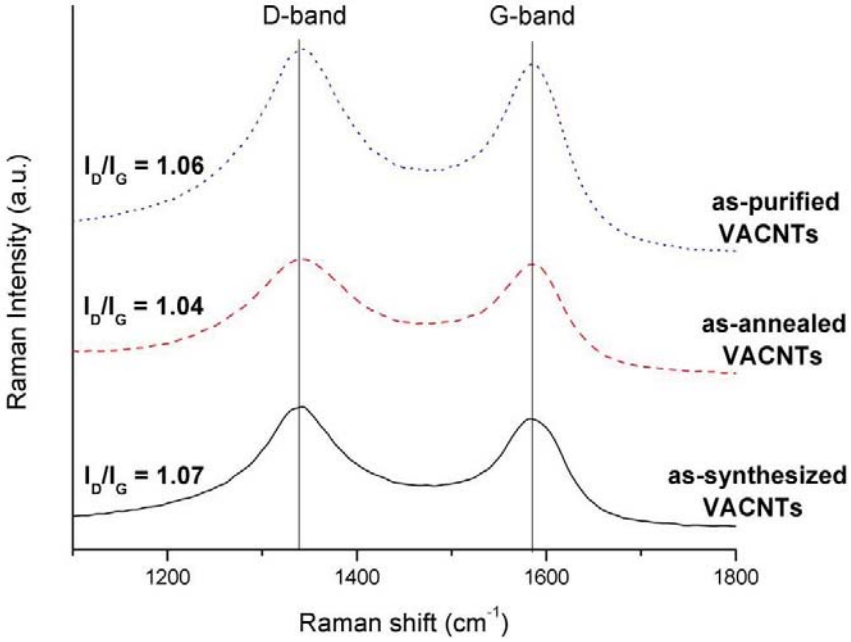

Figure 47 Raman spectra and the I_D/I_G ratios of the tubes prepared at 750 °C via the decomposition of C_2H_2 ("*as-synthesized VACNTs*"), the tubes prepared at 750 °C via the decomposition of C_2H_2 and post-treated by thermal annealing at 1000 °C for 4 h (under N_2 atmosphere) ("*as-annealed VACNTs"*) and the tubes prepared at 750 °C via the decomposition of C_2H_2, post-treated by thermal annealing at 1000 °C for 4 h (under N_2 atmosphere) and air oxidation at 500 °C for 1 h (*"as-purified VACNTs"*).

Figure 48 shows the TEM image of the *as-purified sample* evidencing the formation of VACNTs. As the tubes were broken during the sonication process, some short tube fractions can be seen in the image. The outer diameter of the tubes is found to be variable due to a range of diameters in the AAO template itself, the average diameter of the tubes being < 200 nm. The tubes are found to be branched at the ends and some ends are closed because of the nature of the commercial AAO template, however most tubes have an open end.

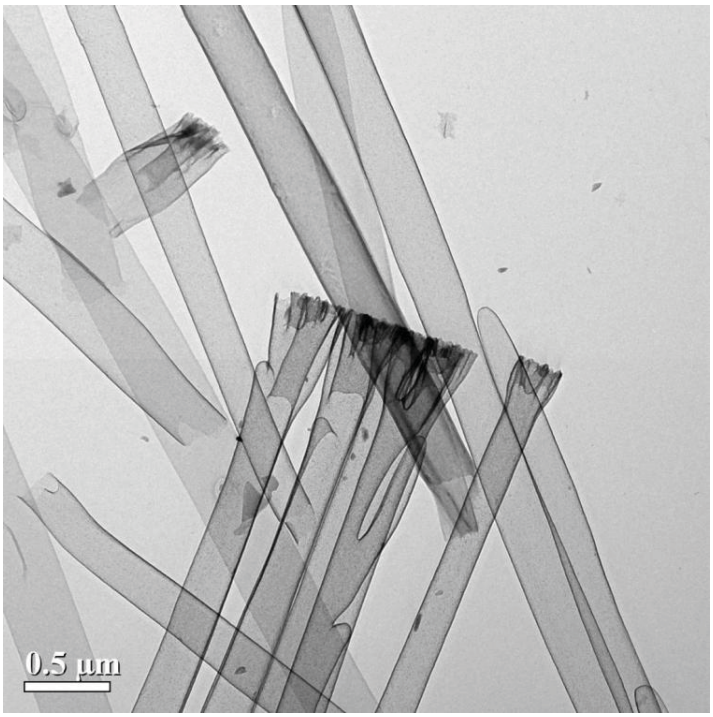

Figure 48 TEM image of the tubes prepared at 750 °C via the decomposition of C_2H_2, post-treated by thermal annealing at 1000 °C and air oxidized at 500 °C for 1 h (*"as-purified VACNTs"*).

3.2. Asymmetric electrografting of 4-aminobenzene on VACNTs via bipolar electrochemical reduction of 4-nitrobenzenediazonium salts

For the bipolar configuration, a disposable cuvette was used as bipolar cell. In order to simplify the experimental set-up, the ion-selective membranes were not used in this work. These membranes are usually used to avoid the classical electrochemical reactions at the feeder electrodes, and thus a loss of the ions supplied for the redox reactions on the bipolar electrode and also to avoid disturbing the reactions at the BPE. The obtained VACNT/AAO membrane, which was post-treated by the thermal annealing at 1000 °C for 4 h and the air oxidation at 500 °C for 1 h, was introduced into the cuvette with their top surfaces facing the walls of the cuvette and located in the middle of the

cuvette (see Figure 49). The sample was not in Ohmic contact with the feeder electrodes. The feeder electrodes were arranged vertically and parallel to the top surfaces of the VACNT/AAO membrane and connected to a high-voltage power supply by using steel crocodile clips. Only the membrane and the ends of the feeder electrodes were suspended in the solution.

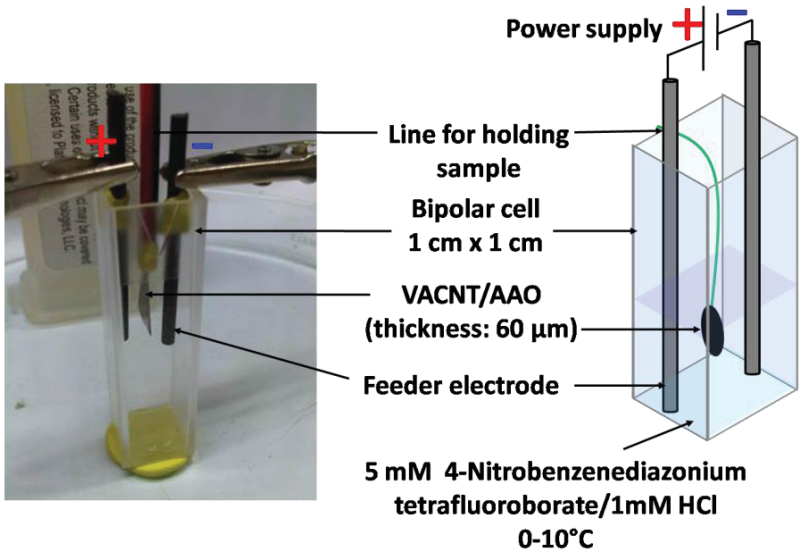

Figure 49 Photo and schematic illustration showing the experimental set-up for asymmetric electrografting of 4-aminobenzene on VACNTs embedded in the AAO membrane with the feeder electrodes being arranged vertically.

For this configuration, we found that it is not possible to apply the desired electric field to the system for a long time. After a few seconds of the application of electric field, the electrical current in the system reached the maximum limitation of the power supply. Then, the electric field was automatically stopped. This reaction time (few seconds) is too short to provide the desired deposition. For this reason, in the next step, we attempted to reduce the current of the system by reducing the surface area of the feeder electrodes immersed in the solution. The feeder electrodes were arranged horizontally (see Figure 50).

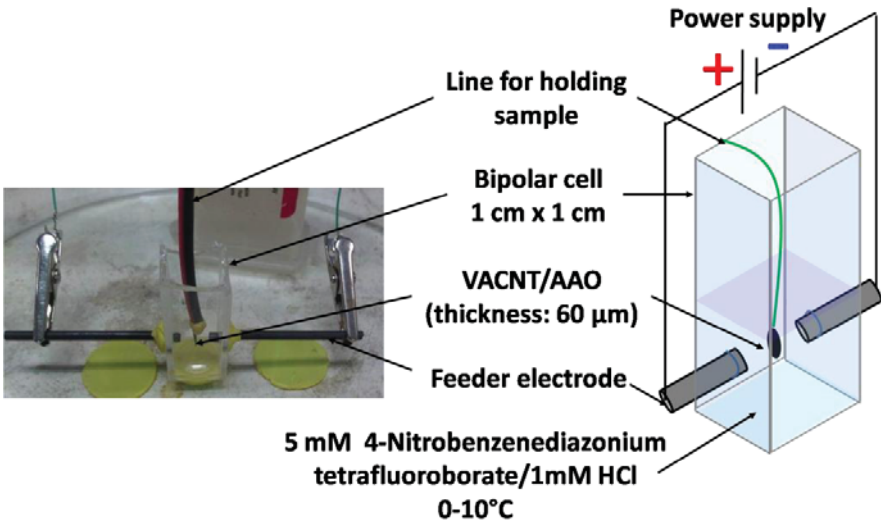

Figure 50 Photo and schematic illustration showing the experimental set-up for asymmetric electrografting of 4-aminobenzene on VACNTs embedded in the AAO membrane with the feeder electrodes being arranged horizontally.

With this configuration, we could apply a voltage of 400 V to the system for a longer time of up to 30 s. However, we found that during the application of the electric field, the temperature of the solution was increasing due to the passage of an electric current through the solution. This temperature increase can induce the grafting of diazonium on the tube surface via a thermal reaction, which cannot be controlled to be site-selective (Delamar *et al.*, 1992; Sagar, 1996). Thus, the asymmetric deposition on VACNTs was then expected to be not achieved. For this reason, we tried to keep the temperature of the solution as constant as possible. The cooling unit, simply constructed by using an ice bath composed of a container filled with ice, water and sodium chloride (NaCl) salt, was introduced around the bipolar cell (see Figure 51). This configuration allows us to apply a voltage of 400 V for up to 120 s without boiling of the working solution. Thus, we used this configuration for the asymmetric electrografting of 4-

aminobenzene on VACNTs via the bipolar electrochemical reduction of 4-nitrobenzenediazonium salts.

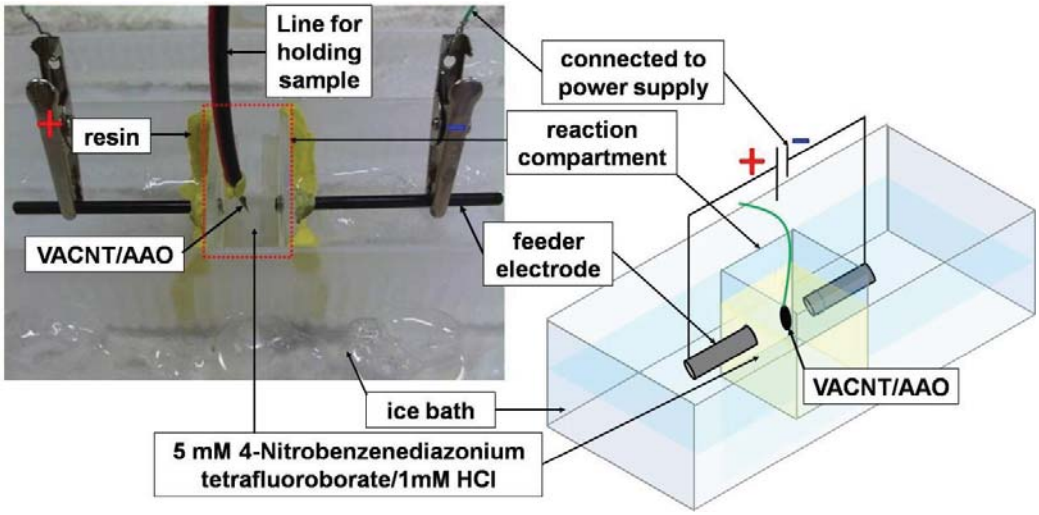

Figure 51 Photo and schematic illustration showing the experimental set-up for asymmetric electrografting of 4-aminobenzene on VACNTs embedded in the AAO membrane with a cooling unit around the bipolar cell.

Nevertheless, it was observed from the TEM image of the tubes, which were obtained after i) the grafting of 4-aminobenzene moieties onto the inner surface of the tubes by using the voltage of 400 V and a deposition time ranging from 30 to 120 s, ii) the protonation of the amine groups of the 4-aminobenzene moieties in an HCl solution, iii) the electrostatic coupling of the protonated amine groups with the labeling materials (the negatively charged citrate-capped AuNPs), and iv) the removal of AAO template (by using HF) that there are no AuNPs present on the surface of CNTs. In other words, there is no grafting of the 4-aminobenzene moieties on the tube surface. AuNPs cannot be observed from the TEM images both in the cases of individual tubes (Figure 52a) and CNT bundles (Figure 52b). We suggest that this is because the VACNT/AAO membrane was not conductive enough to allow the electron transfer necessary for the bipolar reactions. This is due to the insulating nature of the AAO material (alumina). For this

reason, in the next step, we attempted to enhance the efficiency of the bipolar electrografting by disclosing partly the ends of the VACNT bundle that is embedded in the AAO membrane via the removal of the AAO top surface using HF solution.

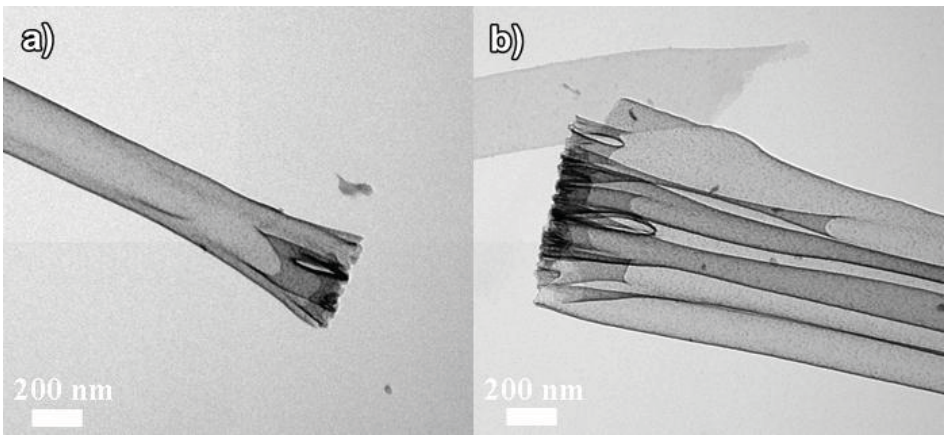

Figure 52 TEM images of (a) an individual CNT and (b) a CNT bundle obtained after i) the grafting of 4-aminobenzene moieties onto the inner surface of the tubes by using a voltage of 400 V and a deposition time ranging from 30 to 120 s, ii) the protonation of the amine groups of the 4-aminobenzene moieties in an HCl solution, iii) the electrostatic coupling of the protonated amine groups with the labeling materials (the negatively charged citrate-capped AuNPs), and iv) the removal of the AAO template (by using HF).

3.2.1. Opening of both ends of the VACNT bundle

Hydrofluoric acid solutions with different concentrations (including 50%, 25% and 12.5% w/v) were used to remove alumina partly from the top surface at both ends of the as-prepared VACNT/AAO membrane together with the use of the suction filter system. It was found that, by dropping only few drops of the 50% HF solution onto the surface of the VACNT/AAO membrane for a short time, the membrane was corroded

immediately to small pieces (see Figure 53a). This result indicates that this acid concentration is too high for keeping the membrane structure. The SEM image taken from the top of the treated membrane (see Figure 53b) shows that the treatment causes severe corrosion of the alumina from the membrane surface. The outer surface of the tubes was highly opened by the treatment (see Figure 53c). This makes the sample not suitable to be used for the selective grafting of the organic layer onto the inner surface of the tubes because the grafting is expected to occur also at the outer surface of the tubes. In the next step, we then used the HF solution with the lower concentration of 25%.

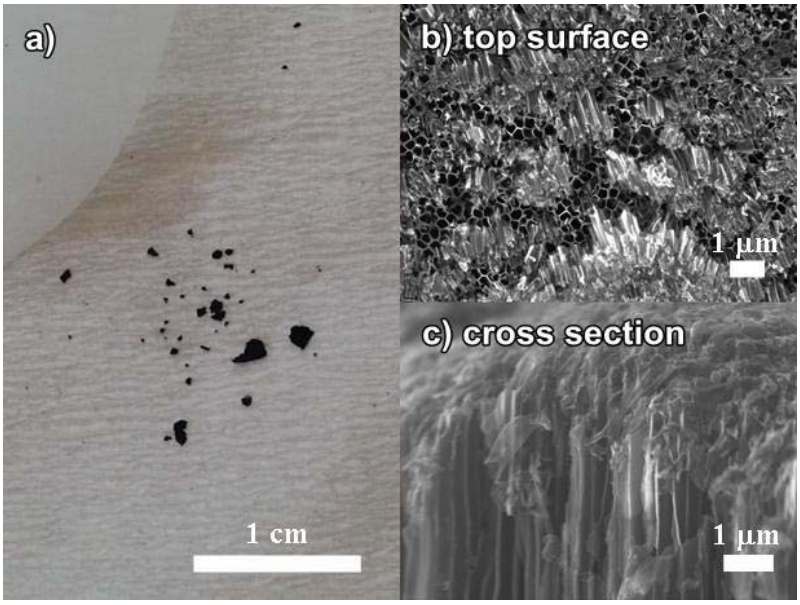

Figure 53 (a) Photograph and (b-c) SEM images with the (b) top-surface and (c) cross-section views of the VACNT/AAO sample prepared at 750 °C via the decomposition of C_2H_2, post-treated by thermal annealing at 1000 °C for 4 h (under N_2 atmosphere) and air oxidation at 500 °C for 1 h in which both ends of the VACNT bundle were partly exposed by using a 50% HF solution.

In the case of using the 25% HF acid solution, the resultant was similar to the case of using the 50% HF acid solution. Therefore, we used the HF solution with the lower concentration of 12.5%.

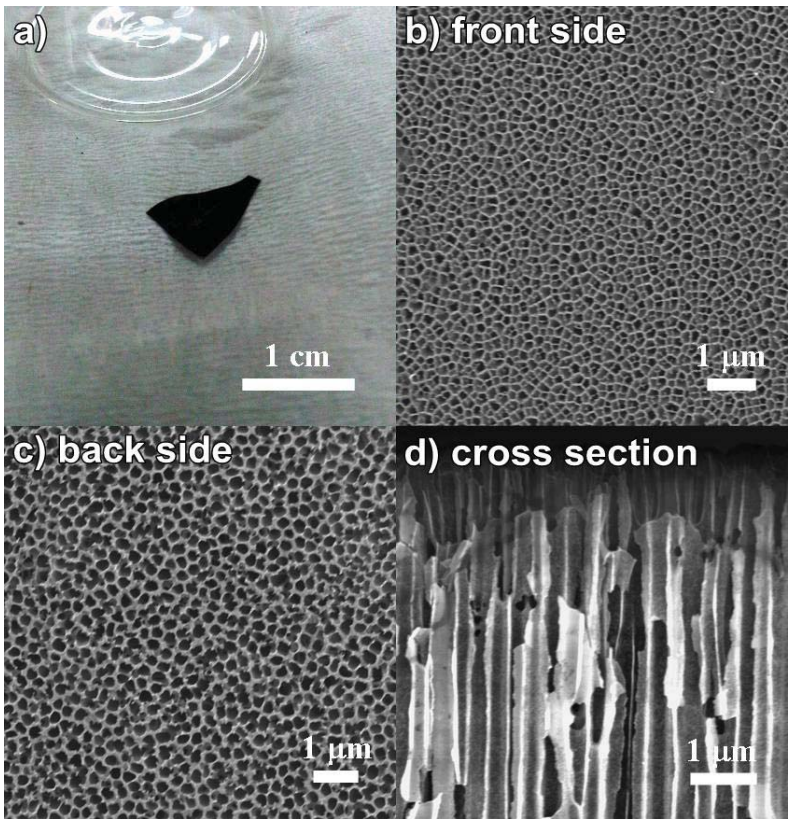

Figure 54 (a) Photograph and (b-d) SEM images with the (b-c) top-surface (at both sides) and (d) cross-section views of the VACNT/AAO sample prepared at 750 °C via the decomposition of C_2H_2, post-treated by thermal annealing at 1000 °C for 4 h (under N_2 atmosphere) and air oxidation at 500 °C for 1 h in which both ends of the VACNT bundle were partly exposed to a 12.5% HF solution.

By using the 12.5% HF acid solution, the membrane structure could be preserved (see Figure 54a). The SEM images with low magnification taken from the top of the

treated membrane on both sides (Figure 54b-c) show that the treatment did not remove significantly alumina from the membrane surface. The membrane surface on both sides still looks similar to that of the untreated one. However, via the image with high magnification, the opening of the VACNT bundle at the ends was clearly observed. Then, we further used this treatment for the selective grafting of the organic layer onto the inner surface of the tubes.

To promote the asymmetric electrografting of the organic layer onto the inner surface of the tubes embedded in the VACNT/AAO membrane, we first attempted to use a voltage of 400 V (corresponding to an electric field of 40 kV m^{-1}), which was expected to be enough to drive the desired redox reactions across tubes with a length of < 60 μm in the bipolar cell with the distance between the feeder electrodes of 1 cm. During that experiment, we observed the generation of a substance with orange color and gas bubbles at the cathodic and the anodic sides of the BPE, respectively. This finding corresponds well to the redox reactions expected to occur at both sides of the BPE (see Figure 55). The evolution of the substance with orange color corresponds well to the reduction of 4-nitrobenzenediazonium salts (see step 2 in Figure 34). While the gas bubbles are expected to be the evolution of the oxygen bubbles due to water oxidation that occurs rapidly until the gas bubbles can be seen (Warakulwit, 2007). Although gas bubbles were formed, we assumed that they will not disturb the grafting of the organic layer on the other side of the membrane. This is because in our set-up the membrane is fixed. The SEM images of the VACNT/AAO sample obtained after i) the grafting of 4-aminobenzene moieties onto the inner surface of the tubes by using a voltage of 400 V and a deposition time of 30 s, ii) the protonation of the amine groups of the 4-aminobenzene moieties in an HCl solution and iii) the electrostatic coupling of the protonated amine groups with the labeling materials (the negatively charged citrate-capped AuNPs) (see Figure 56) suggest that electrografting of the 4-aminobenzene moieties on the tube surface occurred under the current experimental conditions as AuNPs can be observed.

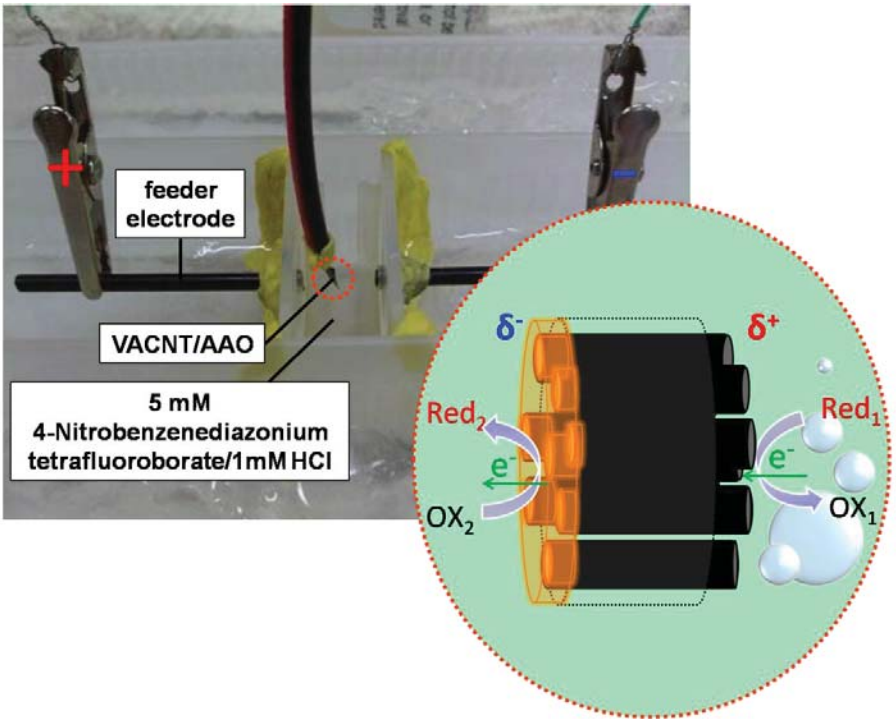

Figure 55 Photo and schematic illustration showing the experimental set-up and the redox reactions that are expected to occur at both sides of the BPE (the VACNT/AAO membrane). The reduction of 4-nitrobenzenediazonium salts (the coating with orange color) and the water oxidation (the evolution of gas bubbles) are expected to occur at the cathodic and anodic sides of the BPE, respectively.

The top-view high magnification SEM image of the cathodic side of the modified membrane is shown in Figure 56a. The presence of AuNPs in the images confirms the successful grafting of the 4-aminobenzene moieties on the inner surface of the tubes at the cathodic side of the membrane. The top-view high magnification SEM image of the anodic side of the membrane (see Figure 56b) in which AuNPs cannot be seen confirms the selective grafting of the organic layer on one side (the cathodic side) of the VACNT/AAO membrane.

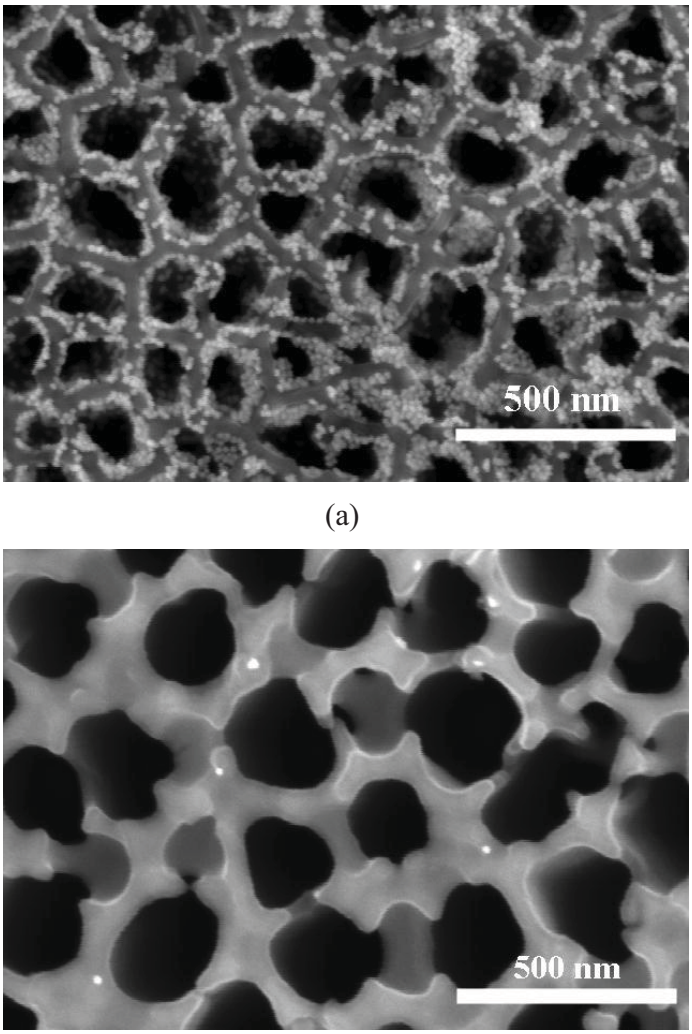

Figure 56 High-magnification FE-SEM images with the top-surface view of the VACNT/AAO sample at the (a) cathodic and (b) anodic sides. The sample was obtained after i) the grafting of 4-aminobenzene moieties onto the inner surface of the tubes by using a voltage of 400 V (corresponding to an electric field of 40 kV m^{-1}) and a deposition time of 30 s, ii) the protonation of the amine groups of the 4-aminobenzene moieties in an HCl solution and iii) the electrostatic coupling of the protonated amine groups with the labeling materials (the negatively charged citrate-capped AuNPs).

The chemical composition of the anodic and cathodic side has been characterized via the EDX technique (Figure 57). The EDX data corresponding to the SEM images of the cathodic side indicate the presence of carbon (C) (from CNTs), oxygen (O) and aluminium (Al) (from the alumina composition) and gold (Au) (derived from AuNPs). The calculated Au content is rather high (7.91 atomic %) at this side and neglectable (0.051 atomic %) at the anodic side (while other chemical compositions are almost preserved). This finding confirms again the selective grafting of the organic layer on the cathodic side of the VACNT/AAO membrane.

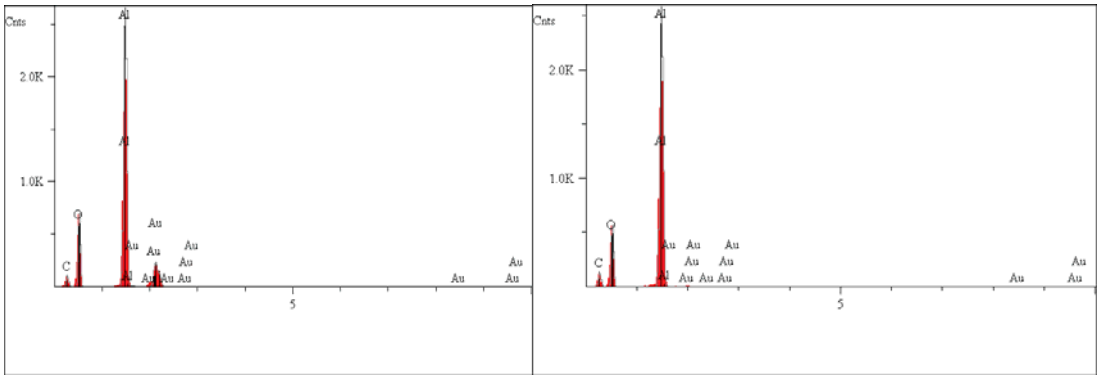

(a) (b)

Figure 57 The EDX data corresponding to the SEM images of Figure 56a and 56b for the (a) cathodic and (b) anodic sides.

After that the sample was treated with a 50% HF acid solution in order to remove completely the AAO template. The SEM images of the resulting sample are shown in Figure 58a-b, respectively. Figure 58a clearly shows the presence of AuNPs on the tube surface at the cathodic side although the amount of the particles is less than that found in the as-prepared sample (before the removal of AAO). We suggest that the remaining particles have a strong interaction with the tube surface. Thus, they could withstand the removal of AAO by using the strong HF solution. Figure 58b clearly shows the absence of AuNPs on the tube surface at the anodic side. This finding clearly confirms the

selective grafting of the organic layer on the cathodic side of the VACNT/AAO membrane.

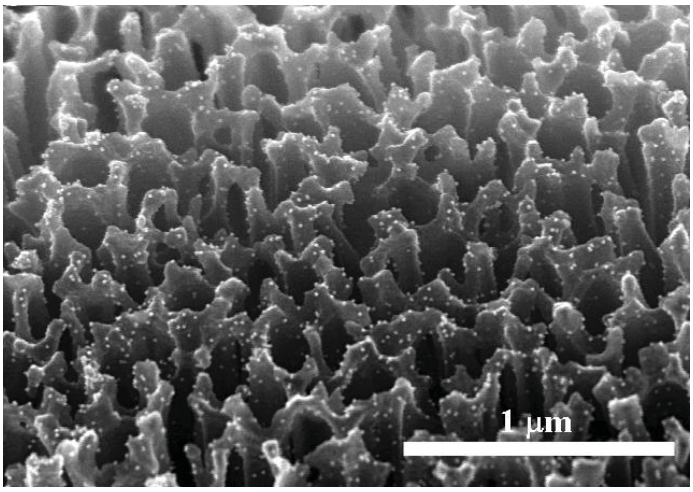

(a)

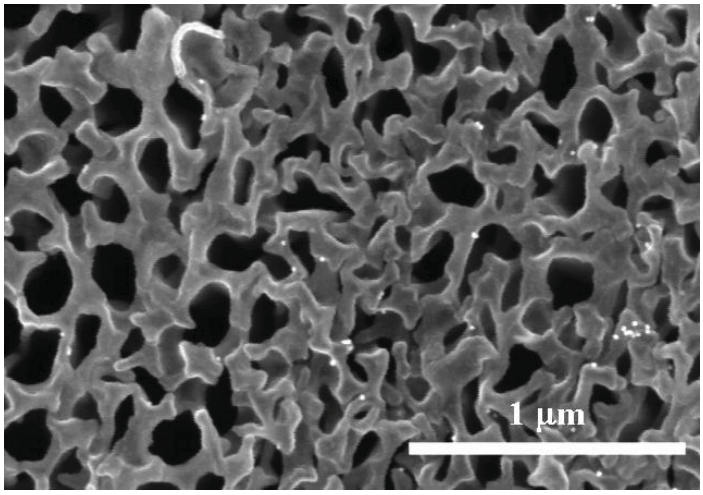

(b)

Figure 58 FE-SEM images with the top-surface view of a bundle of VACNTs focused on the (a) cathodic and (b) anodic sides obtained from the removal of AAO template (by using HF) from the sample corresponding to Figure 56a and 56b, respectively.

The low magnification TEM images of the sample are shown in Figure 59. It can be seen from the images that AuNPs are located selectively at one end of the tubes although most of the tubes were shortened due to the sonication employed in the step of sample preparation for the TEM characterization.

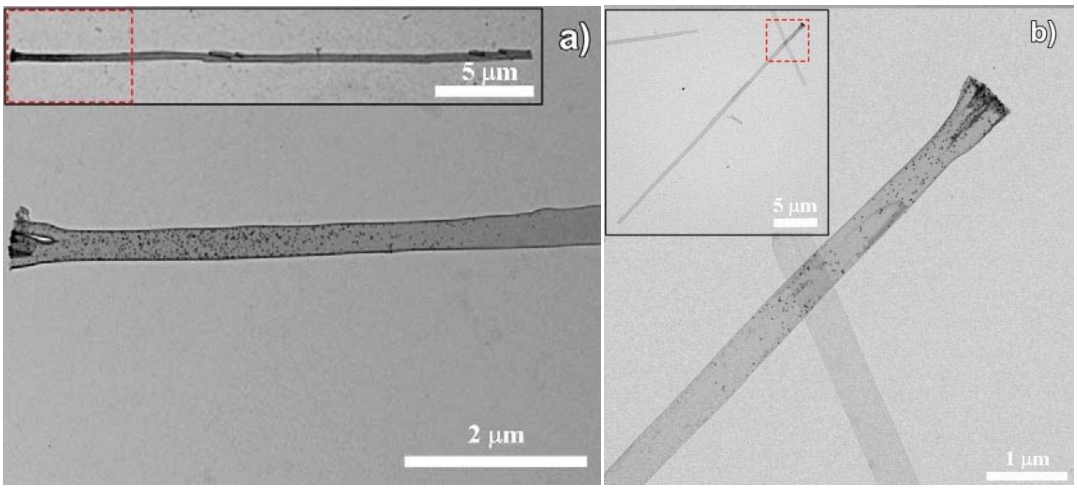

Figure 59 TEM images of the tubes obtained after the bipolar electrografting of 4-aminobenzene moieties onto the inner surface of the tubes by using an electric field of 40 kV m^{-1} for 30 s, the protonation of the 4-aminobenzene moieties in HCl solution, the coupling with the citrate-capped AuNPs, and the removal of AAO template.

The high magnification TEM images of the sample are shown in Figure 60a-b. It can be seen from the images that AuNPs are located selectively inside of the tubes revealing the successful asymmetric electrografting of 4-aminobenzene on the inner surface of the tubes. Figure 60c shows that the particles located at the tube surface have comparable size compared to the as-prepared particles although the sample underwent the harsh treatment with the concentrated HF. For this reason, we suggested that the technique using the citrate-capped AuNPs is suitable for labeling the asymmetric electrografting of 4-aminobenzene on CNTs.

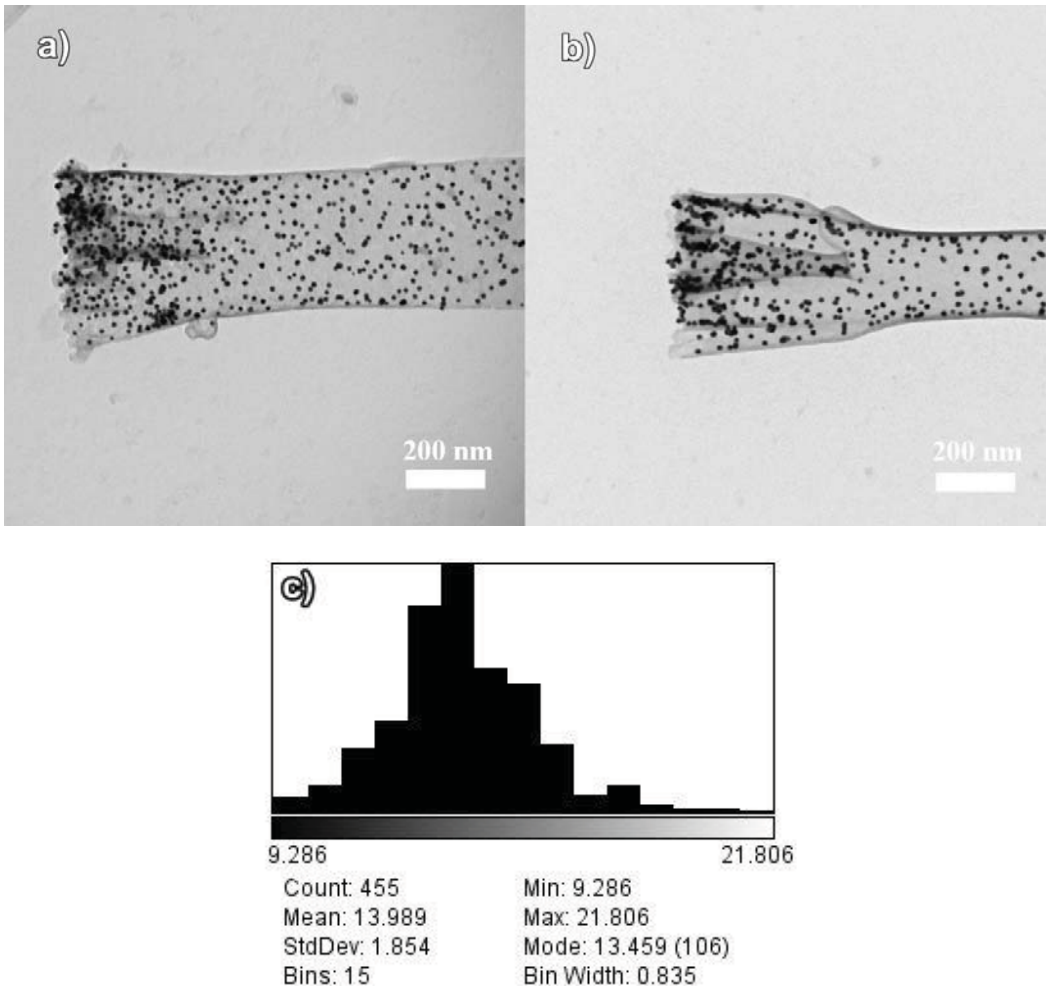

Figure 60 (a-b) High-magnification TEM images of the tubes corresponding to the TEM image of Figure 59 for the cathodic side. (c) Histogram showing the particle size distribution of AuNPs deposited onto the tube surface.

In order to investigate the role of the deposition time on the bipolar electrografting of 4-aminobenzene onto VACNTs, an additional experiment was performed by using the same bipolar configuration and a voltage of 400 V (corresponding to an electric field of 40 kV m^{-1}), but with a longer deposition time of 120 s.

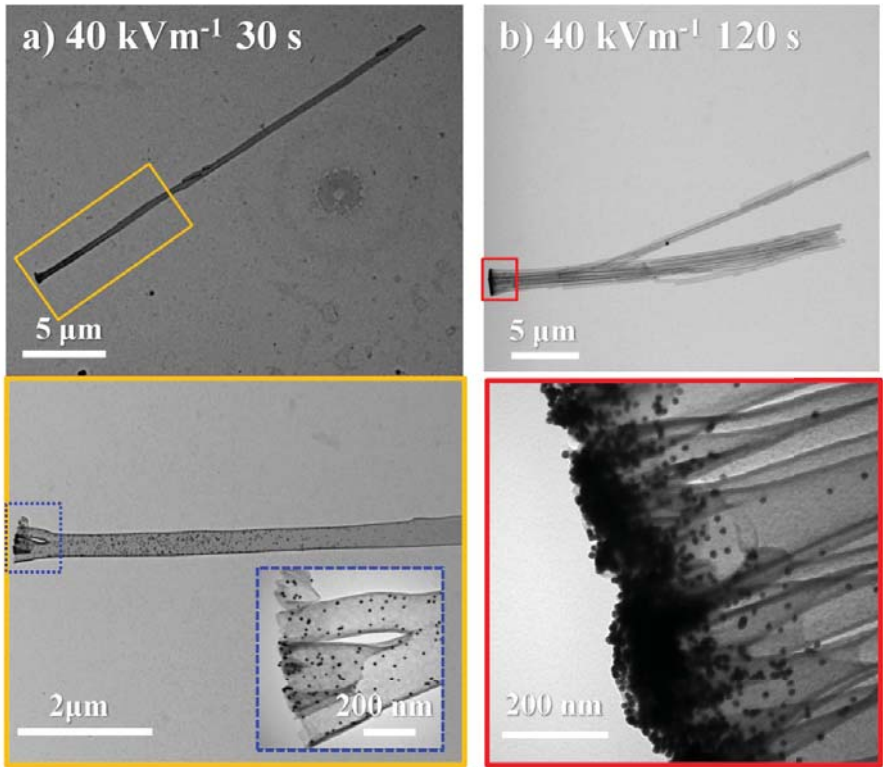

Figure 61 TEM images of the tubes obtained after the bipolar electrografting of 4-aminobenzene moieties onto the inner surface of the tubes by using the electric field of 40 kV m^{-1} and the deposition time of 30 s (a) and 120 s (b), the protonation of the 4-aminobenzene moieties in HCl solution, the coupling with the citrate-capped AuNPs, and the removal of AAO template.

Figure 61 shows the TEM images of the obtained sample. It is interesting that we found that the increase of deposition time does not result in an increase in the area where AuNPs are deposited on the tube surface. In other words, there is no increase of the area that is grafted by 4-aminobenzene moieties, but it results in the grafting of the dense organic layer onto the tube inner surface (see Figure 61b). This leads to the clogging of the entrance of the tube channels that can be revealed by the high amount of AuNPs located at the tube extremity. We suggest that this is because, in the case of CNTs, their average diameter is rather small (< 200 nm). Then, when the inner surface of the tubes

undergoes the deposition for a relatively long time, the organic layer may be too dense, and thus, preventing the penetration of the redox active ions into the tube channels. As a result, the deposition continues only at the tube extremity where the ions can be supplied. From this finding, we conclude that the bipolar electrochemical technique employed in this work can not only introduce an organic layer or a biocompatible functional groups on the tube surface but also can be employed to create a dense organic layer as a cap of the tubes opening up applications in the field of drug delivery.

4. Conclusions

In conclusion, the asymmetric electrografting of the amino-terminated substituted aryl moieties (4-aminobenzene) onto carbon nanotubes was performed via the bipolar electrochemical reduction of 4-nitrobenzenediazonium salts as a proof-of-concept experiment with the aim to establish bipolar electrochemistry as a technique for the production of nanoscale Janus-type objects. Vertically aligned multi-walled carbon nanotubes prepared in the pores of an aluminum oxide template via chemical vapor deposition were used. Prior to the bipolar experiments, they were thermally annealed (re-ordering of the structure) under nitrogen atmosphere and air oxidized (removing the carbonaceous impurities such as the amorphous carbon from the sample). It was found that the employed treatment can remove the amorphous carbon from the sample without a significant change in the graphiticity (crystallinity) of the tubes compared to the as-synthesized ones. After that, the membrane was treated with HF acid solution to expose partly the tube ends, thus improving the polarization by the applied electric field in the bipolar experiments. It was found that an HF solution with a concentration of 12.5% is suitable. The membrane structure is preserved. Only the part at the tube extremities was removed. Then, the modification can be controlled to occur almost only on the inner surface of the tubes. By using an in-house bipolar cell simply made of a disposal cuvette as the solution reservoir equipped with two carbon rods that were horizontally aligned in the cell as the feeder electrodes, a power supply and a water cooling unit, an organic layer

of 4-aminobenzene was selectively grafted over the inner surface at the cathodic side of the tubes (whereas the water oxidation was generated at the anodic side) under an electric field of 40 kV m^{-1} and a deposition time of 30 s. For this reason, the bipolar electrochemical technique employed in this work can introduce an organic layer or biocompatible functional groups onto the tube surface selectively, thus extending the applications of CNTs in the fields of bio-fuel cell, bio-electrocatalyst and bio-sensing. For a prolonged deposition time of 120 s, we obtained a dense organic layer at the tube ends. For this reason, the bipolar electrochemical technique employed in this work can also serve to create a dense organic layer as a cap of the tubes, opening up applications in the fields of drug delivery and storage.

CHAPTER IV: CONCLUDING REMARKS

This thesis presents the use of bipolar electrochemistry as a new technique for generating Janus-type objects with hybrid organic-inorganic composition. The surface of carbon objects with various natures ranging from isotropic to anisotropic and various sizes ranging from micro- to nano-scale have been modified in a controllable manner based on a precise control of the deposition time and the applied electric field.

The asymmetric modification of micrometer-sized glassy carbon beads were first performed via two different strategies, the bipolar electrochemical reduction of 4-nitrobenzenediazonium salts and *in situ* generated 4-carboxyphenyl diazonium salts as proof-of-concept experiments. These strategies lead to the successful grafting of different functional groups such as amino and carboxylic acid substituents selectively on one side (cathodic side) of the carbon beads whereas water is oxidized at another side, generating the oxygen bubbles (anodic side). The asymmetric grafting of the amino groups was revealed by charging the modified bead positively under acidic condition, and subsequent coupling with negatively-charged gold nanoparticles via the electrostatic interactions. The carbon beads modified with carboxylic acid groups were indirectly visualized by coupling the carboxylic acid moieties and the functional amino groups of a fluorescent molecule in the presence of carbodiimide reagent as the coupling agent. Additionally, we found that the asymmetric grafting of Janus-type beads in terms of geometric area can be easily tuned by varying the deposition time and/or the applied electric field used for the reduction of the diazonium salts. The Janus-type beads obtained via the asymmetric grafting of aryl diazonium salts with various substituents can be further developed in a straight forward way. It is now possible to create a platform for linking other molecules, leading to promising perspectives in the field of bio-sensing applications and enzymatic bio-fuel cells.

Apart from the production of microscale Janus-type beads, this versatile and attractive approach on bipolar electrochemistry can be also generalized for the production of nanoscale asymmetric objects. Vertically aligned carbon nanotubes (VACNTs) grown over the inner wall of the pores of an anodic aluminum oxide (AAO) template (VACNT/AAO) were prepared via a CVD technique and used as bipolar electrode. The presence of AAO during the bipolar experiments intrinsically protects the outer surface of the tubes from the grafting of the 4-aminobenzene moieties. Therefore the organic layer is not only selectively grafted at the cathodic side of the tubes but also selectively grafted onto the inner surface of the tubes. Depending on the deposition time, the grafted area can be controlled. For short deposition times (30 s), the inner surface of the tubes was selectively modified with the organic layer at the cathodic side. Interestingly, for a longer deposition time (120 s), the ends of the tubes were capped with a dense organic layer of 4-aminobenzene. For this reason, the employed bipolar electrochemical technique can not only generate CNTs bearing organic functionalities on the tube surface for bio-sensing or bio-electrocatalytic applications, but also can create a dense organic layer as a cap at one end of the tubes, opening up applications in the fields of drug delivery and storage.

LITERATURE CITED

Adenier, A., N. Barré, E. Cabet-Deliry, A. Chaussé, S. Griveau, F. Mercier, J. Pinson and C. Vautrin-Ul. 2006. Study of the spontaneous formation of organic layers on carbon and metal surfaces from diazonium salts. **Surf. Sci.** 600(21):4801-4812.

Allongue, P., M. Delamar, B. Desbat, O. Fagebaume, R. Hitmi, J. Pinson and J.-M. Savéant. 1997. Covalent Modification of Carbon Surfaces by Aryl Radicals Generated from the Electrochemical Reduction of Diazonium Salts. **J. Am. Chem. Soc.** 119(1):201-207.

Altalhi, T., M. Ginic-Markovic, N. Han, S. Clarke and D. Losic. 2010. Synthesis of Carbon Nanotube (CNT) Composite Membranes. **Membranes** 1(1):37-47.

Andrews, R., D. Jacques, A.M. Rao, F. Derbyshire, D. Qian, X. Fan, E.C. Dickey and J. Chen. 1999. Continuous production of aligned carbon nanotubes: a step closer to commercial realization. **Chem. Phys. Lett.** 303(5–6):467-474.

Andrieux, C.P. and J. Pinson. 2003. The Standard Redox Potential of the Phenyl Radical/Anion Couple. **J. Am. Chem. Soc.** 125(48):14801-14806.

Aveyard, R., B.P. Binks and J.H. Clint. 2003. Emulsions stabilised solely by colloidal particles. **Adv. Colloid Interface Sci.** 100–102(0):503-546.

Avouris, P., J. Appenzeller, R. Martel and S.J. Wind. 2003. Carbon nanotube electronics. **P. IEEE** 91(11):1772-1784.

Babu, S., P. Ndungu, J.-C. Bradley, M. Rossi and Y. Gogotsi. 2005. Guiding water into carbon nanopipes with the aid of bipolar electrochemistry. **Microfluid. Nanofluid.** 1(3):284-288.

Bahr, J.L., J. Yang, D.V. Kosynkin, M.J. Bronikowski, R.E. Smalley and J.M. Tour. 2001. Functionalization of Carbon Nanotubes by Electrochemical Reduction of Aryl Diazonium Salts: A Bucky Paper Electrode. **J. Am. Chem. Soc.** 123(27):6536-6542.

Baranton, S. and D. Bélanger. 2005. Electrochemical Derivatization of Carbon Surface by Reduction of in Situ Generated Diazonium Cations. **J. Phys. Chem. B** 109(51):24401-24410.

Barbier, B., J. Pinson, G. Desarmot and M. Sanchez. 1990. Electrochemical Bonding of Amines to Carbon Fiber Surfaces Toward Improved Carbon-Epoxy Composites. **J. Electrochem. Soc.** 137(6):1757-1764.

Bard, A.J. and L.R. Faulkner. 2001. **Electrochemical Methods: Fundamentals and Applications.** 2nd. John Wiley & Sons, Inc.

Bard, A.J., R. Parsons and J. Jordan. 1985. **Standard Potentials in Aqueous Solution.** Dekker. New York.

Barone, P.W. and M.S. Strano. 2006. Reversible Control of Carbon Nanotube Aggregation for a Glucose Affinity Sensor. **Angew. Chem. Int. Edit.** 45(48):8138-8141.

Belanger, D. and J. Pinson. 2011. Electrografting: a powerful method for surface modification. **Chem. Soc. Rev.** 40(7):3995-4048.

Binks, B.P. and S.O. Lumsdon. 2001. Pickering Emulsions Stabilized by Monodisperse Latex Particles: Effects of Particle Size. **Langmuir** 17(15):4540-4547.

Bouffier, L. and A. Kuhn. 2013. Design of a wireless electrochemical valve. **Nanoscale** 5(4):1305-1309.

Bourdillon, C., M. Delamar, C. Demaille, R. Hitmi, J. Moiroux and J. Pinson. 1992. Immobilization of glucose oxidase on a carbon surface derivatized by electrochemical reduction of diazonium salts. **J. Electroanal. Chem.** 336(1–2):113-123.

Bradley, J.-C., S. Babu, A. Mittal, P. Ndungu, B. Carroll and B. Samuel. 2001. Pulsed Bipolar Electrodeposition of Palladium onto Graphite Powder. **J. Electrochem. Soc.** 148(9):C647-C651.

Bradley, J.-C. and Z. Ma. 1999. Contactless Electrodeposition of Palladium Catalysts. **Angew. Chem. Int. Edit.** 38(11):1663-1666.

Bradley, J.C., S. Babu and P. Ndungu. 2005. Contactless Tip-Selective Electrodeposition of Palladium onto Carbon Nanotubes and Nanofibers. **Fuller. Nanotub. Car. N.** 13(3):227-237.

Bradley, M. and B.S. Garcia-Risueño. 2011. Symmetric and asymmetric adsorption of pH-responsive gold nanoparticles onto microgel particles and dispersion characterisation. **J. Colloid Interf. Sci.** 355(2):321-327.

Brooksby, P.A. and A.J. Downard. 2004. Electrochemical and Atomic Force Microscopy Study of Carbon Surface Modification via Diazonium Reduction in Aqueous and Acetonitrile Solutions. **Langmuir** 20(12):5038-5045.

Brooksby, P.A. and A.J. Downard. 2005. Multilayer Nitroazobenzene Films Covalently Attached to Carbon. An AFM and Electrochemical Study. **J. Phys. Chem. B** 109(18):8791-8798.

Casagrande, C., P. Fabre, E. Raphaël and M. Veyssié. 1989. "Janus Beads": Realization and Behaviour at Water/Oil Interfaces. **Europhys. Lett.** 9(3):251.

Cayre, O., V.N. Paunov and O.D. Velev. 2003a. Fabrication of asymmetrically coated colloid particles by microcontact printing techniques. **J. Mater. Chem.** 13(10):2445-2450.

Cayre, O., V.N. Paunov and O.D. Velev. 2003b. Fabrication of dipolar colloid particles by microcontact printing. **Chem. Commun.** (18):2296-2297.

Ceccato, M., A. Bousquet, M. Hinge, S.U. Pedersen and K. Daasbjerg. 2011. Using a Mediating Effect in the Electroreduction of Aryldiazonium Salts To Prepare Conducting Organic Films of High Thickness. **Chem. Mater.** 23(6):1551-1557.

Che, G., B.B. Lakshmi, E.R. Fisher and C.R. Martin. 1998a. Carbon nanotubule membranes for electrochemical energy storage and production. **Nature** 393(6683):346-349.

Che, G., B.B. Lakshmi, C.R. Martin, E.R. Fisher and R.S. Ruoff. 1998b. Chemical Vapor Deposition Based Synthesis of Carbon Nanotubes and Nanofibers Using a Template Method. **Chem. Mater.** 10(1):260-267.

Chen, T. and L. Dai. 2013. Carbon nanomaterials for high-performance supercapacitors. **Mater. Today** 16(7–8):272-280.

Clayden, J., N. Greeves and S. Warren. 2012. **Organic Chemistry.** 2nd. Oxford University Press. UK.

Collins, A.T. 1993. The Optical and Electronic Properties of Semiconducting Diamond. **Philos. T. R. Soc. A** 342(1664):233-244.

Collins, T.J. 2007. ImageJ for microscopy. **Biotechniques**. 43:S25 - S30.

Colomer, J.F., C. Stephan, S. Lefrant, G. Van Tendeloo, I. Willems, Z. Kónya, A. Fonseca, C. Laurent and J.B. Nagy. 2000. Large-scale synthesis of single-wall carbon nanotubes by catalytic chemical vapor deposition (CCVD) method. **Chem. Phys. Lett.** 317(1–2):83-89.

Cowlard, F.C. and J.C. Lewis. 1967. Vitreous carbon — A new form of carbon. **J. Mater. Sci.** 2(6):507-512.

Dai, H., A.G. Rinzler, P. Nikolaev, A. Thess, D.T. Colbert and R.E. Smalley. 1996. Single-wall nanotubes produced by metal-catalyzed disproportionation of carbon monoxide. **Chem. Phys. Lett.** 260(3–4):471-475.

Dai, L. 2006. **Carbon Nanotechnology: Recent Developments in Chemistry, Physics, Materials Science and Device Applications.** Elsevier. Amsterdam.

Das, D. and P.K. Das. 2009. Superior Activity of Structurally Deprived Enzyme−Carbon Nanotube Hybrids in Cationic Reverse Micelles. **Langmuir** 25(8):4421-4428.

Datsyuk, V., M. Kalyva, K. Papagelis, J. Parthenios, D. Tasis, A. Siokou, I. Kallitsis and C. Galiotis. 2008. Chemical oxidation of multiwalled carbon nanotubes. **Carbon** 46(6):833-840.

Davis, J.J., K.S. Coleman, B.R. Azamian, C.B. Bagshaw and M.L.H. Green. 2003. Chemical and Biochemical Sensing with Modified Single Walled Carbon Nanotubes. **Chem. Eur. J.** 9(16):3732-3739.

De Volder, M.F.L., S.H. Tawfick, R.H. Baughman and A.J. Hart. 2013. Carbon Nanotubes: Present and Future Commercial Applications. **Science** 339(6119):535-539.

Delamar, M., G. Desarmot, O. Fagebaume, R. Hitmi, J. Pinson and J. Saveant. 1997. Modification of carbon fiber surfaces by electrochemical reduction of aryl diazonium salts: application to carbon epoxy composites. **Carbon** 35(6):801-807.

Delamar, M., R. Hitmi, J. Pinson and J.M. Saveant. 1992. Covalent modification of carbon surfaces by grafting of functionalized aryl radicals produced from electrochemical reduction of diazonium salts. **J. Am. Chem. Soc.** 114(14):5883-5884.

Dementev, N., S. Osswald, Y. Gogotsi and E. Borguet. 2009. Purification of carbon nanotubes by dynamic oxidation in air. **J. Mater. Chem.** 19(42):7904-7908.

Deprez, N. and D.S. McLachlan. 1988. The analysis of the electrical conductivity of graphite conductivity of graphite powders during compaction. **J. Phys. D Appl. Phys.** 21(1):101.

Downard, A.J. 2000a. Electrochemically Assisted Covalent Modification of Carbon Electrodes. **Electroanal.** 12(14):1085-1096.

Downard, A.J. 2000b. Potential-Dependence of Self-Limited Films Formed by Reduction of Aryldiazonium Salts at Glassy Carbon Electrodes. **Langmuir** 16(24):9680-9682.

Duval, J., J.M. Kleijn and H.P. van Leeuwen. 2001. Bipolar electrode behaviour of the aluminium surface in a lateral electric field. **J. Electroanal. Chem.** 505(1–2):1-11.

Dyke, C.A. and J.M. Tour. 2003. Unbundled and Highly Functionalized Carbon Nanotubes from Aqueous Reactions. **Nano Lett.** 3(9):1215-1218.

Eklund, P.C., J.M. Holden and R.A. Jishi. 1995. Vibrational modes of carbon nanotubes; Spectroscopy and theory. **Carbon** 33(7):959-972.

Endo, M., T. Hayashi and Y.-A. Kim. 2006. Large-scale production of carbon nanotubes and their applications. **Pure Appl. Chem.** 78(9):1703-1713.

Fan, S., M.G. Chapline, N.R. Franklin, T.W. Tombler, A.M. Cassell and H. Dai. 1999. Self-Oriented Regular Arrays of Carbon Nanotubes and Their Field Emission Properties. **Science** 283(5401):512-514.

Faria, J., M.P. Ruiz and D.E. Resasco. 2010. Phase-Selective Catalysis in Emulsions Stabilized by Janus Silica-Nanoparticles. **Adv. Synth. Catal.** 352(14-15):2359-2364.

Fattah, Z., P. Garrigue, B. Goudeau, V. Lapeyre, A. Kuhn and L. Bouffier. 2013. Capillary electrophoresis as a production tool for asymmetric microhybrids. **Electrophoresis** 34(14):1985-1990.

Fattah, Z., P. Garrigue, V. Lapeyre, A. Kuhn and L. Bouffier. 2012. Controlled Orientation of Asymmetric Copper Deposits on Carbon Microobjects by Bipolar Electrochemistry. **J. Phys. Chem. C** 116(41):22021-22027.

Fattah, Z., G. Loget, V. Lapeyre, P. Garrigue, C. Warakulwit, J. Limtrakul, L. Bouffier and A. Kuhn. 2011. Straightforward single-step generation of microswimmers by bipolar electrochemistry. **Electrochim. Acta** 56(28):10562-10566.

Fleischmann, M., J. Ghoroghchian, D. Rolison and S. Pons. 1986. Electrochemical behavior of dispersions of spherical ultramicroelectrodes. **J. Phys. Chem.** 90(23):6392-6400.

Fonseca, A., K. Hernadi, J.B. Nagy, D. Bernaerts and A.A. Lucas. 1996. Optimization of catalytic production and purification of buckytubes. **J. Mol. Catal. A: Chem.** 107(1–3):159-168.

Frackowiak, E. and F. Béguin. 2001. Carbon materials for the electrochemical storage of energy in capacitors. **Carbon** 39(6):937-950.

Frens, G. 1973. Controlled Nucleation for the Regulation of the Particle Size in Monodisperse Gold Suspensions. **Nat. Phys. Sci.** 241:20-22.

Furniss, B.S., A.J. Hannaford, P.W.G. Smith and A.R. Tatchell. 1989. **Vogel's Textbook of Practical Organic Chemistry.** 5th. Longman. London.

Geng, J., C. Singh, D.S. Shephard, M.S.P. Shaffer, B.F.G. Johnson and A.H. Windle. 2002. Synthesis of high purity single-walled carbon nanotubes in high yield. **Chem. Commun.** (22):2666-2667.

Gong, K., S. Chakrabarti and L. Dai. 2008. Electrochemistry at Carbon Nanotube Electrodes: Is the Nanotube Tip More Active Than the Sidewall? **Angew. Chem. Int. Edit.** 47(29):5446-5450.

Gu, H., Z. Yang, J. Gao, C.K. Chang and B. Xu. 2004. Heterodimers of Nanoparticles: Formation at a Liquid−Liquid Interface and Particle-Specific Surface Modification by Functional Molecules. **J. Am. Chem. Soc.** 127(1):34-35.

Guerrette, J.P., S.M. Oja and B. Zhang. 2012. Coupled Electrochemical Reactions at Bipolar Microelectrodes and Nanoelectrodes. **Anal. Chem.** 84(3):1609-1616.

Guo, D.J. and H.L. Li. 2005. Highly dispersed Ag nanoparticles on functional MWNT surfaces for methanol oxidation in alkaline solution. **Carbon** 43(6):1259-1264.

Guo, T., P. Nikolaev, A.G. Rinzler, D. Tomanek, D.T. Colbert and R.E. Smalley. 1995. Self-Assembly of Tubular Fullerenes. **J. Phys. Chem.** 99(27):10694-10697.

Haddon, R.C., J. Sippel, A.G. Rinzler and F. Papadimitrakopoulos. 2004. Purification and Separation of Carbon Nanotubes. **MRS Bulletin** 29(04):252-259.

Harris, P.J.F. 1999. **Carbon Nanotubes and Related Structures: New Materials for the Twenty-First Century.** Cambridge University Press. New York.

Harris, P.J.F. 2004. Fullerene-related structure of commercial glassy carbons. **Philos. Mag.** 84(29):3159-3167.

Harris, P.J.F. and K. Kawamura. 1976. **Polymeric carbons - Carbon Fibre, Glass and Char.** Cambridge University Press.

Hata, K., D.N. Futaba, K. Mizuno, T. Namai, M. Yumura and S. Iijima. 2004. Water-Assisted Highly Efficient Synthesis of Impurity-Free Single-Walled Carbon Nanotubes. **Science** 306(5700):1362-1364.

Heilmann, A., N. Teuscher, A. Kiesow, D. Janasek and U. Spohn. 2003. Nanoporous Aluminum Oxide as a Novel Support Material for Enzyme Biosensors. **J. Nanosci. Nanotechnol.** 3(5):375-379.

Hernadi, K., A. Fonseca, J.B. Nagy, D. Bemaerts, A. Fudala and A.A. Lucas. 1996. Catalytic synthesis of carbon nanotubes using zeolite support. **Zeolites** 17(5–6):416-423.

Hertel, T., R.E. Walkup and P. Avouris. 1998. Deformation of carbon nanotubes by surface van der Waals forces. **Phys. Rev. B** 58(20):13870-13873.

Himmelhaus, M. and H. Takei. 2000. Cap-shaped gold nanoparticles for an optical biosensor. **Sensor. Actuat. B-Chem.** 63(1–2):24-30.

Hiura, H., T.W. Ebbesen and K. Tanigaki. 1995. Opening and purification of carbon nanotubes in high yields. **Adv. Mater.** 7(3):275-276.

Hoffman, W.P., W.C. Hurley, T.W. Owens and H.T. Phan. 1991. Advantage of the scanning tunnelling microscope in documenting changes in carbon fibre surface morphology brought about by various surface treatments. **J. Mater. Sci.** 26(17):4545-4553.

Hong, L., S. Jiang and S. Granick. 2006. Simple Method to Produce Janus Colloidal Particles in Large Quantity. **Langmuir** 22(23):9495-9499.

Hou, P.-X., C. Liu and H.-M. Cheng. 2008. Purification of carbon nanotubes. **Carbon** 46(15):2003-2025.

Hu, C., H. Liao, F. Li, J. Xiang, W. Li, S. Duo and M. Li. 2008. Noncovalent functionalization of multi-walled carbon nanotubes with siloxane polyether copolymer. **Mater. Lett.** 62(17–18):2585-2588.

Huang, W., Y. Wang, G. Luo and F. Wei. 2003. 99.9% purity multi-walled carbon nanotubes by vacuum high-temperature annealing. **Carbon** 41(13):2585-2590.

Hunter, R.J. 1981. **Zeta Potential in Colloid Science.** Academic Press. New York.

Hunter, R.J. 1993. **Introduction to Modern Colloid Science.** Oxford University Press. New York.

Iijima, S. 1991. Helical microtubules of graphitic carbon. **Nature** 354(6348):56-58.

Iijima, S. and T. Ichihashi. 1993. Single-shell carbon nanotubes of 1-nm diameter. **Nature** 363(6430):603-605.

Inagi, S., Y. Ishiguro, M. Atobe and T. Fuchigami. 2010. Bipolar Patterning of Conducting Polymers by Electrochemical Doping and Reaction. **Angew. Chem. Int. Edit.** 49(52):10136-10139.

Jenkins, G.M., K. Kawamura and L.L. Ban. 1972. Formation and Structure of Polymeric Carbons. **P. Roy. Soc. Lond. A Mat.** 327(1571):501-517.

Jeong, S.-H., H.-Y. Hwang, S.-K. Hwang and K.-H. Lee. 2004. Carbon nanotubes based on anodic aluminum oxide nano-template. **Carbon** 42(10):2073-2080.

Jirage, K.B., J.C. Hulteen and C.R. Martin. 1997. Nanotubule-Based Molecular-Filtration Membranes. **Science** 278(5338):655-658.

José-Yacamán, M., M. Miki-Yoshida, L. Rendón and J.G. Santiesteban. 1993. Catalytic growth of carbon microtubules with fullerene structure. **Appl. Phys. Lett.** 62(6):657-659.

Kariuki, J.K. and M.T. McDermott. 1999. Nucleation and Growth of Functionalized Aryl Films on Graphite Electrodes. **Langmuir** 15(19):6534-6540.

Kariuki, J.K. and M.T. McDermott. 2001. Formation of Multilayers on Glassy Carbon Electrodes via the Reduction of Diazonium Salts. **Langmuir** 17(19):5947-5951.

Keller, F., M.S. Hunter and D.L. Robinson. 1953. Structural Features of Oxide Coatings on Aluminum. **J. Electrochem. Soc.** 100(9):411-419.

Kimling, J., M. Maier, B. Okenve, V. Kotaidis, H. Ballot and A. Plech. 2006. Turkevich Method for Gold Nanoparticle Synthesis Revisited. **J. Phys. Chem. B** 110(32):15700-15707.

Kong, J., H.T. Soh, A.M. Cassell, C.F. Quate and H. Dai. 1998. Synthesis of individual single-walled carbon nanotubes on patterned silicon wafers. **Nature** 395(6705):878-881.

Kooi, S.E., U. Schlecht, M. Burghard and K. Kern. 2002. Electrochemical Modification of Single Carbon Nanotubes. **Angew. Chem. Int. Edit.** 41(8):1353-1355.

Kowalska, E., P. Kowalczyk, J. Radomska, E. Czerwosz, H. Wronka and M. Bystrzejewski. 2006. Influence of high vacuum annealing treatment on some properties of carbon nanotubes. **J. Therm. Anal. Calorim.** 86(1):115-119.

Kumsapaya, C., M.-F. Bakaï, G. Loget, B. Goudeau, C. Warakulwit, J. Limtrakul, A. Kuhn and D. Zigah. 2013. Wireless Electrografting of Molecular Layers for Janus Particle Synthesis. **Chem. Eur. J.** 19(5):1577-1580.

Kyotani, T., L.-f. Tsai and A. Tomita. 1995. Formation of Ultrafine Carbon Tubes by Using an Anodic Aluminum Oxide Film as a Template. **Chem. Mater.** 7(8):1427-1428.

Kyotani, T., L.-f. Tsai and A. Tomita. 1996. Preparation of Ultrafine Carbon Tubes in Nanochannels of an Anodic Aluminum Oxide Film. **Chem. Mater.** 8(8):2109-2113.

Lee, C.J., D.W. Kim, T.J. Lee, Y.C. Choi, Y.S. Park, W.S. Kim, Y.H. Lee, W.B. Choi, N.S. Lee, J.M. Kim, Y.G. Choi and S.C. Yu. 1999. Synthesis of uniformly distributed carbon nanotubes on a large area of Si substrates by thermal chemical vapor deposition. **Appl. Phys. Lett.** 75(12):1721-1723.

Lehman, J.H., M. Terrones, E. Mansfield, K.E. Hurst and V. Meunier. 2011. Evaluating the characteristics of multiwall carbon nanotubes. **Carbon** 49(8):2581-2602.

Lewis, J.C., B. Redfern and F.C. Cowlard. 1963. Vitreous carbon as a crucible material for semiconductors. **Solid State Electron.** 6(3):251-IN254.

Li, W.Z., J.G. Wen, M. Sennett and Z.F. Ren. 2003. Clean double-walled carbon nanotubes synthesized by CVD. **Chem. Phys. Lett.** 368(3–4):299-306.

Li, W.Z., S.S. Xie, L.X. Qian, B.H. Chang, B.S. Zou, W.Y. Zhou, R.A. Zhao and G. Wang. 1996. Large-Scale Synthesis of Aligned Carbon Nanotubes. **Science** 274(5293):1701-1703.

Li, Y., W. Zhou, H. Wang, L. Xie, Y. Liang, F. Wei, J.-C. Idrobo, S.J. Pennycook and H. Dai. 2012. An oxygen reduction electrocatalyst based on carbon nanotube-graphene complexes. **Nat. Nano.** 7(6):394-400.

Lin, W., K.-S. Moon, S. Zhang, Y. Ding, J. Shang, M. Chen and C.-p. Wong. 2010. Microwave Makes Carbon Nanotubes Less Defective. **ACS Nano** 4(3):1716-1722.

Liu and J.J. Gooding. 2006. An Interface Comprising Molecular Wires and Poly(ethylene glycol) Spacer Units Self-Assembled on Carbon Electrodes for Studies of Protein Electrochemistry. **Langmuir** 22(17):7421-7430.

Liu, G., M.N. Paddon-Row and J. Justin Gooding. 2007. A molecular wire modified glassy carbon electrode for achieving direct electron transfer to native glucose oxidase. **Electrochem. Commun.** 9(9):2218-2223.

Loget, G. 2012. **Electric Field-Generated Asymmetric Reactivity : From Materials Science to Dynamic Systems.** Ph.D. Thesis, Université Bordeaux 1. Bordeaux.

Loget, G. and A. Kuhn. 2010. Propulsion of Microobjects by Dynamic Bipolar Self-Regeneration. **J. Am. Chem. Soc.** 132(45):15918-15919.

Loget, G. and A. Kuhn. 2011a. Electric field-induced chemical locomotion of conducting objects. **Nat. Commun.** 2:535.

Loget, G. and A. Kuhn. 2011b. Shaping and exploring the micro- and nanoworld using bipolar electrochemistry. **Anal. Bioanal. Chem.** 400(6):1691-1704.

Loget, G. and A. Kuhn. 2012. Bipolar electrochemistry for cargo-lifting in fluid channels. **Lab Chip** 12(11):1967-1971.

Loget, G., V. Lapeyre, P. Garrigue, C. Warakulwit, J. Limtrakul, M.-H. Delville and A. Kuhn. 2011. Versatile Procedure for Synthesis of Janus-Type Carbon Tubes. **Chem. Mater.** 23(10):2595-2599.

Loget, G., G. Larcade, V. Lapeyre, P. Garrigue, C. Warakulwit, J. Limtrakul, M.H. Delville, V. Ravaine and A. Kuhn. 2010. Single point electrodeposition of nickel for the dissymmetric decoration of carbon tubes. **Electrochim. Acta** 55(27):8116-8120.

Loget, G., J. Roche and A. Kuhn. 2012. True Bulk Synthesis of Janus Objects by Bipolar Electrochemistry. **Adv. Mater.** 24(37):5111-5116.

Loget, G., D. Zigah, L. Bouffier, N. Sojic and A. Kuhn. 2013. Bipolar Electrochemistry: From Materials Science to Motion and Beyond. **Acc. Chem. Res.** 46:2513-2523.

Losic, D. and S. Simovic. 2009. Self-ordered nanopore and nanotube platforms for drug delivery applications. **Expert Opin. Drug Deliv.** 6(12):1363-1381.

Mahouche-Chergui, S., S. Gam-Derouich, C. Mangeney and M.M. Chehimi. 2011. Aryl diazonium salts: a new class of coupling agents for bonding polymers, biomacromolecules and nanoparticles to surfaces. **Chem. Soc. Rev.** 40(7):4143-4166.

Mano, N. and A. Heller. 2005. Bioelectrochemical Propulsion. **J. Am. Chem. Soc.** 127(33):11574-11575.

Marcoux, P.R., P. Hapiot, P. Batail and J. Pinson. 2004. Electrochemical functionalization of nanotube films: growth of aryl chains on single-walled carbon nanotubes. **New J. Chem.** 28(2):302-307.

Mardilovich, P.P., A.N. Govyadinov, N.I. Mukhurov, A.M. Rzhevskii and R. Paterson. 1995. New and modified anodic alumina membranes Part I. Thermotreatment of anodic alumina membranes. **J. Membr. Sci.** 98(1–2):131-142.

Martin, C.R. 1994. Nanomaterials: A Membrane-Based Synthetic Approach. **Science** 266(5193):1961-1966.

Masuda, H. and K. Fukuda. 1995. Ordered Metal Nanohole Arrays Made by a Two-Step Replication of Honeycomb Structures of Anodic Alumina. **Science** 268(5216):1466-1468.

Mavré, F.o., R.K. Anand, D.R. Laws, K.-F. Chow, B.-Y. Chang, J.A. Crooks and R.M. Crooks. 2010. Bipolar Electrodes: A Useful Tool for Concentration, Separation, and Detection of Analytes in Microelectrochemical Systems. **Anal. Chem.** 82(21):8766-8774.

Mavré, F.o., K.-F. Chow, E. Sheridan, B.-Y. Chang, J.A. Crooks and R.M. Crooks. 2009. A Theoretical and Experimental Framework for Understanding Electrogenerated Chemiluminescence (ECL) Emission at Bipolar Electrodes. **Anal. Chem.** 81(15):6218-6225.

Meyyappan, M., D. Lance, C. Alan and H. David. 2003. Carbon nanotube growth by PECVD: a review. **Plasma Sources Sci. Technol.** 12(2):205.

Mittal, V. 2011. **Surface Modification of Nanotube Fillers.** Wiley-VCH Verlag GmbH & Co. KGaA. Weinheim.

Nativ-Roth, E., R. Shvartzman-Cohen, C. Bounioux, M. Florent, D. Zhang, I. Szleifer and R. Yerushalmi-Rozen. 2007. Physical Adsorption of Block Copolymers to SWNT and MWNT: A Nonwrapping Mechanism. **Macromolecules** 40(10):3676-3685.

Nayak, R.R., K.Y. Lee, A.M. Shanmugharaj and S.H. Ryu. 2007. Synthesis and characterization of styrene grafted carbon nanotube and its polystyrene nanocomposite. **Eur. Polym. J.** 43(12):4916-4923.

Nie, Z., W. Li, M. Seo, S. Xu and E. Kumacheva. 2006. Janus and Ternary Particles Generated by Microfluidic Synthesis: Design, Synthesis, and Self-Assembly. **J. Am. Chem. Soc.** 128(29):9408-9412.

Nikolaev, P., M.J. Bronikowski, R.K. Bradley, F. Rohmund, D.T. Colbert, K.A. Smith and R.E. Smalley. 1999. Gas-phase catalytic growth of single-walled carbon nanotubes from carbon monoxide. **Chem. Phys. Lett.** 313(1–2):91-97.

Nisisako, T. and T. Torii. 2007. Formation of Biphasic Janus Droplets in a Microfabricated Channel for the Synthesis of Shape-Controlled Polymer Microparticles. **Adv. Mater.** 19(11):1489-1493.

Nisisako, T., T. Torii, T. Takahashi and Y. Takizawa. 2006. Synthesis of Monodisperse Bicolored Janus Particles with Electrical Anisotropy Using a Microfluidic Co-Flow System. **Adv. Mater.** 18(9):1152-1156.

O'Connell, M.J., P. Boul, L.M. Ericson, C. Huffman, Y. Wang, E. Haroz, C. Kuper, J. Tour, K.D. Ausman and R.E. Smalley. 2001. Reversible water-solubilization of single-walled carbon nanotubes by polymer wrapping. **Chem. Phys. Lett.** 342(3–4):265-271.

Ohno, H., D. Takagi, K. Yamada, S. Chiashi, A. Tokura and Y. Homma. 2008. Growth of Vertically Aligned Single-Walled Carbon Nanotubes on Alumina and Sapphire Substrates. **Jpn. J. Appl. Phys.** 47(4R):1956.

Osswald, S., E. Flahaut, H. Ye and Y. Gogotsi. 2005. Elimination of D-band in Raman spectra of double-wall carbon nanotubes by oxidation. **Chem. Phys. Lett.** 402(4–6):422-427.

Paunov, V.N. and O.J. Cayre. 2004. Supraparticles and "Janus" Particles Fabricated by Replication of Particle Monolayers at Liquid Surfaces Using a Gel Trapping Technique. **Adv. Mater.** 16(9-10):788-791.

Pazo-Llorente, R., C. Bravo-Diaz and E. Gonzalez-Romero. 2004. pH Effects on Ethanolysis of Some Arenediazonium Ions: Evidence for Homolytic Dediazoniation Proceeding through Formation of Transient Diazo Ethers. **Eur. J. Org. Chem.** 2004(15):3221-3226.

Pellissier, M., F. Barrière, A.J. Downard and D. Leech. 2008a. Improved stability of redox enzyme layers on glassy carbon electrodes via covalent grafting. **Electrochem. Commun.** 10(6):835-838.

Pellissier, M., D. Zigah, F.d.r. Barrière and P. Hapiot. 2008b. Optimized Preparation and Scanning Electrochemical Microscopy Analysis in Feedback Mode of Glucose Oxidase Layers Grafted onto Conducting Carbon Surfaces. **Langmuir** 24(16):9089-9095.

Philip, B., J. Xie, J.K. Abraham and V.K. Varadan. 2005. Polyaniline / carbon nanotube composites: starting with phenylamino functionalized carbon nanotubes. **Polym. Bull.** 53(2):127-138.

Pinson, J. and F. Podvorica. 2005. Attachment of organic layers to conductive or semiconductive surfaces by reduction of diazonium salts. **Chem. Soc. Rev.** 34(5):429-439.

Poinern, G.E.J., X.T. Le, M. Hager, T. Becker and D. Fawcett. 2013. Electrochemical Synthesis, Characterisation, and Preliminary Biological Evaluation of an Anodic Aluminium Oxide Membrane with a pore size of 100 nanometres for a Potential Cell Culture Substrate. **Am. J. Biomed. Eng.** 3(6):119-131.

Qin, L.C., D. Zhou, A.R. Krauss and D.M. Gruen. 1998. Growing carbon nanotubes by microwave plasma-enhanced chemical vapor deposition. **Appl. Phys. Lett.** 72(26):3437-3439.

Radi, A.-E., V. Lates and J.-L. Marty. 2008. Mediatorless Hydrogen Peroxide Biosensor Based on Horseradish Peroxidase Immobilized on 4-Carboxyphenyl Film Electrografted on Gold Electrode. **Electroanal.** 20(23):2557-2562.

Rahimi-Razin, S., V. Haddadi-Asl, M. Salami-Kalajahi, F. Behboodi-Sadabad and H. Roghani-Mamaqani. 2012. Matrix-grafted multiwalled carbon nanotubes/poly(methyl methacrylate) nanocomposites synthesized by in situ RAFT polymerization: A kinetic study. **Int. J. Chem. Kinet.** 44(8):555-569.

Ren, Z.F., Z.P. Huang, J.W. Xu, J.H. Wang, P. Bush, M.P. Siegal and P.N. Provencio. 1998. Synthesis of Large Arrays of Well-Aligned Carbon Nanotubes on Glass. **Science** 282(5391):1105-1107.

Robert, T.M., N.B. Robert and S.K. Bhattacharjee. 2011. **Organic Chemistry.** 6th. Pearson Prentice Hall. New Delhi.

Ruoff, R.S., J. Tersoff, D.C. Lorents, S. Subramoney and B. Chan. 1993. Radial deformation of carbon nanotubes by van der Waals forces. **Nature** 364(6437):514-516.

Sagar, R. 1996. **Together With Chemistry XII.** 1st. Rachana Sagar Pvt. Ltd. New Delhi.

Schneider, J.J., N.I. Maksimova, J. Engstler, R. Joshi, R. Schierholz and R. Feile. 2008. Catalyst free growth of a carbon nanotube–alumina composite structure. **Inorg. Chim. Acta.** 361(6):1770-1778.

Sheridan, E., K.N. Knust and R.M. Crooks. 2011. Bipolar electrode depletion: membraneless filtration of charged species using an electrogenerated electric field gradient. **Analyst** 136(20):4134-4137.

Shim, M., N.W. Shi Kam, R.J. Chen, Y. Li and H. Dai. 2002. Functionalization of Carbon Nanotubes for Biocompatibility and Biomolecular Recognition. **Nano Lett.** 2(4):285-288.

Shul, G., C.A.C. Ruiz, D. Rochefort, P.A. Brooksby and D. Bélanger. 2013. Electrochemical functionalization of glassy carbon electrode by reduction of diazonium cations in protic ionic liquid. **Electrochim. Acta** 106(0):378-385.

Silverstein, R.M., G.C. Bassler and T.C. Morrill. 1991. **Spectrometric Identification of Organic Compounds.** 5th. John Wiley & Sons. New York.

Singh, C., M.S.P. Shaffer, K.K.K. Koziol, I.A. Kinloch and A.H. Windle. 2003. Towards the production of large-scale aligned carbon nanotubes. **Chem. Phys. Lett.** 372(5–6):860-865.

Suh, J.S. and J.S. Lee. 1999. Highly ordered two-dimensional carbon nanotube arrays. **Appl. Phys. Lett.** 75(14):2047-2049.

Sui, Y.C., D.R. Acosta, J.A. González-León, A. Bermúdez, J. Feuchtwanger, B.Z. Cui, J.O. Flores and J.M. Saniger. 2001. Structure, Thermal Stability, and Deformation of Multibranched Carbon Nanotubes Synthesized by CVD in the AAO Template. **J. Phys. Chem. B** 105(8):1523-1527.

Sulka, G.D. and K.G. Parkoła. 2007. Temperature influence on well-ordered nanopore structures grown by anodization of aluminium in sulphuric acid. **Electrochim. Acta** 52(5):1880-1888.

Takei, H. and N. Shimizu. 1997. Gradient Sensitive Microscopic Probes Prepared by Gold Evaporation and Chemisorption on Latex Spheres. **Langmuir** 13(7):1865-1868.

Tan, P., S.-L. Zhang, K.T. Yue, F. Huang, Z. Shi, X. Zhou and Z. Gu. 1997. Comparative Raman Study of Carbon Nanotubes Prepared by D.C. Arc Discharge and Catalytic Methods. **J. Raman Spectrosc.** 28(5):369-372.

Teranishi, T., Y. Inoue, M. Nakaya, Y. Oumi and T. Sano. 2004. Nanoacorns: Anisotropically Phase-Segregated CoPd Sulfide Nanoparticles. **J. Am. Chem. Soc.** 126(32):9914-9915.

Terrones, M., N. Grobert, J. Olivares, J.P. Zhang, H. Terrones, K. Kordatos, W.K. Hsu, J.P. Hare, P.D. Townsend, K. Prassides, A.K. Cheetham, H.W. Kroto and D.R.M. Walton. 1997. Controlled production of aligned-nanotube bundles. **Nature** 388(6637):52-55.

Thess, A., R. Lee, P. Nikolaev, H. Dai, P. Petit, J. Robert, C. Xu, Y.H. Lee, S.G. Kim, A.G. Rinzler, D.T. Colbert, G.E. Scuseria, D. Tománek, J.E. Fischer and R.E. Smalley. 1996. Crystalline Ropes of Metallic Carbon Nanotubes. **Science** 273(5274):483-487.

Tsang, S.C., Y.K. Chen, P.J.F. Harris and M.L.H. Green. 1994. A simple chemical method of opening and filling carbon nanotubes. **Nature** 372(6502):159-162.

Tuinstra, F. and J.L. Koenig. 1970. Raman Spectrum of Graphite. **J. Chem. Phys.** 53(3):1126-1130.

Turkevich, J., P.C. Stevenson and J. Hillier. 1951. A study of the nucleation and growth processes in the synthesis of colloidal gold. **Discuss. Faraday Soc.** 11(0):55-75.

Ulrich, C., O. Andersson, L. Nyholm and F. Björefors. 2008. Formation of Molecular Gradients on Bipolar Electrodes. **Angew. Chem. Int. Edit.** 47(16):3034-3036.

Van der Linden, W.E. and J.W. Dieker. 1980. Glassy carbon as electrode material in electro- analytical chemistry. **Anal. Chim. Acta** 119(1):1-24.

Walker, P.L., J.F. Rakszawski and G.R. Imperial. 1959. Carbon Formation from Carbon Monoxide-Hydrogen Mixtures over Iron Catalysts.I. Properties of Carbon Formed. **J. Phys. Chem.** 63(2):133-140.

Walther, A., M. Drechsler and A.H.E. Muller. 2009. Structures of amphiphilic Janus discs in aqueous media. **Soft Matter** 5(2):385-390.

Wang, J. and Y. Lin. 2008. Functionalized carbon nanotubes and nanofibers for biosensing applications. **Trends Analyt. Chem.** 27(7):619-626.

Warakulwit, C. 2007. **Functionalizations of Carbon Nanotubes: An Experimental and Theoretical Study.** Ph.D. Thesis, Kasetsart University. Bangkok and Université Bordeaux 1. Bordeaux.

Warakulwit, C., T. Nguyen, J. Majimel, M.-H. Delville, V. Lapeyre, P. Garrigue, V. Ravaine, J. Limtrakul and A. Kuhn. 2008. Dissymmetric Carbon Nanotubes by Bipolar Electrochemistry. **Nano Lett.** 8(2):500-504.

Wei, B.Q., R. Vajtai and P.M. Ajayan. 2001. Reliability and current carrying capacity of carbon nanotubes. **Appl. Phys. Lett.** 79(8):1172-1174.

Wepasnick, K., B. Smith, J. Bitter and D. Howard Fairbrother. 2010. Chemical and structural characterization of carbon nanotube surfaces. **Anal. Bioanal. Chem.** 396(3):1003-1014.

Wildgoose, G.G., N.S. Lawrence, H.C. Leventis, L. Jiang, T.G.J. Jones and R.G. Compton. 2005. X-Ray photoelectron spectroscopy studies of graphite powder and multiwalled carbon nanotubes covalently modified with Fast Black K: evidence for a chemical release mechanism via electrochemical reduction. **J. Mater. Chem.** 15(9):953-959.

Wong, Y.M., S. Wei, W.P. Kang, J.L. Davidson, W. Hofmeister, J.H. Huang and Y. Cui. 2004. Carbon nanotubes field emission devices grown by thermal CVD with palladium as catalysts. **Diam. Relat .Mater.** 13(11–12):2105-2112.

Wu, P., X. Chen, N. Hu, U.C. Tam, O. Blixt, A. Zettl and C.R. Bertozzi. 2008. Biocompatible Carbon Nanotubes Generated by Functionalization with Glycodendrimers. **Angew. Chem. Int. Edit.** 47(27):5022-5025.

Xu, Y.-Q., E. Flor, M.J. Kim, B. Hamadani, H. Schmidt, R.E. Smalley and R.H. Hauge. 2006. Vertical Array Growth of Small Diameter Single-Walled Carbon Nanotubes. **J. Am. Chem. Soc.** 128(20):6560-6561.

Yan, L.Y., Y.F. Poon, M.B. Chan-Park, Y. Chen and Q. Zhang. 2008. Individually Dispersing Single-Walled Carbon Nanotubes with Novel Neutral pH Water-Soluble Chitosan Derivatives. **J. Phys. Chem. C** 112(20):7579-7587.

Yang, H.-H. and R.L. McCreery. 1999. Effects of Surface Monolayers on the Electron-Transfer Kinetics and Adsorption of Methyl Viologen and Phenothiazine Derivatives on Glassy Carbon Electrodes. **Anal. Chem.** 71(18):4081-4087.

Yang, S., F. Guo, B. Kiraly, X. Mao, M. Lu, K.W. Leong and T.J. Huang. 2012. Microfluidic synthesis of multifunctional Janus particles for biomedical applications. **Lab Chip** 12(12):2097-2102.

Yang, X., S.B. Hall and S.N. Tan. 2003. Electrochemical Reduction of a Conjugated Cinnamic Acid Diazonium Salt as an Immobilization Matrix for Glucose Biosensor. **Electroanal.** 15(10):885-891.

Yu, H., M. Chen, P.M. Rice, S.X. Wang, R.L. White and S. Sun. 2005. Dumbbell-like Bifunctional Au−Fe3O4 Nanoparticles. **Nano Lett.** 5(2):379-382.

Zhang, X., A. Cao, Y. Li, C. Xu, J. Liang, D. Wu and B. Wei. 2002. Self-organized arrays of carbon nanotube ropes. **Chem. Phys. Lett.** 351(3–4):183-188.

Zhao, W., B. Basnet and I. Kim. 2012. Carbon nanotube formation using zeolite template and applications. **J. Adv. Ceram.** 1(3):179-193.

Zhong, G., S. Hofmann, F. Yan, H. Telg, J.H. Warner, D. Eder, C. Thomsen, W.I. Milne and J. Robertson. 2009. Acetylene: A Key Growth Precursor for Single-Walled Carbon Nanotube Forests. **J. Phys. Chem. C** 113(40):17321-17325.

Zollinger, H. 2003. **Color Chemistry. Syntheses, Properties, Application of Organic Dyes and Pigments.** 3rd. Wiley-VCH.

Appendix A

Details of thermal decomposition of VACNTs by Thermal Gravimetric Analysis (TGA)

The thermal gravimetric analysis (TGA) weight loss profile of VACNTs prepared at 750 °C via the decomposition of C_2H_2 using the AAO membrane as the template, post-treated with the thermal annealing at 1000 °C for 4 h (under N_2 atmosphere) and the air oxidation at 500 °C for 1 h after the removal of AAO by using the 50% HF solution is shown below. The data was taken by using a PYRIS 1 TGA, PERKIN-ELMER equipment in the temperature range of 100 ^oC to 1000 ^oC with a heating rate of 10 ^oC/min under an air flow. The weight loss profile shows that the tubes are thermally stable until < 500 °C in air.

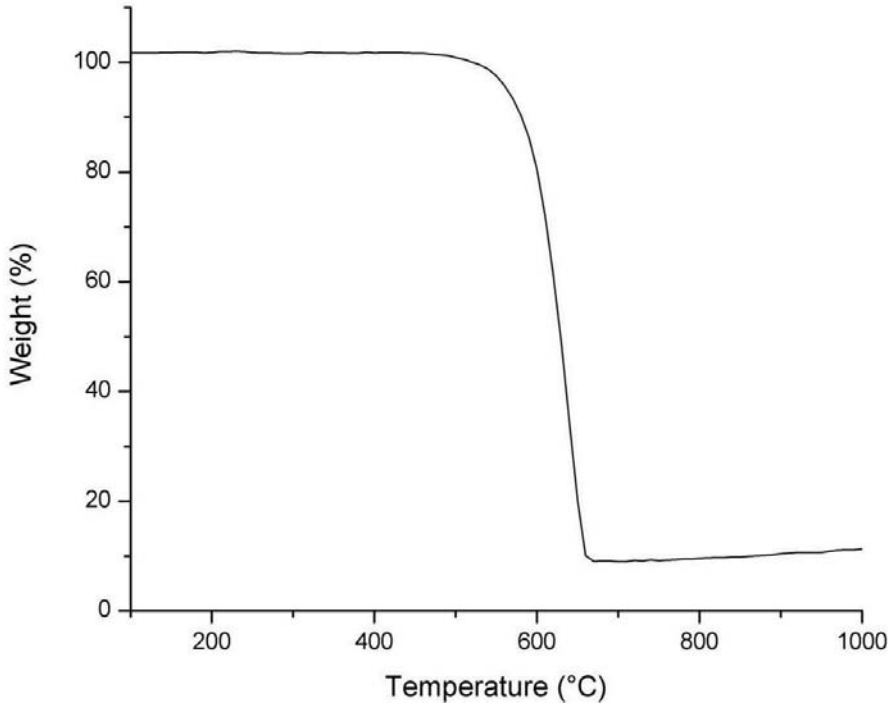

Appendix Figure A1 TGA weight loss profile of VACNTs prepared at 750 °C via the decomposition of C_2H_2 using the AAO membrane as the template, post-treated with the thermal annealing at 1000 °C for 4 h (under N_2 atmosphere) and the air oxidation at 500 °C for 1 h after the removal of AAO by using the 50% HF solution

Appendix B

Details of EDX spectra of the as-purified VACNT/AAO sample

The SEM images with the top-surface view of the VACNT/AAO sample at both sides of the membrane and corresponding EDX spectra are shown below. The chemical compositions including carbon (C) (derived from CNTs), oxygen (O) and aluminium (Al) (derived from the alumina composition) are observed.

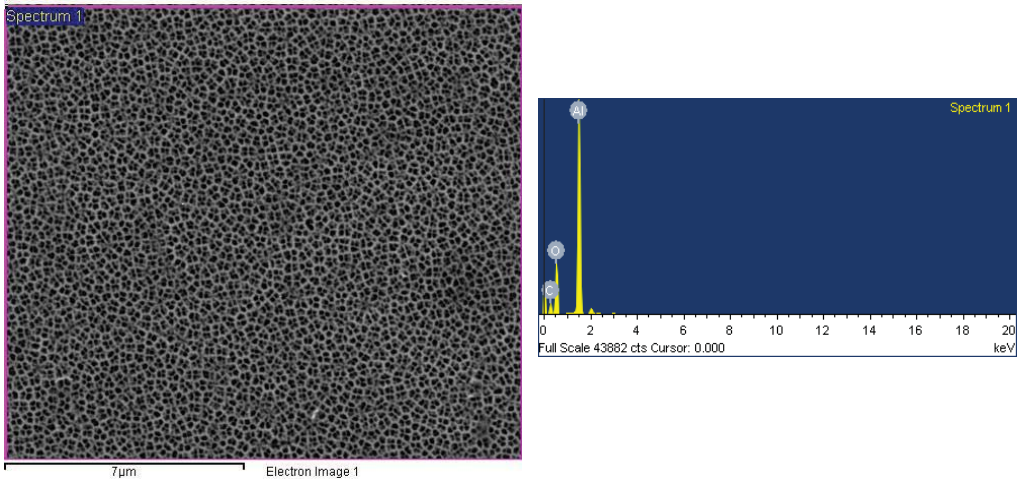

(a)

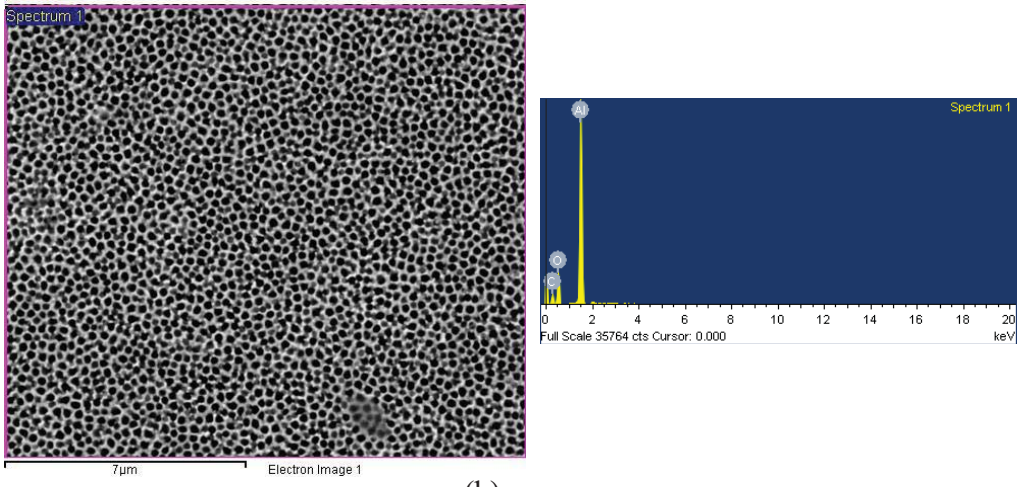

(b)

Appendix Figure B1 (a-b) Low-magnification SEM images with the top-surface view of the VACNT/AAO sample at both sides of the membrane and corresponding EDX spectra

CURRICULUM VITAE

NAME : Miss Chawanwit Kumsapaya

BIRTH DATE : October 13, 1982

BIRTH PLACE : Ratchaburi, Thailand

EDUCATION :

YEAR	INSTITUTE	DEGREE/DIPLOMA
2005	Chiangmai Univ.	B.Sc. (Chemistry, 1st class honour)
2008	Kasetsart Univ.	M.Sc. (Chemistry)

SCHOLARSHIPS :

2004-2008 The Development and Promotion of Science and Technology talents (DPST) project, the institute for the Promotion of Teaching Science and Technology (IPST)

2008-2011 The Commission on Higher Education (CHE), Ministry of Education, under the program "Strategic Scholarships for Frontier Research Network for the Joint Ph.D. Program Thai Doctoral degree"

PUBLICATIONS :

C. Kumsapaya, K. Bobuatong, P. Kongpracha, Y. Tantirungrotechai, and J. Limtrakul 2009**.** Mechanistic Investigation on 1,5- to 2,6-Dimethylnaphthalene Isomerization Catalyzed by Acidic β Zeolite: ONIOM Study with an M06-L Functional. **J. Phys. Chem. C** 113(36):16128–16137. **(Impact Factor: 4.805)**

C. Kumsapaya, K. Bobuatong, S. Choomwattana, P. Kongpracha, Y. Tantirungrotechai, and J. Limtrakul 2009. A Mechanistic Investigation on 1,5- to 2,6-Dimethylnaphthalene Isomerization Catalyzed by Acidic Beta Zeolite: An ONIOM Study with a Newly Developed Density Functional Theory. **NSTI-Nanotech** 3: 276–279. (Proceeding)

C. Kumsapaya, M.-F. Bakaï, G. Loget, B. Goudeau, C. Warakulwit, J. Limtrakul, A. Kuhn, and D. Zigah 2013. Wireless Electrografting of Molecular Layers for Janus Particle Synthesis. **Chem. Eur. J.** 19:1577-1580. **(Impact Factor: 5.925)**

PRESENTATIONS :

Poster Presentations

C. Kumsapaya, K. Bobuatong, S. Choomwattana, P. Kongpracha, Y. Tantirungrotechai, and J. Limtrakul. A Mechanistic Investigation on 1,5- to 2,6-Dimethylnaphthalene Isomerization Catalyzed by Acidic Beta Zeolite: An ONIOM Study with a Newly Developed Density Functional Theory. The 2009 NSTI Nanotechnology Conference and Trade Show, Houston, Texas, USA (May 3-7, 2009).

C. Kumsapaya, K. Bobuatong, S. Choomwattana, P. Kongpracha, Y. Tantirungrotechai, and J. Limtrakul. Mechanistic Investigation on 1,5- to 2,6-Dimethylnaphthalene Isomerization Catalyzed by Acidic β Zeolite: An ONIOM Study with an M06-L Functional. Sokendai Asian Winter School "Molecular Science – Central Role in Multidisciplinary Fields", Institute for Molecular Science (IMS), School of Physical Sciences, the Graduate University for Advanced Studies (SOKENDAI), Okazaki, Japan (December 1-4, 2009).

C. Kumsapaya, A. Kuhn, C. Warakulwit, and J. Limtrakul. Generation of Hybrid Au-Pt Nanostructures by Bipolar Electrochemical Deposition. NanoThailand 2010 conference "NanoThailand 2010: Nanotechnology for a Sustainable World", Pathumthani, Thailand (November 18-20, 2010).

Oral Presentations

Y. Kumsapaya (old name) and A. Rujiwatra. Cadmium removal abilities via column method of Na-x and Sodalite zeolites synthesized from coal fly ash. Science and Technology Conference "Science and Technology lead Thai Progress to International", Bangkok International Trade & Exhibition Centre, Bangna, Bangkok, Thailand (March 10 – 11, 2005).

Y. Kumsapaya (old name), K. Bobuatong, T. Nanok, and J. Limtrakul. A Mechanistic Investigation on the Isomerization of 1,5- into 2,6-Dimethylnaphthalene Catalyzed by an Acidic Beta Zeolite: An ONIOM Method. 33rd Congress on Science and Technology of Thailand (STT. 33rd: 2007), Walailak University, Nakhon Si Thammarat, Thailand (October 18 – 20, 2007).